

12-2013

BASIS FOR TARGETING MET ACTIVATION MEDIATED RESISTANCE TO PI3K INHIBITION IN BREAST CANCER

Ana M. Gonzalez-Angulo

Follow this and additional works at: http://digitalcommons.library.tmc.edu/utgsbs_dissertations

 Part of the [Medicine and Health Sciences Commons](#)

Recommended Citation

Gonzalez-Angulo, Ana M., "BASIS FOR TARGETING MET ACTIVATION MEDIATED RESISTANCE TO PI3K INHIBITION IN BREAST CANCER" (2013). *UT GSBS Dissertations and Theses (Open Access)*. Paper 418.

This Dissertation (PhD) is brought to you for free and open access by the Graduate School of Biomedical Sciences at DigitalCommons@The Texas Medical Center. It has been accepted for inclusion in UT GSBS Dissertations and Theses (Open Access) by an authorized administrator of DigitalCommons@The Texas Medical Center. For more information, please contact laurel.sanders@library.tmc.edu.

**BASIS FOR TARGETING MET ACTIVATION MEDIATED
RESISTANCE TO PI3K INHIBITION IN BREAST CANCER**

by

Ana Maria Gonzalez-Angulo, M.D.

Approved:



Gordon B. Mills, M.D., Ph.D. (Advisor)



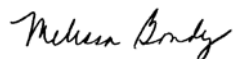
Lajos Pusztai, M.D., D.Phil



Faye M. Johnson, M.D., PhD.



Naoto Tada Ueno, M.D., PhD., F.A. C.P



Melissa L. Bondy, Ph.D.

Approved:

Dean, The University of Texas
Graduate School of Biomedical Sciences at Houston

**BASIS FOR TARGETING MET ACTIVATION MEDIATED RESISTANCE
TO PI3K INHIBITION IN BREAST CANCER**

**A
DISSERTATION**

Presented to the Faculty of
The University of Texas
Health Science Center at Houston
and
The University of Texas
MD Anderson Cancer Center
Graduate School of Biomedical Sciences
in Partial Fulfillment
of the Requirements
for the Degree of
DOCTOR OF PHILOSOPHY

by

Ana Maria Gonzalez-Angulo, M.D.

Houston, TX

(December, 2013)

ABSTRACT

BASIS FOR TARGETING MET ACTIVATION MEDIATED RESISTANCE TO PI3K INHIBITION IN BREAST CANCER

Ana Maria Gonzalez-Angulo, M.D.

Supervisory Professor: Gordon B. Mills, M.D., PhD.

The identification of resistance mechanisms to emerging therapies, such as those targeting the PI3K pathway and the MET receptor, has the potential to benefit a significant number of patients with breast cancer. In this study we hypothesized that concurrent aberrations in *PI3K* and *MET* will render breast cancers resistant to therapies targeting each pathway, and that combination therapy targeting the PI3K and MET pathway will optimize therapy-effect by preventing the acquisition of resistance.

We analyzed cMET and phospho-cMET levels in 257 breast cancer samples and found that high levels of both the proteins were seen in all breast cancer subtypes, which correlated with poor prognosis.(1) We also analyzed DNA from 971 FFPE early breast tumors, and showed that *MET* and *PIK3CA* are frequently co-amplified, and a high copy number of either gene is associated with poorer prognostic features and the triple negative disease.(2) Additionally, we determined the effect of MET-T1010I, MET-Y1253D and MET overexpression, found in breast cancers, on the activity of the two most common breast cancer *PIK3CA* mutations (E545K and H1047R), in a model of breast epithelial cells (MCF-10A) and a cell line breast cancer model (HCC1954). Our results suggest that tumors with concurrent aberrations in *MET* and *PIK3CA* are likely to be more aggressive and resistant to therapies targeting each pathway, and that combinatorial therapy (with MET and PI3K pathway inhibitors) could circumvent this resistance.

This is the first study to investigate the significance of differential expression of cMET and p-cMET in different breast cancer subtypes, to report p-cMET levels as a prognostic factor in breast cancer, and also, the first to report *MET* gene copy number, its distribution by tumor subtype, and correlation with patient outcome.(2) Our study is also unique for showing that the

presence of *MET* aberrations enhances the tumorigenic effects induced by the *PIK3CA* mutations in breast cancer/epithelial cells; results from our tumor xenograft models corroborate with these *in vitro* findings. Moreover, we are the first to provide evidence for the potential activity of combinatorial therapy using MET and PI3K pathway inhibitors against breast cancer.

TABLE OF CONTENTS

Approval Sheet	i
Title Page	ii
ABSTRACT.....	iii
Table of Contents.....	v
List of Figures	vi
List of Tables.....	viii
CHAPTER 1: INTRODUCTION.....	1
CHAPTER 2: cMET and phospho-cMET protein levels in breast cancers and survival outcomes	8
INTRODUCTION.....	8
MATERIALS AND METHODS.....	12
RESULTS.....	14
DISCUSSION.....	18
CHAPTER 3: Frequency of <i>MET</i> and <i>PIK3CA</i> copy number elevation and correlation with outcome in patients with early stage breast cancer	21
INTRODUCTION.....	21
MATERIALS AND METHODS.....	21
RESULTS.....	23
DISCUSSION.....	27
CHAPTER 4: <i>In vitro</i> effects of <i>MET</i> and <i>PIK3CA</i> co-aberrations in breast cancer	32
INTRODUCTION.....	32
MATERIALS AND METHODS.....	35
RESULTS.....	40
DISCUSSION.....	75
CHAPTER 5: DISCUSSION.....	86
APPENDIX 1.....	93
APPENDIX 2.....	95
BIBLIOGRAPHY	96
VITA.....	123

LIST OF FIGURES

<i>Figure 1 The hepatocyte growth factor HGF-cMET axis signaling network and ongoing targeted therapy strategies.....</i>	<i>10</i>
<i>Figure 2. Kaplan-Meier estimates illustrating the RFS of patients.....</i>	<i>16</i>
<i>Figure 3. Kaplan-Meier estimates illustrating (A) OS and (B) RFS</i>	<i>17</i>
<i>Figure 4. Distribution of MET and catalytic subunit of PIK3CA copy number shown by breast cancer subtype.....</i>	<i>24</i>
<i>Figure 5. Kaplan-Meier recurrence-free survival curves</i>	<i>26</i>
<i>Figure 6. Kaplan-Meier recurrence-free survival curves</i>	<i>27</i>
<i>Figure 7. Establishment of stable cells</i>	<i>41</i>
<i>Figure 8. Development of Lentiviral Constructs.....</i>	<i>43</i>
<i>Figure 9. Effect of wild type or mutant PIK3CA/cMETS on Cell Growth.....</i>	<i>44</i>
<i>Figure 10. The Effects of PIK3CA/cMET mutations on Colony Formation</i>	<i>46</i>
<i>Figure 11. The Effects of cMET or PIK3CA aberrations on Mammary Acinar Morphogenesis.</i>	<i>47</i>
<i>Figure 12. The Effects of cMET and/or PIK3CA overexpression or mutations on Cell Invasion</i>	<i>49</i>
<i>Figure 13. The Effect of mutant and wild type cMET and /or PIK3CA on Cell Signaling</i>	<i>51</i>
<i>Figure 14. Effects of mutant and wild type cMET on cell proliferation in PIK3CA-mutated breast cancer cells.....</i>	<i>56</i>
<i>Figure 15. Effects of mutant and wild type cMET on cell survival and anchorage-independent proliferation in PIK3CA-mutated breast cancer cells.....</i>	<i>57</i>
<i>Figure 16. Effects of wild type cMET or its mutants on tumor xenograft formation and progression in hHGF transgenic mice</i>	<i>59</i>
<i>Figure 17. Effect of wild type or mutant cMET on Cell Signaling in PIK3CA-mutated breast cancer cells.....</i>	<i>62</i>

Figure 18. Effects of wild type or mutant cMETs on cell response to PI3K inhibitors in PIK3CA-mutated breast cancer cells 63

Figure 19. Effects of targeting cMET or PI3K on cell signaling in PIK3CA-mutated breast cancer cell..... 64

Figure 20. Effects of combinations of PI3K inhibitors with cMET antibody, onartuzumab, or cMET inhibitor, EMD1214063, on Cell Proliferation..... 68

Figure 21. Effects of combinations of PI3K inhibitors with cMET antibody, onartuzumab, or cmet inhibitor, EMD1214063, on Cell Invasion..... 69

Figure 22. Effects of combinations of PI3K inhibitors with cMET antibody, onartuzumab, or cMET inhibitor, EMD1214063, on Cell Invasion of HCC1954 cells..... 71

LIST OF TABLES

<i>Table 1 Patient and clinical characteristics by total cMET and phospho-cMET.....</i>	<i>14</i>
<i>Table 2. Total cMET and phospho-cMET expressions by tumor subtype</i>	<i>15</i>
<i>Table 3. RFS and OS by total cMET and phospho-cMET levels and breast cancer subtype..</i>	<i>15</i>
<i>Table 4. Multivariable Cox proportional hazards model.....</i>	<i>17</i>
<i>Table 5. Patient and Tumor characteristics</i>	<i>23</i>
<i>Table 6. Five-year relapse-free survival estimates</i>	<i>25</i>
<i>Table 7. Multivariate Cox proportional hazard model.....</i>	<i>29</i>
<i>Table 8.....</i>	<i>39</i>
<i>Table 9. Summarizing the Effects of PIK3CA and MET aberrations on mammary epithelial cells</i>	<i>54</i>
<i>Table 10. Summarizing the Effects of MET aberrations on PIK3CA mutant-HCC1954 cells...</i>	<i>61</i>
<i>Table 11. Summarizing the Effects of selective PI3K pathway inhibitors and MET inhibitors on MET aberrant HCC1954 cells</i>	<i>73</i>
<i>Table 12. Summarizing the Effects of selective PI3K pathway inhibitors and MET inhibitors on MET and/or PIK3CA aberrant MCF -10A cells</i>	<i>75</i>

CHAPTER 1: INTRODUCTION

Breast cancer is the second most common cancer worldwide after lung cancer, the fifth most common cause of cancer death, and the leading cause of cancer death in women. The global burden of breast cancer exceeds all other cancers and the incidence rates of breast cancer are increasing(3). Over 200,000 cases and around 40,000 breast cancer related deaths occurred in the US in 2012.(4)

Breast Cancer is a heterogeneous group of neoplasms originating from the epithelial cells lining the milk ducts(5). Breast tumor heterogeneity has been noted in histology and clinical outcome for a long time, and these differences have served as the basis for disease classification(5). Gene expression studies have identified several major subtypes of breast cancer: the luminal subtypes, which typically express hormone-receptor related genes, and two hormone receptor-negative subtypes- the human epidermal growth factor receptor 2 (HER2) positive/estrogen receptor (ER) negative subtype and the basal-like subtype(6).

In gene arrays, basal breast cancers are characterized by low expression of ER-related genes and HER2-related genes, for this reason in clinical specimens they are usually ER-negative, progesterone receptor (PR) negative and lack HER2 overexpression. This is called the triple-negative phenotype(6). Triple-negative tumors typically have a higher histologic grade, elevated mitotic count, scant stromal content, central necrosis, pushing margins of invasion, a stromal lymphocytic response and multiple apoptotic cells(7, 8). Histologically they are largely ductal, but several unusual histologies are also overrepresented, including metaplastic(7, 9, 10), atypical or typical medullary(7, 11), or adenoid cystic carcinomas. Due to the lack of expression of ER, PR or HER2, these tumors do not respond to hormonal therapies or HER2-targeted therapies, and are associated with poor prognosis. Thus, new systemic therapies are desperately needed.

Detailed understanding of the genetic abnormalities that drive subsets of cancer has led to the development of highly specific inhibitors targeting key oncogenic pathways(12). The PI3K (phosphatidylinositol 3 kinase) and the HGF/MET (hepatocyte growth factor/mesenchymal epithelial transition receptor) are two such pathways. The PI3K pathway is mutationally activated in more tumors than any other pathway making it a highly attractive therapeutic target. Indeed, more drugs are in or about to enter clinical trials targeting this

pathway than any other. Studies suggest that overexpression of HGF (MET ligand) and MET contributes to resistance, both inherent and treatment-acquired, to endocrine therapy as well as to trastuzumab treatment. (13, 14) The anti-apoptotic, prosurvival effect of the HGF/MET signaling pathway makes MET inhibition a potential therapeutic target for breast cancers that are resistant and refractory to conventional therapies.(2) Several small molecule MET kinase inhibitors and antibodies against HGF and MET, are in various stages of development as potential cancer therapies. (15-17) Hence, it is pertinent to understand the role of the PI3K and MET signaling pathway in breast cancer.

The PI3K pathway in breast cancer: This pathway plays a key role in cell growth, protein translation, autophagy, metabolism, and cell survival.(18, 19) Thus, tight regulation of the PI3K pathway is paramount to ensure that cellular inputs are integrated for appropriate cellular outcomes. The PI3K pathway is downstream of most growth factor tyrosine kinase receptors (TKR) including MET, EGFR, HER2 and IGFR that have been implicated in breast cancer. Further, the Akt protein kinase is frequently phosphorylated in breast, NSCLC (non small cell lung cancer), endometrial, prostate, colon, gastric, and pancreatic cancers, as well as glioblastoma, reflecting pathway activation. Increased levels of Akt phosphorylation/activation and PTEN loss are predictors of poor outcome in breast cancer and linked to therapy resistance to TKR inhibitors.(20)

The PI3K pathway is mutationally activated in more tumors than any other cellular pathway making it a highly attractive therapeutic target. PI3K signaling is deregulated through a variety of mechanisms, including overexpression or activation of TKR, activating mutations, gene amplification of *PIK3CA* and *AKT* isoforms, as well as loss of key negative regulators including PTEN and INPP4B as well as aberrations in multiple other pathway members. We have demonstrated activating mutations in *PIK3CA*, the gene encoding the p110alpha catalytic subunit of PI3K, in 22% of breast cancers indicating that the PI3K pathway is an important target in this disease.(21) Further, other forms of deregulation and aberrations of this pathway have been implicated not only in breast cancer development and progression,(22) but also in resistance to targeted therapies directed to TKR and hormone receptors.(23-26) As a result, multiple drugs targeting the PI3K pathway are in early clinical trials as mono or combination therapies in breast cancer.(27) Thus, it is critically important to identify mechanisms of resistance to PI3K pathway inhibitors.

Evidence of importance of the HGF/MET axis and resistance to targeted therapies for cancer: The hepatocyte growth factor (HGF) and its receptor, the transmembrane tyrosine kinase MET, promote cell proliferation, survival, motility, and invasion, as well as morphogenic changes that in normal cells stimulate tissue repair and regeneration but are also co-opted during tumor growth.(28-35) MET over-expression, with or without gene amplification, has been reported in a variety of human cancers including breast, lung, and GI malignancies.(36-38) Further, high levels of HGF and/or MET correlate with poor prognosis in several tumor types, including breast, ovarian, cervical, gastric, head and neck, and non-small cell lung cancer (NSCLC).(38-42) Gene amplification and protein over-expression of MET drive resistance to EGFR inhibitors, both in NSCLC cell lines and in patients.(43) The concept that rational combinatorial therapy will be needed for optimal efficacy is supported by the observation that inhibition of either MET or EGFR was insufficient to fully block signaling in gefitinib-resistant cell lines, whereas the combination completely inhibited signaling.(43) A recent phase II randomized clinical trial evaluating Onartuzumab, an antibody to the MET receptor, in combination with erlotinib, in patients with advanced NSCLC showed that Onartuzumab combined with erlotinib improved progression-free survival PFS (hazard ratio (HR), 0.56) and overall survival (HR 0.55) in patients with tumors with high MET expression.

An additional mechanism that causes MET activation of is the presence of activating mutations. Missense germ-line mutations in kinase domain of MET were initially described in patients with hereditary papillary renal carcinoma.(44) Sporadic and germline mutations have been detected in multiple solid tumors. However, only some of these mutant alleles have been proven to cause malignant transformation as a result of constitutive receptor activation posing a potential for therapeutic target.(45) Oncogenic somatic and germline mutations have been found to be predominantly located in the non-kinase domain, mainly in regions encoding the extracellular semaphorin domain (E168D, L229F, S323G, and N375S) and the intracellular juxtamembrane domain (R988C, T1010I, S1058P, and exon-14 deletions).(45) The juxtamembrane domain regulates ligand-dependent MET internalization by Y1003 phosphorylation in response to HGF binding leading to MET ubiquitination and degradation(33). Somatic or germline mutations in the juxtamembrane domains can result in MET accumulation at the cell surface and persistent HGF-stimulation leading to tumorigenesis.(46) Overall, *MET* mutations occur at a lower frequency than other mechanisms of pathway activation, however, they provide strong evidence of the axis oncogenic potential and may identify patients that can either benefit from MET-directed therapies, or those in

which some of these therapies may not be effective.(47) A strong response to therapeutic inhibition with cMET small-molecule inhibitors has been demonstrated in cell line models harboring *MET* oncogenic mutations when these cause increased MET expression, phosphorylation and downstream signaling.(47) A more in-depth description of the frequency and biological implications of cMET aberrations can be found at the introduction of chapter 2 of this document.

Our preliminary analysis of hotspot mutations with Sequenom showed T1010I and Y1253D as the two most common mutations. The Y1253D activating somatic point mutation is located in *MET* exon 19,(48) and was first identified in the lymph node metastasis of head and neck squamous cell carcinoma (HNSCC).(49) It was found to change one of the two tyrosines (Y1252/Y1253) known as the MET receptor major autophosphorylation sites.(50) MET Y1253D has also been shown to couple and activate signaling pathways, which confer a motile-invasive phenotype on cancer cells.(50) The missense MET sequence alteration T1010I, located in exon 14 encoding for the juxtamembrane domain of MET, has been reported in thyroid carcinoma, renal papillary carcinoma, small cell lung cancer, human gastric carcinoma and in a breast cancer biopsy.(44) T1010I has been reported as a germline mutation in colorectal cancer,(51) thyroid cancer,(52) and hereditary renal papillary cancer,(53) however, its capacity to contribute to oncogenesis has been a topic of debate.(54) Schmidt et al. showed that T1010I lacks the ability to transform NH3T3 cells,(55) wherein, Lee and colleagues observed that it was more active than the wild type MET in the athymic nude mice tumorigenesis assay.(53) Considering the significance of the identification of the two major breast cancer hereditary susceptibility genes, *BRCA1* and *BRCA2*, it is pertinent to throw light on the functionality of other germline mutations. Our study aims to evaluate the functional significance of the T1010I aberration in the pathogenesis of breast cancer. A more in-depth description of the frequency of reported copy number alterations and co-alterations in *cMET* and *PIK3CA* can be found at the introduction of chapter 3 of this document.

In some instances aberrations can occur as germline as well as somatic; for example, the germline versus somatic *BRCA1/2* mutations found in Ovarian Cancers. Germline DNA of 28 ovarian cancer patients, harboring a *BRCA1* or *BRCA2* mutation, was analyzed by Hennessey and colleagues.(56) In these, 11 ovarian tumor *BRCA1* (nine of 21; 42.9%) and *BRCA2* (two of seven; 28.6%) mutations could be demonstrated to be somatic due to an inability to detect the aberration in germline DNA, whereas, 17 mutations (60.7%) were found in both tumor and germline DNA.(56) Hence, it is important to determine the nature of the

T1010I aberration in Breast Cancer, and we are currently in the process of sequencing Breast Cancer tumors for the same. Keeping in mind that the recent TCGA (The Cancer Genome Atlas) report on human breast tumors has excluded all the Database SNPs (dbSNPs),(57) and has not reported T1010I, for the purpose of this study we are addressing T1010I as a Single Nucleotide Polymorphism (SNP); rs56391007.(51, 58)

Studies with breast cancer models are just beginning. Ponzio and colleagues have illustrated that MMTV-driven-MET mutant mouse models produce tumors resembling human basal breast cancer.(59) Their study used mice that were transgenic for oncogenic variants of the MET receptor- M1248T, Y1003F/M1248T. They have demonstrated that these Met^{variants} induce mammary tumors with diverse histology, which, based on immunohistochemistry and expression profiling, includes tumors with basal and luminal characteristics. Our study investigates the role of the SNP *MET* T1010I and the somatic *MET* mutation Y1253D in the pathogenesis of Breast Cancer. Further, in collaborative studies, we have demonstrated that MET overexpression was selected in PI3K driven mouse mammary tumors that were resistant to PI3K inhibition.(60) A recent completed trial is assessing the combination of bevacizumab and paclitaxel +/- Onartuzumab in patients with advanced triple receptor-negative breast cancer.(61)

***PIK3CA* and *MET* and response to targeted therapeutics in cancer:** We and others have demonstrated that PI3K pathway aberrations correlate with resistance to receptor targeted therapies.(23-26) As an example, in lung cancer cells, HGF induces EGFR-TKI resistance by activating MET with restoration of downstream MAPK-ERK1/2 and PI3K signaling. (62) Indeed, transient blockade of the PI3K pathway with PI-103 (PI3K inhibitor) and gefitinib overcame HGF-mediated resistance to EGFR-TKIs by inducing apoptosis in EGFR mutant lung cancer cell lines.(62) The effects may be bidirectional, as in collaborative studies we have shown that *MET* amplification can induce resistance to PI3K pathway inhibition in breast cancer murine model systems.(60) Thus, crosstalk between MET and the PI3K pathway may mediate cross resistance to targeted therapies. A more in-depth description of the biological implications of cMET aberrations in the presence of PIK3CA aberrations is presented in the introduction of chapter 4 of this document.

We completed multiplexed mutational analysis of almost 1000 primary untreated breast cancers in 44 different cancer genes including *PIK3CA*. Strikingly, with one exception, the frequency of co-mutations (mutations in more than one of the 44 different cancer genes

assessed) was lower than predicted by chance indicating that most of the mutations assessed are mutually exclusive. However, mutations in both *PIK3CA* and the cell surface receptor MET were present at much greater than expected frequency. We found that 22% of the tumors (218 of 962) harbored *PIK3CA* mutations, and that 4% of the tumors (39 of 962) harbored MET mutations. Remarkably, 16% (34 of 218) of breast cancers with *PIK3CA* mutations exhibited co-mutations in *MET* suggesting concurrent selection of PI3K and MET pathway aberrations. Thus, 4-5% of breast cancer patients (8,000-10,000 new patients a year in the US) are likely to demonstrate concurrent mutations. This analysis was published prior to the recent TCGA publication(57) on human breast tumors. Our findings differ from the TCGA results, possibly due to the elimination of dbSNPs in their report. When PI3K pathway aberrations (*PIK3CA* amplification, *AKT* mutation and amplification, PTEN and INPP4B loss) and MET aberrations (MET protein and RNA overexpression and gene amplification) were assessed, our preliminary analysis indicated that at least 10% of breast cancers (20,000 cases per year) will exhibit concurrent aberrations. Further, our preliminary data suggests that the incidence of PI3K and MET pathway aberrations and particularly concurrent aberrations varies by breast cancer subtype. *MET* amplification or mutation may be selected by PI3K pathway targeted therapy or vice versa. The frequency of *MET* mutations and PI3K pathway aberrations in patients entering trials (i.e., patients with metastatic disease that have PI3K pathway or MET receptor aberrations) is unknown. However, Dr. Funda Meric-Bernstam has provided preliminary data from 420 metastatic breast cancer patients. Using Ion AmpliSeq™ Cancer Panel they have sequenced 46 cancer-related genes for over 900 known cancer mutations and have found that that 26% of the tumors (109 of 420) harbored *PIK3CA* mutations, and that 4% of the tumors (16 of 420) harbored MET mutations. Interestingly, 9% (10 of 109) of breast cancers with *PIK3CA* mutations exhibited co-mutations in *MET*. It is thus critical to ascertain the role of concurrent mutations in *PIK3CA* and *MET* in response to select therapeutics targeting each pathway in breast cancer.

Hypothesis: We hypothesized that concurrent aberrations in *PI3K* and *MET* will render breast cancers resistant to therapies targeting each pathway, and that combination therapy targeting the PI3K and MET pathway will optimize therapy effectiveness by preventing the acquisition of resistance. We have tested this hypothesis through the following specific aims:

Specific Aims:

- To determine MET protein levels and *MET/PIK3CA* copy number elevations in breast cancers-

- By measuring the protein levels of total cMET and p-cMET by breast cancer subtype, and their correlation with patient outcome.
- By measuring the frequency of *MET* and *PIK3CA* copy numbers in breast cancer patients, and their associations with patient outcome.
- To determine the effect of co-mutations/SNPs in *MET* and *MET* overexpression found in breast cancers, on the activity of the two most common breast cancer *PIK3CA* mutations (E545K and H1047R) *in vitro*-
 - a) Using parental (Wild Type), single mutant (*PIK3CA* or *MET*) and co-mutant (*PIK3CA* and *MET*) immortalized **Breast Epithelial Cells** to:
 - Analyze the effects of the aberrations on their cell growth, proliferation, colony formation, cell morphology, anchorage independent proliferation, cell invasion and cell signaling.
 - Analyze their sensitivity to selective PI3K pathway inhibitors (alone), MET receptor inhibitors (alone), and their combination.
 - b) Using parental (Wild Type), single mutant (*PIK3CA* or *MET*) and co-mutant (*PIK3CA* and *MET*) immortalized **Breast Cancer Cells** to:
 - Analyze the effects of the aberrations on their cell growth, proliferation, colony formation, cell morphology, anchorage independent proliferation, cell invasion and cell signaling.
 - Analyze their sensitivity to selective PI3K pathway inhibitors (alone), MET receptor inhibitors (alone), and their combination.

Based on the proposed specific aims, in the next three chapters there will be more in-depth introduction reviewing 1. The frequency and biological implications of cMET aberrations. 2. The frequency of reported copy number alterations and co-alterations in *cMET* and *PIK3CA*. 3. A more in-depth description of the biological implications of cMET aberrations in the presence of *PIK3CA* aberrations is presented in the introduction of chapter 4 of this document

CHAPTER 2: cMET AND PHOSPHO-cMET PROTEIN LEVELS IN BREAST CANCERS AND SURVIVAL OUTCOMES

INTRODUCTION

The HGF-cMET Axis: The c-MET proto-oncogene is located on chromosome 7q21. The protein product of this gene is a cell surface receptor tyrosine kinase (RTK) that is expressed in the epithelial cells of many organs, including the liver, pancreas, prostate, kidney etc, during both embryogenesis and adulthood. The established form of the cMET receptor is a disulfide-linked heterodimer composed of an extracellular α -chain and a transmembrane β -chain (Figure 1), that results from the proteolytic cleavage of a precursor protein. The β -chain has an extracellular domain, a transmembrane domain and a cytoplasmic portion, wherein the cytoplasmic portion contains juxtamembrane and tyrosine kinase (TK) domains, and a carboxy-terminal tail essential for substrate docking and downstream signaling.(63)

Hepatocyte growth factor (HGF) or scatter factor (SF) acts as a ligand for the cMET receptor. The active form of HGF is made of an amino-terminal domain (N), four Kringle domains (K1 to K4), and a serine protease homology domain (SPH)(64) where the N-K1 portion mediates receptor binding by engaging two cMET molecules, leading to receptor dimerization.(65) Additional contacts with cMET may be provided by the residues within the SPH domain. (64)

Active HGF binds to functionally established cMET resulting in receptor dimerization/multimerization, phosphorylation of multiple tyrosine residues in the intracellular region, catalytic activation, and downstream signaling through docking of a number of substrates transducing multiple biological activities as motility, proliferation, survival, and morphogenesis.(66, 67) (Figure 1)

Kinase activity of the receptor is regulated by HGF binding, which induces cMET autophosphorylation on the tyrosine residues Y1234 and Y1235 at the TK domain. This in turn forms a multifunctional docking site that recruits intracellular adapters through Src homology-2 domains and other motifs, and activates downstream signaling.(66, 68) The main substrates and adapter proteins in this axis are signal transducer and activator of transcription 3 (STAT3), growth factor receptor-bound protein 2 (Grb2), Gab1, phosphatidylinositol 3-kinase (PI3K), phospholipase C- γ , Shc, Src, Shp2, Ship1. Gab1 and Grb2 are critical effectors that interact directly with the receptor. They recruit a network of adaptor proteins that are involved in

signaling and multiple biological effects induced by the activated axis. In order for cMET to achieve its maximal activity in promoting invasive cell growth (Figure 1), it is pertinent to maintain the integrity of the entire signal transduction machinery.(66, 68) Through the renin-angiotensin system/mitogen-activated protein kinase (RAS/MAPK) signaling pathway or the recruitment of the focal adhesion kinase (FAK)/paxillin complex, the HGF-mediated activation of cMET leads to the activation of downstream effectors involved in epithelial-mesenchymal transition (EMT).(69, 70)

The HGF-cMET pathway is modulated by other proteins including $\alpha 6\beta 4$ -integrin, which works as a signaling platform that potentiates HGF-triggered activation of RAS and PI3K,(71) plexin B1, which transactivates cMET in response to semaphorin stimulation (72) and the death receptor Fas, which can associate with cMET preventing Fas-ligand binding and inhibiting Fas-induced apoptosis.(73) In addition, HGF-mediated cMET effects may be potentiated by the activation of other RTKs. EGFR plays a significant role in enhancing HGF-cMET-mediated proliferation and invasion of epithelial cells (74), and cMET can synergize with HER2 to promote a malignant phenotype.(75). cMET and the IGF1 receptor work together to induce migration and invasion of pancreatic cancer cells.(76) In summary, a complex system of interactions modulates and governs the magnitude and duration of cMET signaling in the cell.

The HGF-cMET Axis and Cancer: Under normal conditions, HGF-induced cMET-TK activation is tightly regulated by ligand activation at the cell surface, ligand-activated receptor internalization/degradation, and paracrine ligand delivery. However, pathway deregulation occurs in multiple neoplasms. Persistent ligand stimulation can lead to protein overexpression as HGF upregulates various genes including *cMET*, and the encoding proteases that are required for HGF and cMET metabolism.(66) Other mechanisms of oncogenic pathway activation include aberrant paracrine or autocrine ligand production, constitutive kinase activation in the presence or absence of *cMET* gene amplification, and *cMET* gene mutations.(77, 78)

Several studies have characterized the effects of sustained cMET activation through preclinical models. Through direct involvement of angiogenic pathways *in-vivo* studies have shown that activation of HGF-cMET signaling promotes cell invasiveness and triggers metastases.(79) The oncogenic TPR-MET fusion protein is constitutively active and in animal models its transgenic expression leads to the development of malignancies.(46) In human gastric cancer this rearrangement has been detected in both precursor lesions and in the

adjacent normal mucosa indicating predisposition to develop gastric cancers.(80) Studies have shown that a number of cultured cancer cell lines, from NSCLCs and gastric carcinomas, exhibiting *cMET* gene amplification are dependent on *cMET* for growth and survival, and *cMET* inhibition results in both, decreased proliferation and cell death.(43, 77)

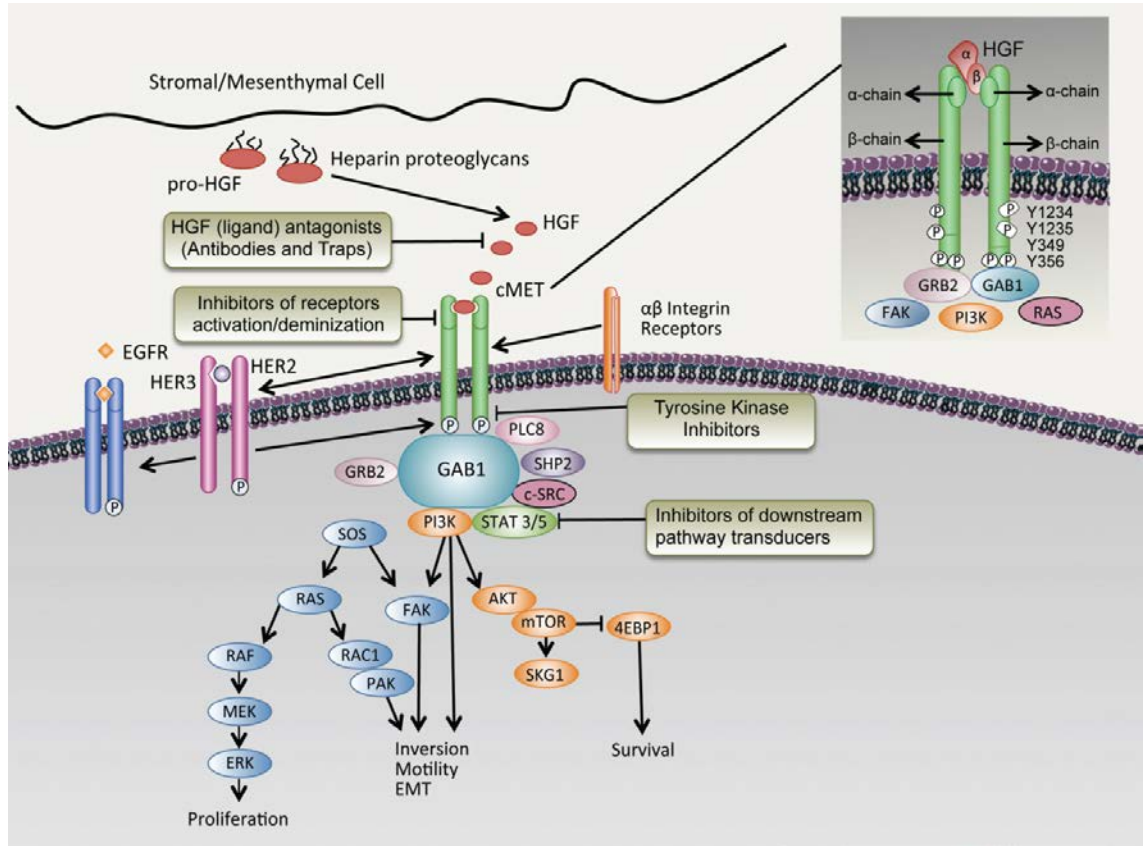


Figure 1 The hepatocyte growth factor HGF-cMET axis signaling network and ongoing targeted therapy strategies.

The pathway, which transduces invasive growth signals from mesenchymal to epithelial cells (secreted by mesenchymal cells), is activated by HGFA and binds to the *cMET* receptor on epithelial cells. *cMET* kinase activation results in *trans*-autophosphorylation and binding of adaptor proteins, forming scaffolds for recruitment and activation of signaling proteins. Signals generated from these structures lead to activation of signaling pathways related to increased proliferation, survival, motility, invasiveness, and stimulation of angiogenesis. EGFR, epidermal growth factor receptor; FAK, focal adhesion kinase; GRB2, growth factor receptor-bound protein 2; HER, human epidermal growth factor receptor; mTOR, mammalian target of rapamycin; PI3K, phosphatidylinositol 3-kinase; RAS, renin-angiotensin system; STAT, signal transducer and activator of transcription.(47)

Reprinted with permission. © (2012) American Society of Clinical Oncology. All rights reserved.

In the absence of gene aberrations, protein overexpression due to transcriptional upregulation is the most frequent cause of constitutive *cMET* activation in human cancers. A variety of epithelial tumors have been found to display elevated levels of *cMET* expression.(81) Multiple studies have been conducted to examine expression/overexpression

of cMET in primary cancers. cMET has been shown to be overexpressed in neoplastic tissue compared to normal surrounding tissue, and the extent of expression correlates with disease extension and outcome in several tumor types.(82-84) Strong cMET expression and p-cMET expression has been observed in up to 60% and 40-100% of NSCLC cases, respectively,(85) depending on the specific lung cancer tissue assessed.(82, 85-87) Over 80%of cases have been observed with cMET overexpression in malignant renal cell carcinoma and pleural mesothelioma.(88) cMET overexpression has also been reported in breast,(89) and seems to be associated with advanced disease stage and poor outcome in NSCLC, colon, breast and ovarian cancer.(84, 87, 90, 91)

Protein overexpression and constitutive activation of the kinase domain is a result of *cMET* gene amplification,(77) and has been observed in both, primary tumors or as a secondary event affecting therapy sensitivity in cancer cells.(43, 92) Additionally, several studies have shown that increased *cMET* copy number is an independent negative prognostic factor in surgically resected NSCLC (93) or is associated with advanced stage and liver metastases in colorectal cancer. (90)

The presence of activating mutations too causes cMET activation. Hereditary papillary renal carcinoma patients are observed with missense germ-line mutations in the TK domain.,(94) Sporadic mutations are more prevalent and can involve the TK, juxtamembrane or sema domains. However, only some of these mutant alleles have been proven to be the cause of constitutive receptor activation resulting in malignant.(85) Oncogenic mutations have been found to be predominantly located in the non-kinase domain, mainly in regions encoding the extracellular semaphorin domain (E168D, L229F, S323G, and N375S) and the intracellular juxtamembrane domain (R988C, T1010I, S1058P, and exon-14 deletions) of NSCLC cell lines, in 12.5% of SCLC cases, as well as in 8% of samples of lung human adenocarcinomas.(85, 95) cMET internalization is regulated by phosphorylation of Y1003 in the juxtamembrane domain, in response to HGF binding, leading to cMET ubiquitination and degradation. (46) Exon-14 deletion leads to the loss of Y1003 followed by cMET accumulation at the cell surface and persistent HGF-stimulation leading to tumorigenesis.(46) Though *cMET* mutations occur at a lower frequency compared to other mechanisms of pathway activation, they provide strong evidence of the axis oncogenic potential. This in turn could help screen patients that can benefit from cMET-directed therapies.

cMET oncogenic mutations lead to elevated phosphorylated cMET and downstream signaling, and cell line models harboring these mutations respond strongly to small-molecule inhibitors against cMET.(85, 96) The presence of *cMET* mutations in lymph nodes and metastatic sites could suggest the selection of these mutated cells during metastatic progression.(49) The presence of *cMET* activation mutations and prognosis has not been explored extensively as yet.

The HGF/cMET axis plays a key role in tumor progression in breast cancers. Clarifying the prognostic implication and differential impact of cMET expression on survival in breast cancer subtypes is a necessary first step to application of targeted therapy against cMET in breast cancers. We found that high levels of cMET and p-cMET were seen in all breast cancer subtypes and correlated with poor prognosis. Inhibition of the cMET axis is a promising new therapeutic strategy and needs further investigation. We performed an analysis of primary breast cancer specimens to evaluate the protein levels of total cMET and p-cMET by breast cancer subtype using reverse phase protein arrays (RPPA), and their correlation with patient outcome.

MATERIALS AND METHODS

Patients and tumor samples: Fine needle aspirates from 257 primary invasive breast cancers were obtained and snap frozen. All specimens were collected under Institutional Review Board (IRB)-approved protocols. The breast tumors were classified into three clinically relevant subtypes defined by immunohistochemistry (IHC) for estrogen receptor (ER) and progesterone receptor (PR) status and by IHC or fluorescent in situ hybridization (FISH) for HER2 status as per American Society of Clinical Oncology and College of American Pathologists (ASCO/CAP) guidelines (97, 98). These subtypes were defined by the dominant traditional prognostic molecular marker (ER, PR and HER2). Hormone receptor-positive (HR-positive) tumors were ER-positive and/or PR-positive and HER2-negative. Similarly, HER2-positive group included all HER2 positive tumors irrespective of hormone receptor status. Triple negative subtype included all cases that were ER/PR and HER2 negative.

The samples used for the study were archived samples from previously collected tumor specimens from patient treated at MD Anderson Cancer Center between 1986 and 2007. The corresponding clinical data was obtained from the Breast Cancer Management System database at MD Anderson Cancer Center. Missing information from the database was collected by chart review.

Reverse phase protein lysate microarray (RPPA): Protein was extracted from the human tumors and RPPA was performed in our laboratory as described previously (99). Briefly, lysis buffer was used to lyse frozen tumors by homogenization. Tumor lysates were normalized to 1 $\mu\text{g}/\mu\text{L}$ concentration using bicinchoninic acid assay and boiled with 1% SDS, and the supernatants were manually diluted in six or eight 2-

fold serial dilutions with lysis buffer. An Aushon Biosystems (Burlington, MA) 2470 arrayer created 1,056 sample arrays on nitrocellulose-coated FAST slides (Schleicher & Schuell BioScience, Inc.) from the serial dilutions. A slide was then probed with validated primary cMET and p-cMET antibodies (Cell Signaling Technology, Danvers, MA) and the signal was amplified using a DakoCytomation–catalyzed system. The antibodies for cMET (Mouse) and p-cMET (Rabbit, Y1235) were used at a dilution of 1:250 for RPPA. A secondary antibody was used as a starting point for amplification. The slides were scanned, analyzed, and quantitated using Microvigene software (VigeneTech Inc.) to generate serial dilution–signal intensity curves for each sample with the logistic fit model: $\ln(y) = a + (b - a) / (1 + \exp(c * (d - \ln(x))))$. A representative natural logarithmic value of each sample curve on the slide (curve average) was then used as a relative quantification of the amount of each protein in each sample. The level of cMET and p-cMET in each sample was expressed as a log mean centered value after correction for protein loading using the average expression levels of over 150 proteins as previously described (99). Refer to appendix 1 for antibody validation method.

Statistical Methods: Boxplots were generated for original and log₂ transformed expressions of total cMET and p-cMET by breast cancer subtypes. The original expressions were right-skewed but the log₂ transformation data was normally distributed. Hence, all following statistical analyses were based on the log₂ transformation of the original expression values. P values less than 0.05 were considered statistically significant and all tests were two-sided. Statistical analyses were done with R statistical software version 2.12.0 (R Development Core Team, 2010, Vienna, Austria).

Mean and standard deviations were generated for total cMET and p-cMET by tumor subtypes. Linear regression models were used to determine if the mean total cMET and p-cMET expression was different by tumor subtypes. Martingale residual plots with lowess smooth for Cox's model for total cMET and p-cMET separately as covariate by tumor subtypes suggested a non-linear effect of total and p-cMET. A regression tree method was applied to find the best cutoff point for total cMET and p-cMET expression. Combining the results from martingale residual plots and regression trees, total cMET expression was divided into high level (>0) expression and low level (≤0) expression. Similarly, p-cMET was divided as high level (>0.35) and low level (≤0.35). Patient and tumor characteristics including age, stage, grade and subtype were tabulated between high and low level expressions of total cMET and p-cMET individually. Groups were then compared with the Chi-square tests (100).

Overall survival (OS) and corresponding censoring were computed in months from diagnosis to death for each patient. Relapse-free survival (RFS) was regarded as the time to first relapse after diagnosis. Median RFS and OS were estimated nonparametrically with the use of Kaplan-Meier curves by patient characteristics and levels of total cMET and p-cMET expression and compared by the log-rank statistic. Log-rank tests were used to evaluate the hazard ratio by total cMET and p-cMET expression levels among all patients and patients within each subtype. Cox proportional hazards models were fit to determine the association of cMET and p-cMET levels with the risk of recurrence and death after adjustment for other patient and disease characteristics.

Reprinted with permission. © (2012) American Association for Cancer Research. All rights reserved.

RESULTS

Median patient age was 51 years (range 23-85 years). There were a total of 140 (54.5%) hormone receptor (HR)-positive tumors, 53 (20.6%) HER2-positive tumors and 64 (24.9%) triple receptor-negative (TN) tumors. Using the selected cutoffs, a total of 181 (70.4%) and 123 (47.9%) patients had high expression of cMET and p-cMET, respectively.

Patient and clinic characteristics by levels of total cMET and p-cMET are summarized in table 1. There was no statistically significant difference in clinical or pathologic parameters in patients with high or low level of total cMET. Patients with high p-cMET expression tended to be older (Age > 50: 60.2% vs. 41.0%, $P = .003$) and had fewer high grade tumors (Grade III: 60% vs. 72.2% $P = .046$).

No significant differences in mean levels of total cMET expressions ($P = 0.128$) and p-cMET expressions ($P = 0.088$) were seen between different tumor subtypes, as seen in table 2. At a median follow up of 42.23 months (5.17-277.77 months), there were 76 (30%) relapses and 50 (20%) deaths.

	Overall (<i>N</i> = 257) <i>N</i> (%)	cMET		<i>P</i>	p-cMET		<i>P</i>
		High cMET (>0; <i>N</i> = 181) <i>N</i> (%)	Low cMET (≤0; <i>N</i> = 76) <i>N</i> (%)		High p-cMET (>0.35; <i>N</i> = 123) <i>N</i> (%)	Low p-cMET (≤0.35; <i>N</i> = 134) <i>N</i> (%)	
Age							
≤50	128 (49.8)	83 (45.9)	45 (59.2)	0.069	49 (39.8)	79 (59.0)	0.003
>50	129 (50.2)	98 (54.1)	31 (40.8)		74 (60.2)	55 (41.0)	
Stage							
I	8 (3.1)	4 (2.2)	4 (5.3)	0.426	2 (1.6)	6 (4.5)	0.391
II	141 (55.3)	43 (56.4)	40 (52.6)		67 (54.9)	74 (55.6)	
III	106 (41.6)	39 (41.3)	32 (42.1)		53 (43.4)	53 (39.8)	
Grade							
1	12 (4.7)	9 (5.1)	3 (4.0)	0.473	9 (7.5)	3 (2.3)	0.046
2	73 (28.9)	55 (30.9)	18 (24.0)		39 (32.5)	34 (25.6)	
3	168 (66.4)	114 (64.0)	54 (72.0)		72 (60.0)	96 (72.2)	
Chemotherapy							
Anthracycline based	17 (6.7)	11 (6.2)	6 (7.9)	0.228	10 (8.3)	7 (5.3)	0.214
Taxane based	21 (8.3)	16 (16.9)	5 (6.6)		10 (8.3)	11 (8.3)	
Anthracycline & Taxane	180 (70.9)	121 (68.1)	59 (77.6)		79 (65.3)	101 (75.9)	
No chemotherapy	36 (14.1)	30 (16.8)	6 (7.9)		22 (18.2)	14 (10.5)	
Hormone therapy							
Yes	107 (40.5)	70 (38.7)	37 (48.7)	0.178	59 (48.0)	48 (35.8)	0.065
No	150 (59.5)	111 (61.3)	39 (51.3)		64 (52.0)	86 (64.2)	
Radiation therapy							
Yes	164 (63.8)	108 (59.7)	56 (73.7)	0.046	79 (64.2)	85 (63.4)	0.998
No	93 (36.2)	73 (40.3)	20 (26.3)		44 (35.8)	49 (36.6)	
Subtype							
HER2 positive	53 (20.6)	40 (22.1)	13 (17.1)	0.079	25 (20.3)	28 (20.9)	0.064
HR positive	140 (54.5)	103 (56.9)	37 (48.7)		75 (61.0)	65 (48.5)	
Triple negative	64 (24.9)	38 (31.0)	26 (34.2)		23 (18.7)	41 (30.6)	

Abbreviations: cMET, total cMET; p-cMET, phospho-cMET; HR-positive, hormone receptor positive.

Table 1 Patient and clinical characteristics by total cMET and phospho-cMET (1)
Reprinted with permission. © (2012) American Association for Cancer Research. All rights reserved.

Subtype	N	Total cMET			Phospho-cMET		
		Mean	SD	F-test P value	Mean	SD	F-test P value
HER2 positive	53	0.355	0.0799		0.180	0.1027	
Hormone receptor positive	140	0.391	0.0541	0.128	0.257	0.0651	0.088
Triple receptor negative	64	0.192	0.0904		0.001	0.0990	

Table 2. Total cMET and phospho-cMET expressions by tumor subtype (1)

Reprinted with permission. © (2012) American Association for Cancer Research. All rights reserved.

Table 3 summarizes the median RFS estimates by c-MET and p-cMET expression and by tumor subtypes. Dichotomized total cMET expression (cutoff point 0) was a significant prognostic factor for RFS (HR: 2.44, 95% CI: 1.34-4.44, P = 0.003). Estimated 5-year RFS rates were 61.3% (95% CI: 53.2%-70.7%) and 78.9% (95% CI: 68.6%-90.8%) for patients with high cMET and low cMET level, respectively (P = 0.003). Likewise, dichotomized p-cMET expression (cutoff point 0.35) was also a significant prognostic factor for RFS (HR: 1.64, 95% CI: 1.04-2.60, P = 0.033) and estimated 5-year RFS rates for patients with high p-cMET and low p-cMET levels were 58.9% (95% CI: 49.1%-70.7%) and 73.8% (95% CI: 65.6%-83.1%), respectively (P = 0.033). Total cMET was also a significant predictor of RFS within the HR-positive subtype (HR: 3.44, 95% CI: 1.21-9.81, P = 0.014). In contrast, p-cMET was a significant predictor of RFS within the HER2-positive subtype (HR: 3.02, 95% CI: 1.15-7.96, P = 0.019). The Kaplan-Meier survival curves for RFS for all patients and by breast tumor subtypes are as shown in figure 2. Although, there was a trend towards worse RFS with high cMET levels (HR 2.36; 95% CI: 0.86-6.51) in triple-negative subtype, this did not reach statistical significance (P = 0.086).

Tumor subtypes	Protein level	Patients	RFS				OS				
			Events	5-year RFS (%)	95% CI	P	Events	5-year OS (%)	95% CI	P	
Overall	cMET	High	181	63	61.3	53.2-70.7	0.003	43	72.4	64.7-81.0	0.003
		Low	76	13	78.9	68.6-90.8		7	93.3	87.8-99.2	
	p-cMET	High	123	45	58.9	49.1-70.7	0.033	32	72.4	63.7-82.3	0.025
		Low	134	31	73.8	65.6-83.1		18	85.8	79.4-92.7	
Hormone receptor positive	cMET	High	103	31	65.4	54.7-78.2	0.014	17	82.8	75.0-91.3	0.006
		Low	37	4	85.3	78.2-100		1	100	NA-NA	
	p-cMET	High	75	21	67.6	55.6-82.2	0.519	11	85.2	77.0-94.2	0.519
		Low	65	14	75.1	63.3-89.2		7	90.4	82.6-99.0	
HER2 positive	cMET	High	40	17	55.5	40.8-75.4	0.530	13	59.4	41.4-85.2	0.138
		Low	13	4	0.00	NA-NA		1	100	NA-NA	
	p-cMET	High	25	15	36.5	19.5-68.3	0.019	12	52.3	33.3-82.2	0.014
		Low	28	6	74.1	57.4-95.5		2	91.7	81.3-100	
Triple receptor negative	cMET	High	38	15	59.5	45.5-77.7	0.086	13	56.1	38.0-82.7	0.187
		Low	26	5	80.4	66.4-97.4		5	66.2	66.2-97.4	
	p-cMET	High	23	9	60.9	43.9-84.5	0.251	9	58.8	41.1-84.1	0.128
		Low	41	11	72.3	59.6-87.7		9	74.2	60.5-91.0	

Abbreviations: CI, confidence interval; cMET, total cMET; p-cMET, phospho-cMET.

Table 3. RFS and OS by total cMET and phospho-cMET levels and breast cancer subtype

RFS and OS by total cMET and phospho-cMET levels and breast cancer subtype (1)

Reprinted with permission. © (2012) American Association for Cancer Research. All rights reserved.

Table 3 summarizes the median OS estimates by c-MET and p-cMET expression and by tumor subtypes. At the time of analysis, 207 of the 257 patients (80.5%) were still alive. As was seen with RFS analysis, dichotomized cMET level was

a significant prognostic factor of OS (HR: 3.18, 95% CI: 1.43-7.11, $P = 0.003$). Estimated 5-year OS rates were 72.4% (95% CI: 64.7%-81.0%) and 93.3% (95% CI: 87.8%-99.2%) for patients with high cMET and low cMET levels, respectively ($P = 0.003$). Dichotomized p-cMET level was a significant prognostic factor of OS (HR: 1.92, 95% CI: 1.08-3.44, $P = 0.025$). The estimated 5-year OS rates for patients with high p-cMET and low p-cMET levels were 72.4% (95% CI: 63.7%-82.3%) and 85.8% (95% CI: 79.4%-92.7%), respectively ($P = 0.025$). With regards to breast cancer subtypes, total cMET (HR: 8.28, 95% CI: 1.10-62.59, $P = 0.006$) and p-cMET (HR: 5.49, 95% CI: 1.20-25.10, $P = 0.014$) were significant predictor of OS within HR-positive tumors and HER2-positive tumors, respectively. The Kaplan-Meier survival curves for OS for all patients and by subtypes are as shown in figure 3. Although, there was a trend towards worse OS with high p-cMET levels (HR 2.02; 95% CI: 0.80-5.13) in triple-negative subtype, this did not reach statistical significance ($P = 0.128$).

Multivariable models for RFS and OS are summarized on table 4. After adjustment for patient factors, tumor characteristics and treatment, patients with tumors expressing high levels of cMET had a significant higher risk of recurrence (HR 2.06; 95% CI: 1.08-3.94; $P = 0.028$) and death (HR 2.81; 95% CI: 1.19-6.64; $P = 0.019$) compared to patients with low cMET levels. Also, patients with tumors expressing high levels of p-cMET had a significant higher risk of recurrence (HR 1.79; 95% C: 1.08-2.95; $P = 0.020$) compared to patients with high p-cMET levels.

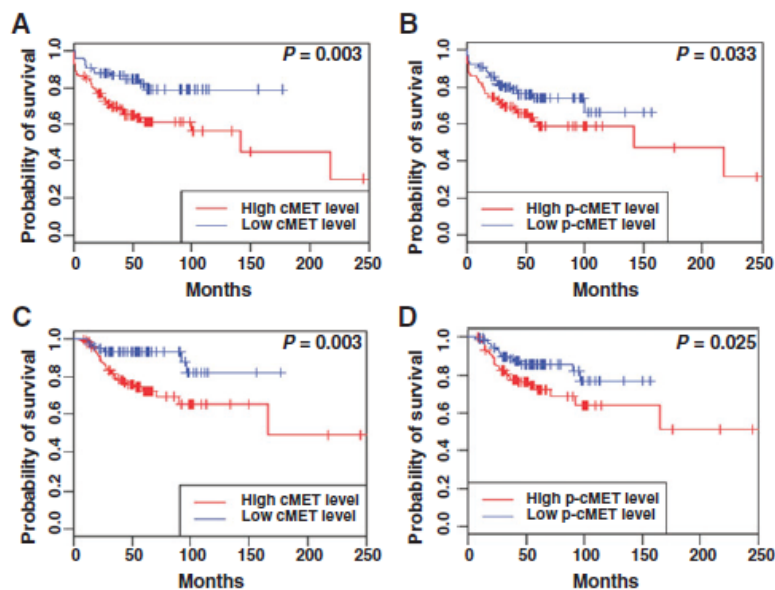


Figure 2. Kaplan-Meier estimates illustrating the RFS of patients

Kaplan-Meier estimates illustrating the RFS of patients by (A) total cMET and (B) p-cMET expression levels and OS of patients by (C) total cMET and (D) p-cMET expression levels. High: total cMET > 0, Low: total cMET ≤ 0. High: p-cMET > 0.35, Low: p-cMET ≤ 0.35(1) Reprinted with permission. © (2012) American Association for Cancer Research. All rights reserved.

To evaluate whether cMET confers radio-resistance, we performed an exploratory sub-group analysis among 164 patients who received radiation therapy. Dichotomized total cMET level was a significant prognostic factor for both RFS (HR 3.37; 95% CI: 1.50-7.57, $P = 0.002$) and OS (HR 4.03; 95% CI: 1.39-11.67, $P = 0.006$) for patients who received radiation therapy. Similarly, dichotomized p-cMET was a significant prognostic factor for RFS (HR 2.07; 95% CI: 1.12-3.84, $P = 0.017$) and OS

(HR 2.25; 95% CI: 1.05-4.85, P = 0.033) in this group. In contrast, among 93 patients who did not receive radiation therapy, total cMET and p-cMET were not significant prognostic factors for either RFS or OS.

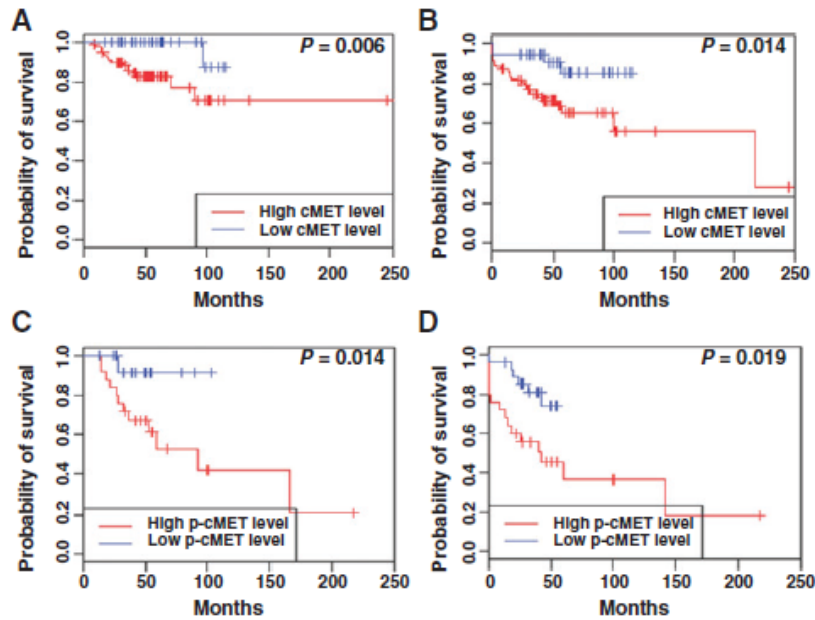


Figure 3. Kaplan-Meier estimates illustrating (A) OS and (B) RFS

Kaplan-Meier estimates illustrating (A) OS and (B) RFS of patients by total cMET in hormone receptor positive breast cancer. Kaplan-Meier estimates illustrating (C) OS and (D) RFS of patients by p-cMET in HER2 positive breast cancer. High: total cMET>0, Low: total cMET<=0. High: p-cMET> 0.35, Low: p-cMET<=0.35(1).

Reprinted with permission. © (2012) American Association for Cancer Research. All rights reserved.

Model	cMET				Model	p-cMET			
	RFS		OS			RFS		OS	
	HR (95% CI)	P	HR (95% CI)	P		HR (95% CI)	P	HR (95% CI)	P
cMET: High vs. low	2.06 (1.08-3.94)	0.028	2.81 (1.19-6.64)	0.019	p-cMET: High vs. low	1.79 (1.08-2.95)	0.020	1.84 (0.97-3.48)	0.062
Subtype:	1.03 (0.54-1.98)	0.925	1.24 (0.53-2.90)	0.621	Subtype:	1.00 (0.52-1.92)	0.999	1.11 (0.48-2.60)	0.803
HER2+ vs. HR+					HER2+ vs. HR+				
Subtype:	0.65 (0.34-1.25)	0.201	2.00 (0.87-4.58)	0.103	Subtype:	0.59 (0.31-1.14)	0.115	1.62 (0.71-3.73)	0.249
TN vs. HR+					TN vs. HR+				
Age: >50 vs. ≤50	0.79 (0.48-1.28)	0.339	0.97 (0.53-1.77)	0.924	Age: >50 vs. ≤50	0.83 (0.51-1.34)	0.441	1.06 (0.58-1.93)	0.848
Chemotherapy:	0.06 (0.01-0.25)	0.0001	0.20 (0.03-1.07)	0.061	Chemotherapy:	0.05 (0.01-0.23)	0.0001	0.15 (0.03-0.78)	0.024
A vs. N					A vs. N				
Chemotherapy:	0.13 (0.05-0.33)	<0.0001	0.26 (0.08-0.82)	0.025	Chemotherapy:	0.13 (0.53-0.34)	<0.0001	0.28 (0.08-0.89)	0.032
T vs. N					T vs. N				
Chemotherapy:	0.10 (0.05-0.18)	<0.0001	0.28 (0.13-0.63)	0.002	Chemotherapy:	0.10 (0.56-0.19)	<0.0001	0.26 (0.13-0.54)	0.0003
B vs. N					B vs. N				
Hormonal therapy:	0.21 (0.10-0.43)	0.0001	0.31 (0.11-0.84)	0.022	Hormonal therapy:	0.16 (0.08-0.33)	<0.0001	0.23 (0.08-0.63)	0.004
Y vs. N					Y vs. N				
Radiation therapy:	0.91 (0.53-1.56)	0.740	0.80 (0.41-1.57)	0.523	Radiation therapy:	0.84 (0.49-1.45)	0.528	0.81 (0.41-1.59)	0.545
Y vs. N					Y vs. N				
Grade: I, II vs. III	0.84 (0.48-1.50)	0.419	0.72 (0.33-1.53)	0.390	Grade: I, II vs. III	0.94 (0.52-1.67)	0.819	0.77 (0.36-1.68)	0.514
Clinical stage:	0.37 (0.22-0.62)	0.0002	0.67 (0.33-1.34)	0.243	Clinical stage: I,	0.40 (0.24-0.69)	0.0009	0.77 (0.38-1.55)	0.458
I, II vs. III					II vs. III				

Abbreviations: cMET, total cMET; p-cMET, phospho-cMET; HR+, hormone receptor positive; TN, triple negative; A, anthracycline based; B, both anthracycline and taxane; T, taxane based.

Table 4. Multivariable Cox proportional hazards model

Multivariable Cox proportional hazards model for RFS and OS relative to total cMET and phosphor-cMET expression(1) American Association for Cancer Research owns the copyright for this content, and has granted us the permission to reuse this material. Reprinted with permission. © (2012) American Association for Cancer Research. All rights reserved.

DISCUSSION

The protein product of the cMET proto-oncogene is a cell surface RTK that binds with high affinity to HGF/SF (101). The receptor ligand interaction results in receptor homodimerization and phosphorylation of tyrosine residues, which in turn activates downstream effectors such as PI3K/AKT, PLC γ (Phospholipase C γ), RAS-MAPK, c-Src, and STATs(102, 103). Strong evidence supports that a cascade of the above events contributes to carcinogenesis and angiogenesis, in a wide variety of human malignancies (102).

We analyzed 257 breast cancer samples, and used RPPA to show that increased levels of total cMET and p-cMET are observed in approximately 70% and 50% of breast cancers, respectively. We have also shown that the levels of total cMET and p-cMET do not significantly differ among different breast cancer subtypes. Survival analysis reveals that total cMET and p-cMET levels are significant prognostic factors for both RFS and OS. When survival outcomes were analyzed among various tumor subtypes, it was observed that elevated levels of cMET and p-cMET were poor prognostic factors for hormone receptor-positive and HER2-positive breast cancers, respectively.

cMET expression has been correlated with progression, aggressive behavior, and poor survival outcomes in breast cancers (42, 91, 104, 105). However, to the best of our knowledge, this is the first study to investigate the significance of differential expression of cMET and p-cMET in different breast cancer subtypes (HR positive, HER2-positive, and TNBC). We are also the first to report p-cMET levels as a prognostic factor in breast cancer. Additionally, we evaluated cMET expression using RPPA, wherein, previous investigators used ELISA, Immunoperoxidase, IHC, and Immunofluorescence techniques to study this receptor. Recent data from our laboratory has shown significant correlations between RPPA and IHC in snap-frozen primary breast tumors and has established reliability of RPPA in functional proteomic "fingerprinting". RPPA is more sensitive when compared to IHC or ELISA as it reduces variability, and avoids observer dependency (106). RPPA analysis of molecular targets can be developed as a clinical application. It allows for a cost-effective, quick, precise, reliable, and reproducible quantification of phosphorylated/non-phosphorylated proteins in multiple samples, simultaneously, with the help of limited clinical material (107, 108).

Several reports suggest that high levels of HGF and cMET expression correlate with poor prognosis in breast cancer. HGF/cMET activation imparts multiple phenotypic properties to tumor cells resulting in the above mentioned clinical outcomes. HGF/cMET signaling enhances the transition from pre-invasive DCIS to invasive carcinoma (37), and promotes cell motility and angiogenesis (109, 110). Bone metastasis in breast cancers is established by HGF-dependent β -catenin stabilization (111). Synergy between HER2 and HGF/cMET signaling promotes the breakdown of cell-cell junctions and enhances cell invasiveness (112). It is possible that the cross-talk results in the poor prognosis observed in HER2-positive breast cancers with increased p-cMET (RFS: P= 0.019 and OS: P=0.014).

Therapy resistance is one of the major obstacles cropping-up in breast cancer treatment. In vitro studies have reported that the HGF/cMET signaling pathway can confer resistance against induction of apoptosis by various DNA damaging agents (radiation and cytotoxic agents such as anthracyclines and taxanes) (113). Additionally, the HGF/cMET signaling pathway also promotes cell survival by enhancing DNA repair (114). It has also been suggested that resistance, both inherent and treatment acquired, to endocrine and trastuzumab therapy could be a consequence of HGF and cMET overexpression (13, 14). Radiotherapy, anthracyclines, taxanes, endocrine therapy, and trastuzumab form the backbone of breast cancer therapy. MET inhibition, owing to the antiapoptotic and prosurvival effect of the HGF/cMET pathway, is emerging as a potential therapeutic target for breast cancers that are resistant to conventional therapies. cMET plays a pivotal role in the acquisition of resistance to treatment, therefore, combining MET inhibitors as first-line therapy with traditional treatments could benefit a subset of breast cancers.

MET expression has been reported to confer radioresistance in cancer cells (115). De Bacco and colleagues reported that human breast cancer cell lines (MDA-MB-231 and MDA-MB-435S) subjected to therapeutic doses of ionizing radiation showed increased MET expression, ligand independent MET phosphorylation/signal transduction, and promoted cell invasion and survival (115). Furthermore, these effects were counteracted by using siRNA against MET and by using kinase inhibitors. In oropharyngeal squamous cell carcinomas treated with radiotherapy, cMET expression correlates with a decrease in the rates of complete remission, shorter disease-free survival, and OS (115). This data suggests that targeting MET may increase the radiosensitivity of tumor cells and could prove to be an attractive target for radiosensitization.

Preclinical data suggests that cMET inhibition in tumor cells impairs cell proliferation, survival, motility, invasion, and angiogenesis (116, 117). Antibodies against HGF and against cMET and small molecule cMET kinase inhibitors are in various stages of development against cancer (15-17). Targeted therapy for breast cancers with preselection based on overexpression of cMET and p-cMET with MET inhibition needs further exploration after adequate optimization of predictive markers.

Our study indicates that total cMET and p-cMET levels are uniformly elevated irrespective of the breast cancer subtype, and are significant prognostic factors for RFS and OS. However, the predictive potential of cMET should be assessed in the clinical trials of cMET targeted therapy, as a retrospective analysis does not allow reliable assessment. cMET inhibition has immense potential to improve breast cancer treatment, and deserves further assessment.

CHAPTER 3: FREQUENCY OF *MET* AND *PIK3CA* COPY NUMBER ELEVATION AND CORRELATION WITH OUTCOME IN PATIENTS WITH EARLY STAGE BREAST CANCER

INTRODUCTION

As mentioned in the previous chapter, the HGF/cMET signaling promotes cell proliferation, survival motility, invasion, as well as morphogenic changes that in normal cells stimulate tissue repair and regeneration but are also co-opted during tumor growth. Additionally, MET over-expression, with or without gene amplification, has been reported in a variety of human cancers including breast, lung, and gastrointestinal malignancies.(28-35) MET over-expression, with or without gene amplification, has been reported in a variety of human cancers including breast, lung, and gastrointestinal malignancies.(36-38) Further, high levels of HGF and/or MET correlate with poor prognosis in several tumor types, including breast, ovarian, cervical, gastric, head and neck, and non-small cell lung cancer.(38-42)

The PI3K pathway plays a key role in cell growth, protein translation, autophagy, metabolism, and cell survival. (18, 19, 22) Therefore, deregulation of this pathway can have detrimental effects on cellular outcomes. Most tyrosine kinase receptors implicated in breast cancer, such as MET, EGFR, HER2 and IGFR, are upstream of the PI3K pathway. Some of the mechanisms involved in the deregulation of the PI3K pathway include overexpression or activation of TKR, activating mutations, gene amplification of *PIK3CA* and *AKT* isoforms, as well as loss of the negative regulators PTEN and INPP4B.(24, 118) Deregulation and aberrations in this pathway have been implicated in breast cancer development and progression. Several studies have suggested the involvement of this pathway in the development of resistance to targeted therapies against tyrosine kinase and hormone receptors.(23-26) As a result, multiple drugs targeting the PI3K pathway are in early clinical trials as mono or combination therapies in breast cancer.(22, 27)

In breast cancer, we have limited information on MET receptor and PI3K pathway aberrations. The purpose of this study is to determine the frequency and association between recurrence-free survival (RFS) and *MET* and *PIK3CA* copy number elevations and their interaction in a large cohort of patients with early stage breast cancer.

MATERIALS AND METHODS

Patients and tumor samples: Adequate tumor DNA from formalin-fixed paraffin-embedded (FFPE) tissue blocks, clinical history, and follow-up data of 1,003

patients diagnosed with early breast cancer between 1985 and 1999 were identified from the Early Stage Breast Cancer Repository (ESBCR) at MD Anderson Cancer Center. Clinical information (including patient's age, race/ethnicity, stage, tumor size, lymph node status, nuclear grade, hormone receptor (HR) status) and primary treatment (including surgery, radiotherapy therapy, chemotherapy, and endocrine therapy) was extracted from the medical records.

Molecular inversion probes and copy number: Tumor DNA was extracted from FFPE tissues and processed for copy number analyses. Briefly, 5-10 (5- μ m) macrodissected tumor sections containing > 80% tumor cells per protocol were pooled and treated three times with proteinase K in ATL Tissue Lysis Buffer™ (Qiagen, Valencia, CA). Following lysis, samples were applied to uncoated Argylla Particles™ (Argylla Technologies, Tucson, AZ) and processed according to manufacturer recommendations. For 129 cases, DNA from non-tumor bearing lymph nodes, stored as FFPE, was isolated as an internal germline reference for the population. Tumor and normal DNA at 10 ng/ μ L was shipped to the Affymetrix™ MIP laboratory for copy number measurement. The laboratory was blinded to all sample and subject information including identity of duplicates. Data from the MIP high-density arrays are deposited at the National Center for Biotechnology Information (NCBI) (GSE31424). Nexus Copy Number v5.1 (BioDiscovery, El Segundo, CA) was used for processing the MIP data of these patients' samples. Nexus Copy Number segmented the data using the SNP-FASST2 segmentation algorithm, and called copy number gains or losses when the estimated copy number of each segment was greater/less than 2.3/1.7 respectively. Thus, copy number values greater than 2.3 were categorized as gains, and copy number values less than 1.7 were categorized as losses. Each sample has, in general, a different set of segments. Common segments were derived in order to perform analyses, with a size of 77,487 of the union of all segment break-points for 971 samples. In order to reduce the dimensionality of the data, similar procedures were followed for the CGH regions. We clustered consecutive segments if no two segments within the cluster had different gain/loss calls for at least 97% of the samples. This simple criterion yielded 3378 segments with common breakpoints across all 971 samples.

Statistical Analysis: Patient characteristics were tabulated and described by their medians and ranges by copy number (high vs. normal/low) with a chi-square test or Wilcoxon's rank sum test as appropriate. Relapse free-survival (RFS) was measured from the date of diagnosis to the date of first local/distant metastasis or last follow-up. Patients who died before experiencing a disease recurrence were considered censored at their date of death in the analysis. Survival outcomes were estimated according to the Kaplan-Meier product limit method. Using log rank statistics, groups were compared between high copy number and normal/low copy number groups for *MET*, *PI3KCA* and their co-amplifications as well as other important clinical variables. Three multivariate Cox proportional hazard models were developed. The first model incorporated *MET*, *PIK3CA*, copy number and their interaction. The second and third models incorporated either *MET* copy number or *PIK3CA* copy number and other prognostic clinical variables. Models were based on a backward selection procedure where all variables of interest were first included in a full model for screening and only variables with $P < 0.1$ were retained. P-values less than 0.05 were considered statistically significant. Analysis was performed by using R 2.11.2. (R Development Core Team, 2010, Vienna, Austria).

Reprinted with permission. © (2012) American Cancer Society. The Material shall at all times remain the exclusive property of John Wiley & Sons, Inc.

Characteristic	All		METCopy No.				P	PI3KCA Copy No.			
	N=971	%	High N=82	%	Normal/Low N=889	%		High N=134	%	Normal/Lost N=837	P
Age at diagnosis, y											
Minimum	25	—	28	—	25	—		25	—	25	—
Median	53	—	52	—	53.5	—		51	—	54	—
Maximum	87	—	86	—	87	—	.3899	84	—	87	—
Tumor size, cm											
<2	566	58.29	34	41.46	532	59.84		62	46.27	504	60.22
≥2	369	38.0	46	56.1	323	36.33	.0009	69	51.49	300	35.84
Lymph node status											
Positive	383	39.44	34	41.46	349	39.26		38	28.36	345	41.22
Negative	565	58.19	47	57.32	518	58.27	.8543	93	69.4	472	56.39
Grade											
1	92	9.47	4	4.88	88	9.9		5	3.73	87	10.39
2	477	49.12	35	42.68	442	49.72		50	37.31	427	51.02
3	336	34.6	41	50.0	295	33.18	.0153	72	53.73	264	31.54
Estrogen receptor											
Negative	293	30.18	38	46.34	255	28.68		71	52.99	222	26.52
Positive	666	68.59	44	53.66	622	69.97	.0018	62	46.27	604	72.16
Progesterone receptor											
Negative	406	41.81	42	51.22	364	40.94		80	59.7	326	38.95
Positive	555	57.16	40	48.78	515	57.93	.109	53	39.55	502	59.98
HER2											
Negative	764	78.68	68	82.93	696	78.29		102	76.12	662	79.09
Positive	207	21.32	14	17.07	193	21.71	.4009	32	23.88	175	20.91
Breast cancer subtype											
HER2positive	207	21.32	14	17.07	193	21.71		32	23.88	175	20.91
Hormone receptorpositive	583	60.04	44	53.66	539	60.63		53	39.55	530	63.32
Triple receptor negative	173	17.82	24	29.27	149	16.76	.0193	49	36.57	124	14.81
Menopausal status											
Perimenopausal/premenopausal	312	32.13	28	34.15	284	31.95		49	36.57	263	31.42
Postmenopausal	624	64.26	52	63.41	572	64.34	.8363	80	59.7	544	64.99
Stage											
I	304	31.31	18	21.95	286	32.17		32	23.88	272	32.5
II	662	68.18	64	78.05	598	67.27	.0694	101	75.37	561	67.03
Histology											
Ductal	898	92.48	78	95.12	820	92.24		128	95.52	770	92.0
Other	58	5.97	3	3.66	55	6.19	.4914	2	1.49	56	6.69
MET											
High copy no.	82	8.44	—	—	—	—		21	15.67	61	7.29
Normal/low copy no.	889	91.56	—	—	—	—		113	84.33	776	92.71
PIK3CA											
High copy no.	134	13.8	21	25.61	113	12.71		—	—	—	—
Normal/low copy no.	837	86.2	61	74.39	776	87.29	.0021	—	—	—	—

Table 5. Patient and Tumor characteristics (2)

Reprinted with permission. © (2012) American Cancer Society. The Material shall at all times remain the exclusive property of John Wiley & Sons, Inc.

RESULTS

Table 5 illustrates the patient and tumor characteristics as well as the therapy received by *MET* and *PIK3CA* copy number groups. Eighty-two (8.44%) were found to have elevated *MET* copy number, 134 (13.8%) had elevated *PIK3CA* copy number respectively, 25.6% of tumors with elevated *MET* copy number, also had elevated *PIK3CA* copy number, and 15.7% of tumors with elevated *PIK3CA* copy number, also had elevated *MET* copy number (Figure 4). Patients with tumors harboring either *MET* or *PIK3CA* high copy number tended to have more aggressive prognostic features

including larger tumor size, higher tumor grade, and negative hormone receptors. There were no significant differences on adjuvant chemotherapy or radiation therapy. However, more patients with normal/low copy number in either *MET* or *PIK3CA* received adjuvant endocrine therapy ($P=0.003$ and <0.000 , respectively). Elevated *MET* or *PIK3CA* copy number were more likely to occur in triple negative disease ($P=0.019$ and <0.001 , respectively).

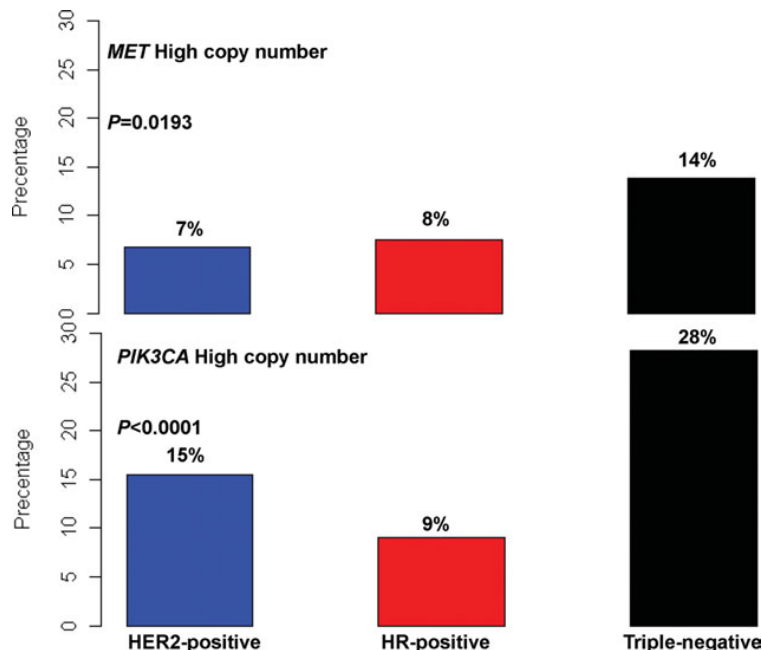


Figure 4. Distribution of *MET* and catalytic subunit of *PIK3CA* copy number shown by breast cancer subtype

HER2 indicates human epidermal growth factor receptor 2; HR, hormone receptor.(2)

Reprinted with permission. © (2012) American Cancer Society. The Material shall at all times remain the exclusive property of John Wiley & Sons, Inc.

At a median follow-up of 7.5 years (range 0-21.1 years), there were 252 recurrences. Table 6 summarizes the 5-year RFS by *MET* and *PIK3CA* copy number and by other patient and tumor characteristics. Five-year RFS was 63.5%, and 83.1% for *MET* high copy number and *MET* normal/low copy number respectively, ($P=0.06$); and 73.1%, and 82.3% for *PIK3CA* high copy number and *PIK3CA* normal/low copy number respectively, ($P=0.15$) (Figures 5A and 5B). To evaluate the interaction of coordinate gene copy elevations in *MET* and *PIK3CA*, patients were classified into four groups: normal/low both *PIK3CA* and *MET* copy number, high both *PIK3CA* and *MET* copy number, *MET* high copy number and *PIK3CA* high copy number. No statistically significant difference in 5-year RFS estimates was found ($P=0.137$) (Figure 5C).

The Kaplan-Meier survival curves by *MET* and *PIK3CA* gene copy number and breast cancer subtype are presented in Figure 6. When looking at *MET* copy number, patients with HR-positive and high *MET* copy number breast cancer had a significant lower 5-year RFS compared with patients with HR-positive and normal/low *MET* copy number breast cancer (76.4% vs. 85.4%, $P=0.034$). There was a trend to worse 5-year RFS in patients with HER2-positive and high *MET* copy number breast cancer compared with patients with HER2-positive and normal/low *MET* copy number breast cancer (64.3% vs. 77.2%, $P=0.061$). No difference was seen in triple receptor-negative disease ($P=0.80$). When looking at *PIK3CA* copy number, there were no differences in 5-year RFS estimates by breast cancer subtype. Exploratory survival analysis to

evaluate the interaction of high gene copy number in both *MET* and *PIK3CA* by breast cancer subtypes showed no statistically significant difference in 5-year RFS estimates (data not shown).

	No.	No. of Events	5-Year RFS Estimates		P
			Survival Rate	95% CI	
All	971	252	81.00%	78.5%-83.6%	
<i>MET</i> copy no.					
High	82	29	72.60%	63.5%-83.1%	.0637
Normal/low	889	223	81.80%	79.3%-84.5%	
<i>PI3KCA</i> copy no.					
High	134	44	73.10%	65.7%-81.3%	.154
Normal/low	837	208	82.30%	79.7%-85.1%	
Subtype					
HER2positive	207	62	76.30%	70.5%-82.5%	.071
Hormone receptorpositive	583	137	84.70%	81.7%-87.8%	
Triple receptornegative	173	49	74.20%	67.8%-81.3%	
Age at diagnosis, y					
<50	371	123	77.40%	73.2%-81.9%	.0003
≥50	595	129	83.30%	80.3%-86.5%	
Tumor size, cm					
<2	566	116	86.50%	83.6%-89.5%	<.0001
≥2	369	123	73.90%	69.4%-78.7%	
Lymph node status					
Positive	383	113	86.60%	83.7%-89.5%	<.0001
Negative	565	130	73.90%	69.5%-78.6%	
Grade					
1	92	22	85.00%	77.8%-92.9%	.249
2	477	113	83.30%	79.9%-86.9%	
3	336	95	77.50%	73.0%-82.2%	
Menopausal status					
Perimenopausal/premenopausal	312	101	76.30%	71.5%-81.3%	.0009
Postmenopausal	624	140	83.90%	81.0%-87.0%	
Stage					
I	304	43	91.90%	88.8%-95.1%	<.0001
II	662	209	76.00%	72.7%-79.5%	
Histology					
Ductal	898	235	80.70%	78.0%-83.4%	.826
Other	58	14	85.30%	76.3%-95.2%	
Chemotherapy					
No	480	102	85.20%	81.9%-88.6%	.001
Anthracyclinebased	323	110	75.50%	70.9%-80.5%	
Anthracycline and taxanebased	114	24	81.60%	74.6%-89.2%	
Radiotherapy					
Yes	410	109	82.50%	78.8%-86.4%	.645
No	535	134	80.60%	77.2%-84.2%	
Endocrine therapy					
Yes	422	79	87.30%	84%-90.6%	.0008
No	522	164	76.80%	73.1%-80.6%	

Abbreviations: 95% CI, 95% confidence interval; HER2, human epidermal growth factor receptor 2; *PI3KCA*, catalytic subunit of phosphoinositide-3-kinase; RFS, recurrence-free survival.

Table 6. Five-year relapse-free survival estimates

Five-year relapse-free survival estimates by copy number and patient and tumor characteristics(2)

Reprinted with permission. © (2012) American Cancer Society. The Material shall at all times remain the exclusive property of John Wiley & Sons, Inc.

Table 7 summarizes the multivariate models *MET*, *PIK3CA*, copy number and their interaction. The results were consistent with the RFS univariate analysis. Overall, patients with tumors harboring high *MET* copy number tended to be at higher risk to develop a recurrence compared to patients with tumors with normal/low *MET* copy

number (HR:1.53, 95% CI:0.98-2.38, P=0.06). High *PIK3CA* copy number was not an independent predictor risk for recurrence (HR:1.3, 95% CI:0.91-1.86, P=0.147), nor was the interaction of both *MET* and *PIK3CA* high copy number (HR:0.7, 95% CI:0.28-1.77, P=0.458). When looking at patients with hormone receptor-positive breast cancer, patients with tumors with high *MET* copy number were more likely to develop recurrences (HR:1.86, 95% CI:1.07-3.25, P=0.029). In multivariate models including patient and tumor characteristics, *MET* or *PIK3CA* high copy number were not independent predictors of RFS after adjustment for age, stage, nodal status, tumor size and breast cancer subtype (HR:1.21, 95% CI:0.8-1.82, P=0.357, and HR:1.29, 95% CI:0.85-1.94, P=0.229).

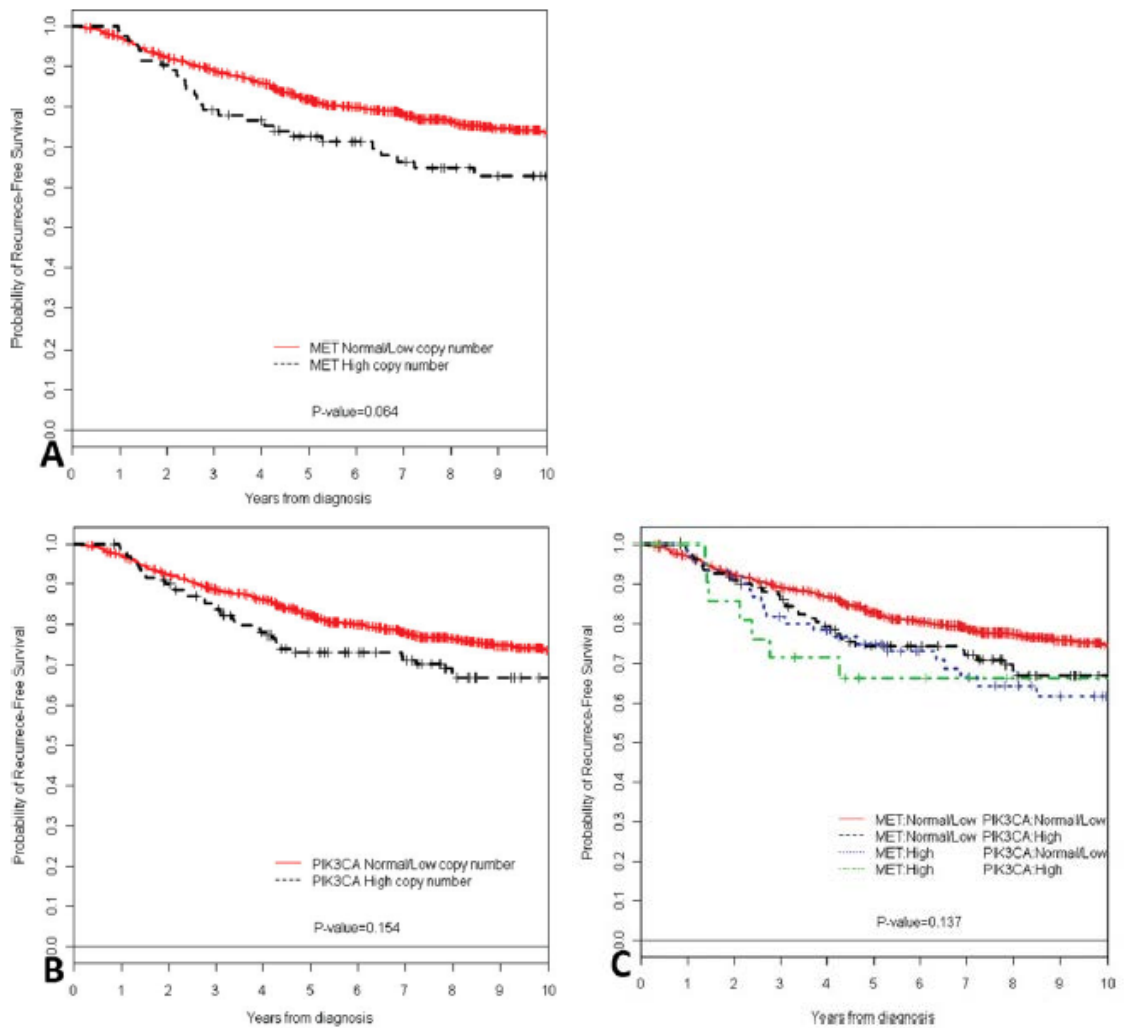


Figure 5. Kaplan-Meier recurrence-free survival curves

Kaplan-Meier recurrence-free survival curves for all patients are shown for (A) *MET* copy number, (B) *PIK3CA* copy number, and (C) *MET* and *PIK3CA* copy number (2)

Reprinted with permission. © (2012) American Cancer Society. The Material shall at all times remain the exclusive property of John Wiley & Sons, Inc.

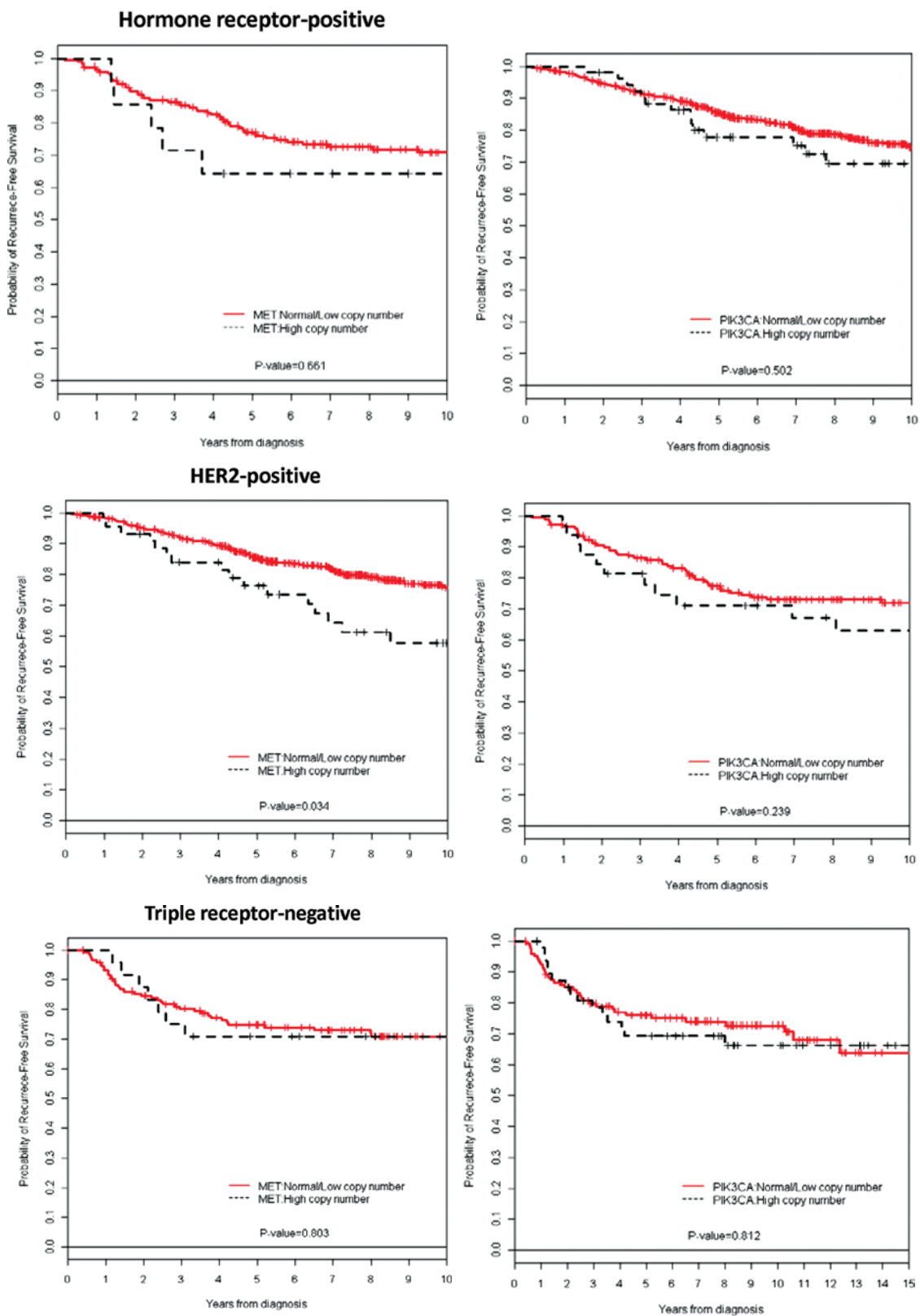


Figure 6. Kaplan-Meier recurrence-free survival curves
Kaplan-Meier recurrence-free survival curves for all patients are shown by breast cancer subtype and *MET* or *PIK3CA* copy number.(2)

DISCUSSION

The purpose of this study was to determine the frequency of *MET* and *PIK3CA* copy number in breast cancer, and their associations with patient outcome. We found that elevated *MET* or *PIK3CA* copy number was found in 82 (8.44%) and 134 (13.8%) of the tumors respectively, and 25.6% of the tumors had high copy numbers of both *PIK3CA* and *MET*. We also observed that high copy number of *MET* or *PIK3CA* was associated with poorer prognostic features and the triple negative disease. Additionally, tumors harboring elevated *MET* copy number tended to have a worse 5-year RFS, ($P=0.06$). A high copy number for either gene was not an independent predictor of RFS.

Germline SNPs, somatic mutations, gene amplification, protein overexpression, and autocrine circuits driven by HGF lead to the deregulation of MET receptor activity.(27) In breast cancer patients, there is limited data which is restricted to the assessment of the overexpressed MET receptor and its ligand HGF in tumor tissues.(40-42, 105, 119) The rate of MET protein overexpression is estimated to be 20% to 30%,(105, 119) and, as in several other tumor types, the increased expression of MET receptor or its ligand HGF in breast cancer is correlated with increased aggressiveness of disease and an overall poorer prognosis.(42, 105, 120) Immunoreactive (ir)-HGF concentrations were assessed in tumor extracts of 258 primary human breast cancers, using an enzyme-linked immunoadsorbent assay, and this initial study demonstrated that the ir-HGF level correlated with large tumor size ($P= .05$). High ir-HGF concentration also correlated with significantly shorter RFS ($P=0.001$) and OS ($P=0.001$) rates, and the ir-HGF level was found to be an independent predictor of RFS ($P = .041$) and overall survival ($P = .036$). (42) In a smaller cohort of 91 tumors, immunofluorescence was used to demonstrate high levels of MET expression, in patients with positive and negative lymph nodes, which correlated with a lower 5-year survival rate ($P = .008$ and $P = .006$, respectively).(119) A small study of 40 primary breast cancers in which MET and HGF were detected by immunofluorescence and immunohistochemistry indicated that MET levels did not correlate with established poor prognostic factors, wherein, overexpression of MET correlated with disease progression ($P = .037$). This study also demonstrated that, irrespective of HER2 positivity, MET overexpression identified a subset of patients with adverse outcomes.(105)

To our knowledge, ours is the first study to assess MET gene copy number in breast cancer, its distribution by tumor subtype, and its correlation with patient outcome. We

observed that patients with high MET copy number and negative hormone receptor status had larger and higher grade tumors. Two interesting findings highlight this study: the correlation of this aberration with the triple negative breast cancer disease and the prognostic significance of copy number in hormone-receptor positive breast cancer patients. This has opened new avenues in the field of breast cancer drug development as these therapeutic targets could activate signaling in triple negative breast cancer patients. This study reflects that MET signaling investigation is paramount in our search for the mechanisms governing endocrine therapy resistance. Finally, we need to define the frequency of MET protein overexpression and its correlation with other aberrations such as gene amplification and activating mutations. Currently, comprehensive work is ongoing in our institution, in this regard.

	Hazard Ratio	95% Confidence Intervals	P-value
All Tumors			
MET Normal/Low copy number	1		
MET High Copy number	1.53	0.98-2.38	0.06
PIK3CA Normal/Low copy number	1		
PIK3CA High Copy number	1.3	0.91-1.86	0.147
MET and PIK3CA high copy number	0.7	0.28-1.77	0.458
HER2-positive			
MET Normal/Low copy number	1		
MET High Copy number	0.92	0.29-2.95	0.886
PIK3CA Normal/Low copy number	1		
PIK3CA High Copy number	1.3	0.67-2.52	0.43
MET and PIK3CA high copy number	2.68	0.4-18.16	0.312
Hormone receptor-positive			
MET Normal/Low copy number	1		
MET High Copy number	1.86	1.07-3.25	0.0287
PIK3CA Normal/Low copy number	1		
PIK3CA High Copy number	1.25	0.7-2.23	0.4418
MET and PIK3CA high copy number	0.59	0.12-2.89	0.515
Triple receptor-negative			
MET Normal/Low copy number	1		
MET High copy number	1.33	0.51-3.43	0.56
PIK3CA Normal/Low copy number	1		
PIK3CA High copy number	1.17	0.6-2.3	0.645
MET and PIK3CA high copy number	0.61	0.12-2.95	0.535

Table 7. Multivariate Cox proportional hazard model

Multivariate Cox proportional hazard model including MET and PIK3CA copy numbers, and their interaction(2)

Reprinted with permission. © (2012) American Cancer Society. The Material shall at all times remain the exclusive property of John Wiley & Sons, Inc.

Some of the PI3K pathway aberrations that are reported in breast cancer include, and are limited to, detection of activating mutations, loss of tumor suppressors, and *PIK3CA* gene

amplification.(20, 21, 26) In a series of 92 primary breast cancers, investigators used quantitative real-time PCR to measure gene copy number and reported that 8.7% (8 of 92) of the tumors harbored a gain of *PIK3CA* gene copy number suggesting that gene amplification is not the main molecular mechanism in activating the PI3K-driven tumorigenesis pathway in breast cancer.(121) In a second cohort of breast cancers, researchers reported that 10 of 161 tumors had *PIK3CA* gene amplification, and 50% of which also had an activation mutation in the gene, suggesting that an additive effect of point mutation and copy number gain can contribute to oncogenesis.(122) We too have demonstrated that 13.8% of all breast cancers have elevated *PIK3CA* copy number, using a large cohort of early breast cancers. 28% of triple negative breast cancers had a high *PIK3CA* copy number, therefore PI3K pathway activation in this subtype could be attributed to gene amplification accompanied by loss of PTEN and INPP4B. Since basal breast cancers have a greater frequency of copy number aberrations, it is pertinent to determine whether *PIK3CA* (or *MET*) amplification is the tumor “driver”. In what to our knowledge was the largest tumor set published to date, which *PIK3CA* amplification was assessed, 292 invasive breast cancers were examined, of which 209 were tested and 28 were found to be amplified (13.4%).(123) Other than *PIK3CA* amplification, these investigators also assessed other PI3K pathway aberrations and correlated them with breast cancer molecular subtype and outcome. Only one cancer was found to encompass both mutation and copy number gain of the *PIK3CA* gene, suggesting that mutations and copy number gains were almost exclusive events. Additionally, neither mutations nor copy number gain were associated with clinicopathological parameters, breast cancer molecular subtype or outcome.(123)

Our results indicate that co-aberrations in the PI3K and MET pathways occur at a sufficient frequency that could contribute to patient outcomes, as 26% of *MET*-amplified tumors are accompanied by *PIK3CA* amplification, which clearly is a higher frequency than that predicted by chance. Further studies are on-going in our group, including the comprehensive analysis of large cohorts of breast cancers (i.e. TCGA- The Cancer Genome Atlas), to determine frequencies of mutations, copy number, methylation as well as translational changes in PI3K pathway-related genes and *MET* alone and in combination to determine the frequency of co-aberrations in the pathways across multiple modalities.

The next step would be to model the *MET* and *PIK3CA* co-aberrations in order to understand their oncogenic effects, and to test the potential activity of combinatorial therapy using MET and PI3K pathway inhibitors against breast cancer. The MET

amplification/mutation needs to be modeled with and without PIK3CA amplification/mutation, in order to elucidate the interactive effects of the MET and PI3K pathway. The following chapter aims to address this.

CHAPTER 4: *IN VITRO* EFFECTS OF MET AND PIK3CA CO-ABERRATIONS IN BREAST CANCER

INTRODUCTION

The PI3K signaling axis is vital for cell metabolism, proliferation, survival, and motility.(124) Class I PI3Ks phosphorylate phosphatidylinositol-4,5-bisphosphate and generate phosphatidylinositol-3,4,5-trisphosphate downstream of growth factor receptors and G protein-coupled receptors.(12) This leads to the activation of several kinases, including protein kinase B (PKB/AKT), mammalian target of rapamycin (mTOR), and p70 ribosomal protein S6 kinase (S6K).(124) More than 25% of breast cancers harbor somatic mutations in the PIK3CA-encoded p110 α catalytic subunit of PI3K.(125-128) These mutations usually occur in the helical region (E545K and E542K) or the kinase domain (H1047R) of p110 α ; H1047R is the most common mutation (>50% of cases).(129) The E545K and E542K mutations are highly enriched within luminal A tumors.(57) Several experimental models have demonstrated that these tumor-associated *PIK3CA* mutations lead to constitutive p110 α activation and oncogenic transformation,(129-133) making the PIK3CA oncogene a target for cancer therapy. Multiple drugs targeting the PI3K pathway are being tested in early clinical trials for breast cancer. As tumors invariably acquire resistance to single agent treatments, the ability to anticipate PI3K inhibitor resistance has enormous clinical value.(134) Genetic and adaptive resistances are major obstacles in translating therapeutic efficacy into curative cancer therapy due to the evolutionary nature of cancer and the unstable genome of some cancers. A thorough understanding of the “wiring diagram” of breast cancer cells and the mechanisms of resistance to PI3K targeted therapy is of paramount importance for designing multidrug combinations.(135, 136)

Using a mouse model of breast cancer that conditionally expresses human PIK3CA^{H1047R} in the presence of doxycycline, it has been demonstrated that 64% of the PIK3CA^{H1047R}- driven mammary tumors recurred after the removal of doxycycline.(129) Analysis of the recurrent tumors identified a tumor with an amplification region encompassing *MET* and, elevated *MET* mRNA and protein expression.(129) These results suggest that *MET* elevation is a mechanism underlying the growth of recurrent tumors that have escaped oncogenic PIK3CA addiction but remain dependent on the PI3K pathway.

MET is a receptor tyrosine kinase that activates the PI3K pathway via ERBB3 and GAB1.(43) The binding of active HGF to functionally established *MET* leads to receptor

dimerization/multimerization, phosphorylation of multiple tyrosine residues in the intracellular region, catalytic activation, and downstream signaling through the docking of a number of substrates leading to the transduction of multiple biological activities such as motility, proliferation, survival, and morphogenesis.(66, 67) MET over-expression, with or without gene amplification, has been reported in a variety of human cancers including breast, lung, and GI malignancies.(36-38) Further, high levels of HGF and/or MET correlate with poor prognosis in several tumor types, including breast, ovarian, cervical, gastric, head and neck, NSCLC.(38-42)

Transgenic expression of the MET receptor in mammary epithelium was sufficient to induce tumors with features of basal breast cancer.(59) Ponzio and colleagues have illustrated that MMTV-driven-MET mutant mouse models produce tumors resembling human basal breast cancer. Their study used mice that were transgenic for oncogenic variants of the MET receptor- M1248T, Y1003F/M1248T. They have demonstrated that these Met^{Mutants} induce mammary tumors with diverse histology, which, based on immunohistochemistry and expression profiling, includes tumors with basal and luminal characteristics. Our study investigates the role of the SNP *MET* T1010I and the somatic *MET* mutation Y1253D in the pathogenesis of Breast Cancer. Lee et al., screened 30 breast cancer samples and found one tumor with the T1010I missense mutation in the intracellular juxtamembrane domain of the MET receptor.(53) This mutation was also present in the DNA from a tumor cell-negative lymph node of the same individual, suggesting that T1010I could be a germline mutation.(53) The T1010I mutation was shown to be more active than the wild-type *MET* in the athymic nude mice tumorigenesis assay, suggesting that it may have effects on tumorigenesis.(53) The juxtamembrane domain regulates ligand-dependent MET internalization by Y1003 phosphorylation in response to HGF binding, leading to MET ubiquitination and degradation(33). When a mutation/SNP occurs in this region, it could result in MET accumulation at the cell surface and persistent HGF-stimulation, leading to tumorigenesis.(46) Overall, ***MET*** mutations occur at a lower frequency than other mechanisms of pathway activation, however, they provide strong evidence of the axis oncogenic potential and may identify patients that can either benefit from MET-directed therapies, or those in which some of these therapies may not work.(47)

As indicated in our published study, a high copy number of *MET* or *PIK3CA* was found to be associated with poorer prognostic features and the triple receptor-negative disease.(2) 16% of breast cancers with activating *PIK3CA* mutations (22% of all breast cancers) exhibited

co-mutations in *MET* suggesting concurrent selection of PI3K and MET pathway aberrations. Thus, 4-5% of breast cancer patients (8,000-10,000 new patients a year in the US) are likely to demonstrate concurrent mutations.

Studies suggest that overexpression of HGF and MET contributes to resistance, both inherent and treatment-acquired, to endocrine therapy and to trastuzumab treatment.(13, 14) The anti-apoptotic prosurvival effect of the HGF/MET signaling pathway makes MET inhibition a potential therapeutic target for breast cancer that are resistant and refractory to conventional therapies.(1)

Since MET participates in the acquisition of resistance, and MET overexpression was selected in PI3K driven mammary tumors that were resistant to PI3K inhibition,(60) it is pertinent to investigate the synergistic effects of PI3K and MET inhibitors on tumorigenesis.

Literature review and previous studies have raised the following questions- Do *MET/PIK3CA* co-aberrations mediate resistance to single targeted therapies directed to PI3K or MET in Breast Cancer?; which leads to the next question - Can combination therapy targeting both PI3K and MET pathways improve treatment efficacy and overcome the resistance from single targeted therapy ? In order to answer these questions, we addressed the following objective-

To determine the effect of co-mutations/SNPs in *MET* and MET overexpression, found in breast cancers, on the activity of the two most common breast cancer *PIK3CA* mutations (E545K and H1047R) *in vitro*

- a) Using parental (Wild Type), single mutant (*PIK3CA* or *MET*) and co-mutant (*PIK3CA* and *MET*) immortalized **Breast Epithelial Cells** to:
 - Analyze the effects of the aberrations on their cell growth, proliferation, colony formation, cell morphology, anchorage independent proliferation, cell invasion and cell signaling.
 - Analyze their sensitivity to selective PI3K pathway inhibitors (alone), MET receptor inhibitors (alone), and their combination.
- b) Using parental (Wild Type), single mutant (*PIK3CA* or *MET*) and co-mutant (*PIK3CA* and *MET*) immortalized **Breast Cancer Cells** to:

- Analyze the effects of the aberrations on their cell growth, proliferation, colony formation, cell morphology, anchorage independent proliferation, cell invasion and cell signaling.
- Analyze their sensitivity to selective PI3K pathway inhibitors (alone), MET receptor inhibitors (alone), and their combination.

MATERIALS AND METHODS

Rationale for construct selection: Parallel construction of recombinant lentiviruses expressing aberrant *PIK3CA* and *MET* was completed. *PIK3CA*-WT was used to mimic gene amplification, its mutants (*PIK3CA*-E545K, *PIK3CA*-H1047R) were chosen as they are the most frequent *PIK3CA* mutations reported in breast cancer. *cMET*-WT was selected to represent the overexpression found in breast cancer (more common than mutations), *cMET*-T1010T was selected to determine if this SNP/mutation alters cell biology and could be related to patient outcomes, and *cMET*-Y1253D was selected since it is a somatic activating mutation in the tyrosine kinase domain of the MET receptor.

Construction of recombinant lentiviruses expressing wild type and mutant *PIK3CA*: The lentiviral constructs (pLenti6/V5-DEST/*PIK3CA*-WT, pLenti6/V5-DEST *PIK3CA*- E545K, pLenti6/V5-DEST *PIK3CA*- H1047R and the control pLenti6/V5-DEST/Lac Z) were gifts from Dr. G. Wu (Karmanos Cancer Institute, Detroit, MI, USA).(137) Virus preps were performed after the sequences were verified. To generate the lentiviruses expressing wild type HA-*PIK3CA* and its mutants, ViraPower Lentiviral Expression System (Invitrogen) was used. The pLenti-HA-*PIK3CA*s or control constructs were co- transfected into the 293FT producer cells with 3 µg pLenti expression plasmid DNA and 9 µg of ViraPower packaging mix using the Lipofectamine 2000 reagent (Invitrogen, Carlsbad, CA, USA). Lentivirus-containing supernatants were collected after 48 h, filtered with 0.45 µm PVDF filters (Millipore) and then used to infect MCF-10A cells. Selection began 48 hours after infection in growth medium with 10 µg/ml Blasticidin (Invitrogen, San Diego, CA).(137) The stable cell lines expressing *PIK3CA*-WT, its mutants (*PIK3CA*-E545K, *PIK3CA*-H1047R), or Lac Z control were further used to establish *PIK3CA*/*cMET* double mutant cells.

Construction of recombinant lentiviruses expressing wild type and mutant *cMET*: GeneART synthesized constructs expressing human wild type (WT) or mutant *cMET*s (*cMET*-

WT-Flag, *cMET* -T1010I-Flag, and *cMET*-Y1253D-Flag) designed by us. pMA vector 2 was used as the backbone in these plasmids. The constructs were sequenced to ensure the validity of the sequence and the orientation. Then the human full-length cDNAs for wild type *cMET* and the two mutants, with Kozak sequence before ATG and Flag-tag after *cMET*, were sub-cloned into pLVX-tdTomato-N1 vectors (Clontech, Mountain View, CA) (Fig. 8A) with XhoI/XmaI enzymes. The constructs (pLVX-*cMET* - WT-tdTomato, pLVX-*cMET*-T1010T-tdTomato, pLVX-*cMET*-Y1253D and the empty vector pLVX-tdTomato-N1) were sequenced by GeneART to confirm the sequence. We confirmed that the orientation of the constructs was correct with restriction enzymes (data not shown).

Generation of Lentiviruses expressing wild type and mutant *cMETs*: To generate the lentiviruses expressing wild type *cMET* and its mutants, we used two expression systems. One of them was the ViraPower Lentiviral Expression System (Invitrogen) that we used for expressing *PIK3CA*, as described previously. In addition, we used the Lenti-XTM Lentiviral Expression System (Clontech). A total amount of 7 µg of pLVX-tdTomato-N1 vector, pLVX-*cMET* WT-tdTomato, pLVX-*cMET* T1010T- tdTomato, or pLVX-*cMET*-Y1253D-tdTomato were co-transfected into the Lenti-X 293T cells, with 36 µg of the Lenti-X HTX packaging Mix, using 7.5 µl Xfect Polymer (Clontech, CA, USA). Lentiviruses containing supernatants were collected after 48 h, followed by a brief centrifugation (500 g for 10 minutes) to remove cellular debris. Then they were used to infect the breast cancer cell line HCC-1954 or mammary epithelial cells, MCF-10A, that expressed *PIK3CA*-WT, *PIK3CA*-E545K, *PIK3CA*-H1047R, or Lac Z as control. Selection began 48 hours after infection in growth medium with 1 µg/ml puromycin for two weeks. Both lentiviral expression systems allowed similar specific expression levels.

Cell culture: MCF-10A, non-transformed mammary epithelial cell line, and HCC1954, human breast cancer cell line, were obtained from Characterized Cell Line Core, UT MD Anderson Cancer Center and grown at 37 °C in humidified 5% CO₂. The MCF-10A cells were maintained in DMEM/F12 (Thermo Scientific, South Logan, Utah) supplemented with 5% horse serum (Invitrogen), 20 ng/ml EGF (Peprotech), 10 µg/ml insulin (Sigma), 100 ng/ml cholera toxin (Sigma), 0.5 µg/ml hydrocortisone (Sigma), 100 units/ml penicillin and 100 µg/ml streptomycin. HCC1954 cells were maintained in RPMI supplemented with 10% FBS, 100 units /ml penicillin and 100 µg/ml streptomycin. Cells were frozen at early passages and used for less than 4 weeks in continuous culture.

Drugs: Onartuzumab (Met-MAbTM), a monovalent, humanized, monoclonal antibody that binds to the receptor tyrosine kinase cMET (Genentech Inc), was used as per manufacturer's instructions. GDC 941 (Genentech) and GDC 980 (Genentech) were dissolved in DMSO (Sigma-Aldrich) to a concentration of 2 mM, stored at -20 °C, and further diluted to an appropriate final concentration in serum-free medium upon use. EMD-1214063 (Merck) was dissolved in DMSO (Sigma-Aldrich) to a concentration of 5 mM, stored at -20 °C, and further diluted to an appropriate final concentration in serum-free medium at the time of use. DMSO in the final solution was 0.1% (v/v). To verify drug effects, we performed preliminary studies and confirmed their inhibitory function on cell signaling (Figure 20).

Cell growth curves: For cell proliferation assay and EGF independent growth, MCF-10A cells expressing wild type or mutant cMET and/or expressing *PIK3CA* mutation were seeded in triplicates, at the density of 2×10^4 cells per well in 12-well plates in low serum medium (2.5% horse serum) lacking EGF and insulin, for 3 days. For HCC1954 cells expressing wild type or mutant cMETs, cells were seeded at the density of 2×10^4 cells per well in 12-well plates in low serum medium (2.5% FBS) for 4 days. Cells were trypsinized and counted on each day with an automated cell counter and cell analyzer, Cellometer Vision (Nexcelom).

Cell Growth Inhibition Assays: Cells were seeded in 96-well plates (2,000 cells per well) in complete growth medium and were allowed to attach for 24 hours. The medium was changed to low serum medium (2.5% horse serum for MCF-10A cells; 2% FBS for HCC1954 cells). Cells were incubated overnight at 37 °C, followed by the addition of serial dilutions of drugs with variable combinations for 72 hours. For testing Onartuzumab or combinations with Onartuzumab, 50 ng/ml HGF was supplemented. Growth inhibition was determined using the CellTiter-Blue viability assay according to the manufacturer's protocol (Promega) and incubated at 37 °C for 3 hours and fluorescence was recorded at 560 Ex/590 Em. Each experiment was repeated at least three times. Cell viability results were calculated on the basis of percentage change versus vehicle-treated control.

Morphogenesis Assay: Three-dimensional culture of cells was carried out on a matrigel basement membrane.(138) Briefly, 4×10^3 cells were resuspended in a modified

growth medium, containing 2% growth factor-reduced matrigel (BD Biosciences) with drugs of variable combinations as designed, and subsequently seeded onto the Matrigel matrix in 8-well chamber slides (BD Bioscience). Medium with drugs was replaced every 3 days. Photographs of representative fields were taken as indicated. Acini were photographed and counted in 10 randomly chosen fields and expressed as means of triplicates, representative of three independent experiments.

***In vitro* Invasion Assay:** Cell *in vitro* invasion was analyzed with 24-well Biocoat Matrigel invasion chambers with 8 µm polycarbonated filters (Becton Dickinson). Cells were starved for 20 hours in serum-free DMEM F12 lacking EGF. After washing with serum-free DMEM F12, 1×10^5 cells in 0.6 ml DMEM F12 were inoculated into the upper chamber, and 0.75 ml DMEM F12 containing fibronectin (5 µg g/ml) was added to the lower chamber. For invasion- inhibition assay, drugs (GDC941, GDC980, Onartuzumab or EMD-1214063) or vehicle was added to both the upper and lower chambers. For testing the effect of Onartuzumab or its combinations, HGF (50 ng/ml) was added. The cells were allowed to pass through the matrigel at 37°C, 5% CO₂, for 22 hours. Non-invasive cells on the upper surface of the filter were removed by wiping with a cotton swab. The cells that penetrated through the pores of the Matrigel to the underside of the filter were stained with 0.25% crystal violet in 20% methanol for 30 min. Invasive cells were photographed and counted in 10 random fields.

Clonogenic Assay: For clonogenic assays, 1,000 cells were seeded in a 60 mm dish, in growth medium, for 11 days. For inhibitory assay, after attaching on the dish, cells were treated for 2 days with drugs in variable combinations as designed. Then the drugs were washed away and cells were allowed to grow in growth media for 11 days. The cells were rinsed with PBS, followed by staining with 0.25% crystal violet / 20% ethanol. Quantitative analysis of the total number and size of clones was performed with AlphaVIEW SA software (Cell Biosciences).

Soft Agar Assay: Cells were suspended in complete growth medium containing 0.3% soft agar, and seeded in triplicates in 35-mm dishes pre-coated with 0.6% agar in growth medium, and incubated at 37°C, 5% CO₂. After 12 days, colonies were photographed and counted in 10 randomly chosen fields and expressed as means of triplicates, representative of three independent experiments.

Tumor Xenografts studies: Human HGF transgenic mice on a severe combined immunodeficiency (SCID) background, named hHGF Tg SCID females(139), at 6 weeks of age and housed in sterile filter-capped cages, were used. All animal studies were carried out under ACUF-approved protocols. Exponentially growing HCC1954/*cMET*-WT, HCC1954/*cMET*-T1010I, HCC1954/*cMET*-Y1253D, and HCC1954/Td Tomato control cells were harvested. After being washed and resuspended in PBS, 1×10^7 cells were injected into the mammary fat pads of mice. Animals were monitored on a daily basis. Each group consisted of 5 mice. Tumor sizes were determined by measuring the length (*l*) and the width (*w*) with calipers twice weekly. Tumor volume was calculated with the formula ($V = lw^2/2$). Differences in tumor volume among groups at each time point were analyzed using ANOVA. At the end of the experiment, mice were sacrificed. Tumors were harvested, followed by measurement of tumor size. Tumors were cut and flash-frozen in liquid nitrogen for Western blot or fixed in 10% neutral-buffered formalin for paraffin- embedding. Xenograft tumors and all the organs, of each mouse, were subjected to double-blind histopathological analysis by a Veterinary pathologist.

Antibody	Source
AKT	Cell Signaling ¹
AKT pS473	Cell Signaling ¹
b-Actin	Sigma ²
c-Jun pS73	Cell Signaling ¹
cMet pY1234/1235	Cell Signaling ¹
cMet	Cell Signaling ¹
ERK2	Santa Cruz ³
Flag M2	Sigma ²
GSK-3a/b pS21/9	Cell Signaling ¹
MAPK (T202/Y204)	Cell Signaling ¹
mTor	Cell Signaling ¹
mTOR pS2448	Cell Signaling ¹
PI3K p110a	Epitomics ⁴
S6 pS240/244	Cell Signaling ¹
Src pY416	Cell Signaling ¹
Stat3 pY705	Cell Signaling ¹
Stat3 pY727	Epitomics ⁴
V5	Invitrogen ⁵

Table 8

Antibodies used for Western blot ¹Beverly, MA; ²Sigma, St Louis, MO; ³Santa Cruz, CA; ⁴Epitomics, Burlingame, CA; ⁵Invitrogen, Carlsbad, CA

Immunoblotting and immunoprecipitation: Cells were washed twice with cold phosphate-buffered saline and lysed in ice-cold lysis buffer [1% Triton X-100, 50mM HEPES, pH 7.4, 150mM NaCl, 1.5mM MgCl₂, 1mM EGTA, 100mM NaF, 10mM Na

pyrophosphate, 1mM Na₃VO₄, 10% glycerol, protease inhibitor cocktail (Roche Applied Science), and phosphatase inhibitors, PhosSTOP (Roche Applied Science)]. Cell lysates were collected after centrifugation at 13,000 rpm for 10 minutes. The cellular protein concentration was determined by BCA reaction with reagents from Pierce (Rockford, IL). For immunoprecipitation, cell lysates were immunoprecipitated with anti-V5 (Invitrogen). Immunocomplexes were collected on Protein A/G plus-conjugated agarose beads (Santa Cruz Biotechnology). Immunocomplexes or cell lysates were separated by SDS-PAGE and transferred to polyvinylidene difluoride (PVDF) membranes. The membranes were blocked with 4% fat free-milk in TBS-T (10 mM Tris-HCl, pH 7.4, 150 mM NaCl, 0.1% Tween 20) for one hour at room temperature, and then incubated overnight with antibodies diluted in 5% BSA in TBS-T (Table 8). The membranes were washed in TBS-T and incubated with HRP-conjugated goat anti-rabbit secondary antibody (1:2500 dilution) or HRP- conjugated goat anti-mouse secondary antibody (1:2500 dilution) for one hour at room temperature. The membranes were washed with TBS-T, and the proteins were visualized using ECL from Amersham Biosciences (Piscataway, NJ).

Statistical Analyses: Statistical analysis was carried out using the ANOVA test (for multiple groups) and the Student *t* test (for two groups). Differences with *P* values < 0.05 were considered statistically significant.

RESULTS

Establishment of stable cells expressing mutant *PIK3CA* (E545K, H1047R) or overexpressing wild type *PIK3CA* genes: In order to study the effects of the cancer-associated *PIK3CA* mutations or *PIK3CA/cMET* double mutations in breast cancer, we first generated different lentiviruses expressing breast cancer-associated mutant *PIK3CA*s (E545K, H1047R) or wild type *PIK3CA* genes or Lac Z constructs, using lentiviral constructs from Dr. G. Wu (Karmanos Cancer Institute, Detroit, MI).(137) E545K mutation is located in the helical domain and H1047R mutation in the kinase domain of *PIK3CA* (Figure 7 A). These viruses were used to infect mammary epithelial cells, MCF10A. After 48 hours, blasticidin was used for selection. The specific expression in these cell lines were verified with immunoprecipitation and Western blot (Fig. 7B).

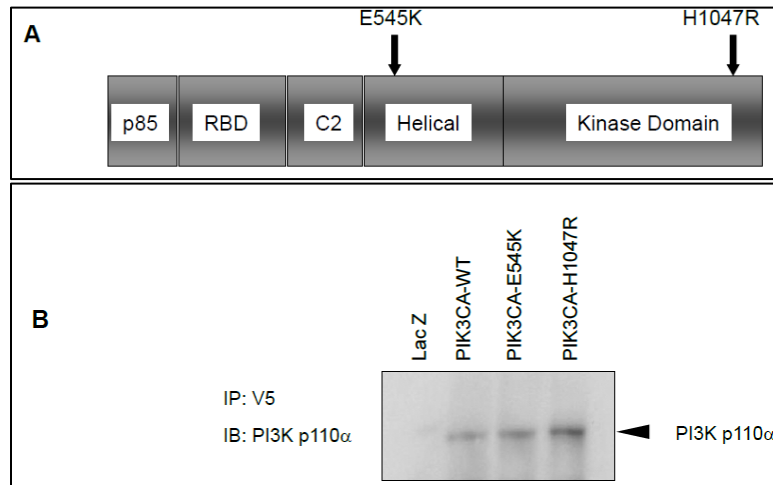
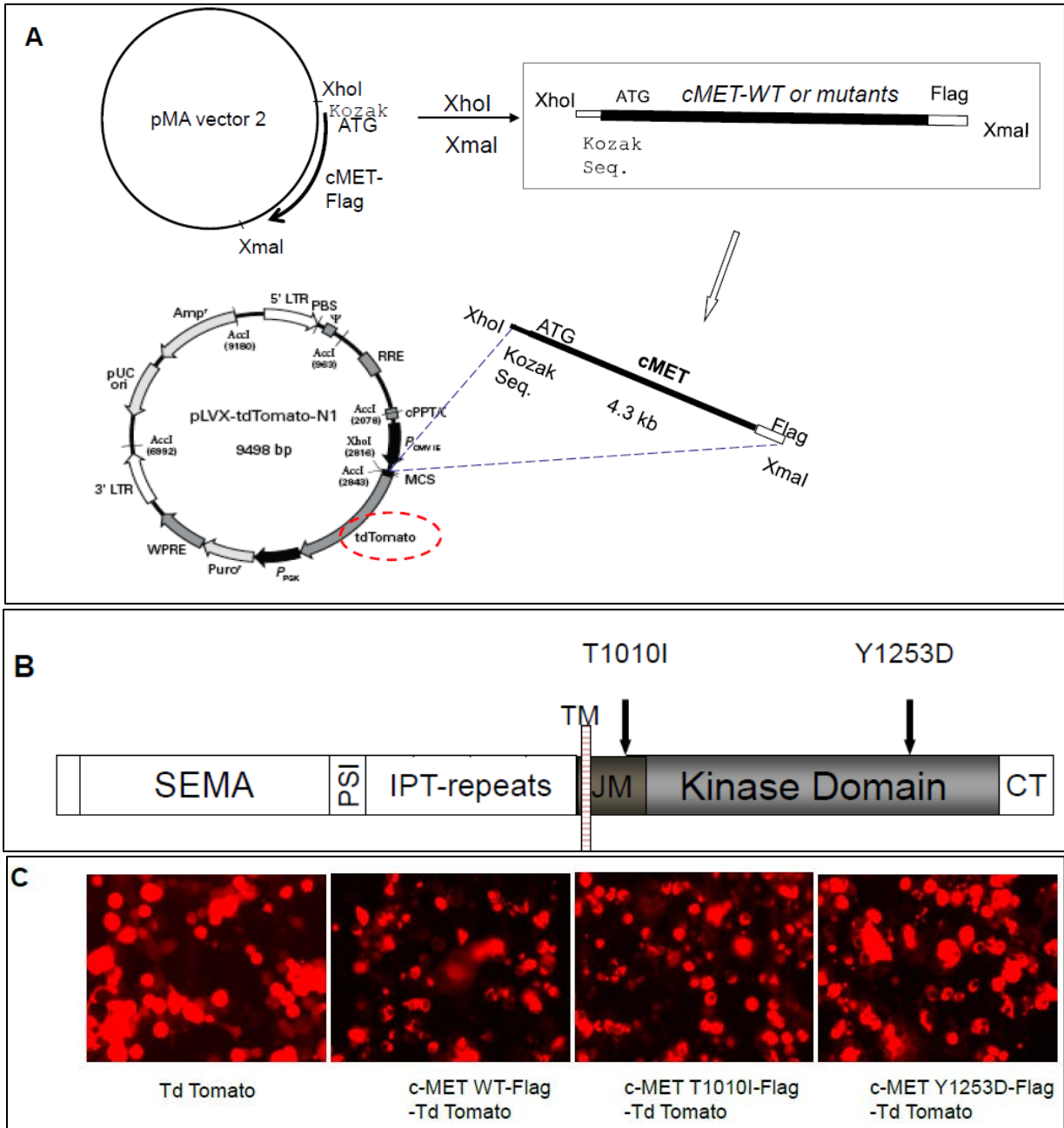


Figure 7. Establishment of stable cells

Establishment of stable cells expressing breast cancer-associated mutant *PIK3CA* genes in the mammary epithelial cell line, MCF-10A cells: **A.** The location of breast cancer-associated E545K and H1047R mutations in the *PIK3CA* molecule. **B.** Immunoprecipitation (IP) and Western blot analysis confirmed the expression of *PIK3CA* in MCF10A cells. To detect the expression of *PIK3CA*-V5, V5 antibody was used for IP and anti-*PI3K* P110 α antibody was used for immunoblot (7B).

Generation of wild type or mutant *cMET* lentiviral constructs and establishment of stable cells expressing different *cMET* genes: To determine whether deregulated expression of *cMET* or its mutation could play a role in progression of breast cancer, we generated wild type or mutant *cMETs* lentiviral constructs with wild type (WT), full-length human *cMET*, or mutant *cMETs* (T1010I, Y1253D) using Flag epitope-tagged cDNA based on pLVX-tdTomato-N1 (Clontech, Mountain View, CA). We named the constructs as pLVX-tdTomato/*cMET* WT-Flag, pLVX-tdTomato/*cMET*-E545K-Flag and pLVX-tdTomato/*cMET*-Y1253D-Flag. pLVX- TdTomato vector was used as control (Figure 8A). The sequence and orientation of the inserted cDNAs were confirmed (data not shown). T1010I is located in the Juxtamembrane (JM) domain, while Y1253D is in the kinase domain (Figure 8B). Using the lentiviral constructs, we generated different lentiviruses and used the viruses to infect MCF10A mammary epithelial cells. To establish stable cells expressing *PIK3CA/cMET* double genes, the stable cells expressing the *PIK3CA* genes were further infected with lentivirus expressing variable *cMETs*. Pooled stable cells expressing wild type or mutant *cMET* genes were generated after puromycin selection. The specific expression of infected genes was detected by the Td Tomato fluorescence in 293FT packaging cells (Figure 8C). We generated 20 stable cell lines based on MCF-10A using the viruses. Here we present representative cell lines to show their expression levels and patterns (Figure 8 D). Control cells infected with the viruses expressing Td Tomato alone showed specific expression in the whole cell (Figure 8C, D). The expression of *cMET*-Flag-Td Tomato in different *cMET*-

Flag-Td Tomato cell lines was observed on the cell membrane and in the cytoplasm (Figure 8C, D), in levels lower than the control cells. We further confirmed the cMET-Flag expression in the 20 stable cell lines with Western blot using anti-Flag M2 antibody. As expected, control cells did not show cMET-Flag expression (Figure 8E). It is important to note that, in this study, cMET WT and PIK3CA WT represent overexpression of cMET and PIK3CA wild type, respectively.



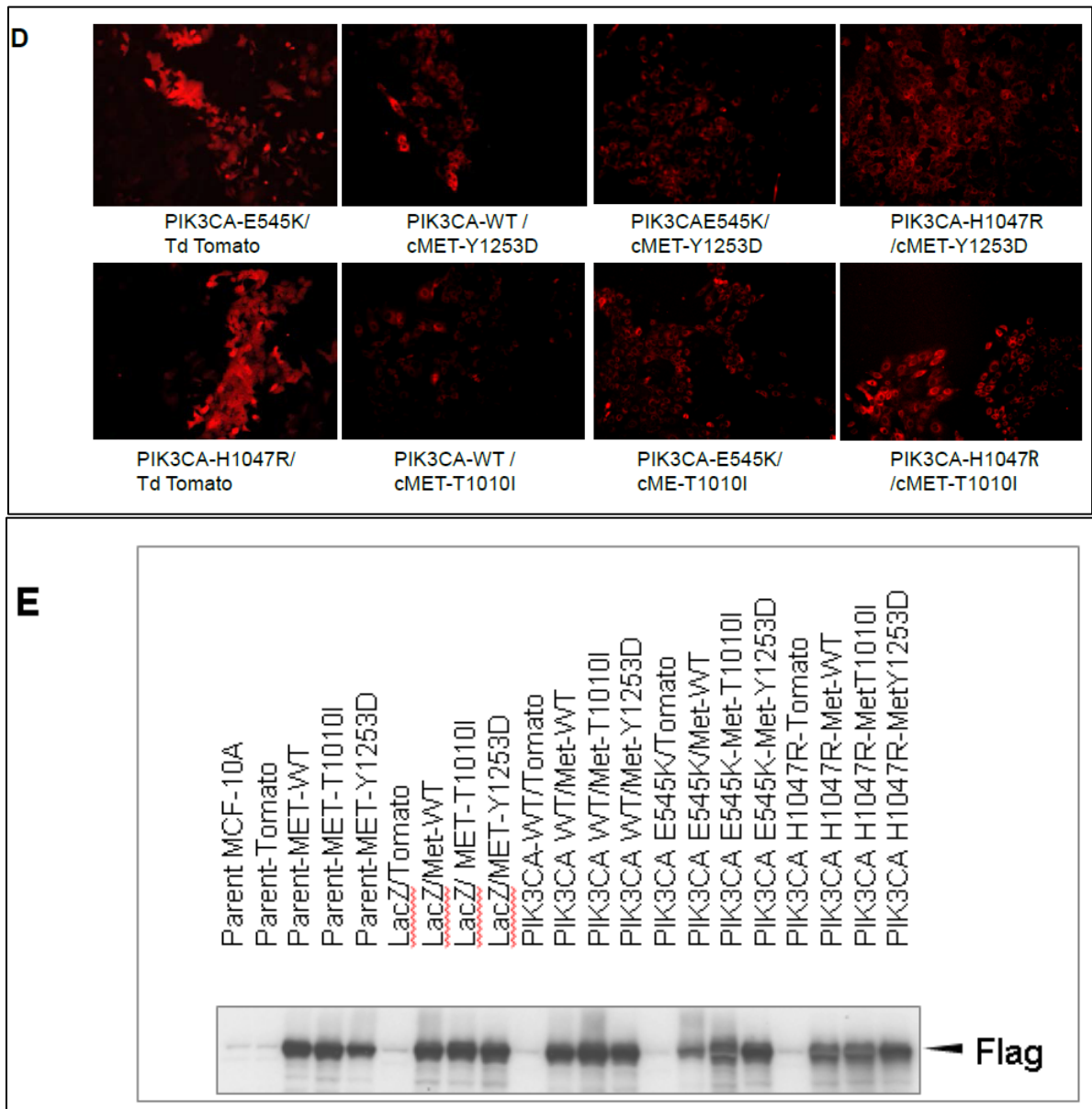


Figure 8. Development of Lentiviral Constructs

Development of lentiviral constructs for human wild type c-MET and its mutants: **A.** Human *cMET* genes, including wild type and two mutants (T1010I and Y1253D), were synthesized by GeneART following our design. The backbone of the plasmids is pMA vector 2. The fragments of Kozak-*cMETs*-Flag were excised from pMA vector 2 with XhoI/XmaI and inserted into pLVX-tdTomatoN1, a lentiviral vector (Clontech, Mountain View, CA). **B.** The location of *cMET* -T1010I and *cMET*-Y1253D in *MET*. **C.** Specific protein expressions in 293FT packaging cells. **D.** Specific protein expression in drug-selected colonies of MCF-10A infected with Lenti-virus expressing *cMET*-FLAG-Td Tomato. **E.** Western blot analysis to confirm the expression of *cMET*-flag-Td Tomato in MCF10A cells. Anti-Flag M2 antibody was used to detect the specific expression.

cMET overexpression and its cancer-associated mutations cooperate with *PIK3CA* mutations to promote cell proliferation: MCF-10A cells are non-tumorigenic mammary epithelial cells. The components of growth medium for the non-transformed cells are much more complex than that for tumor cells. The supplements including 5% horse

serum, EGF, insulin, cholera toxin, and hydrocortisone are required for growth. EGF requirement can be overcome by the exogenous expression of mutant PI3KCA E545K and H1047R(131), which is one of the important molecular effects of the oncogenes.(140) To investigate whether the *PIK3CA/cMET* double mutation affects cell proliferation, we cultured the cells in a less optimal environment, including low serum (2.5% horse serum) medium, and withdrawal of EGF and other supplements for 3 days. We found that MCF10A cells expressing both mutant PI3KCA and aberrant cMETs showed a significant higher proliferation than cells with mutant PI3KCA alone ($P < 0.05-0.001$) or aberrant *cMET* alone (#, $P < 0.05$, ## $P < 0.01$, ### $P < 0.001$ vs *cMET*s alone. ANOVA) (Figure 9A,B). Interestingly, overexpression of wild type *cMET*, in PI3KCA mutant cells, had a similar effect on cell proliferation, on monolayer, as mutant *cMET*. However, among these cell lines, PI3KCA mutant/*cMET*-Y1253D cells exhibited the highest growth ability suggesting a differential effect from wild type *cMET* (Fig. 9A, B). There could be a possible interaction between aberrant PI3KCA and *cMET*, since the co-aberrant cells exhibit higher proliferation when compared to the corresponding PI3KCA or *cMET* only aberrant cells.

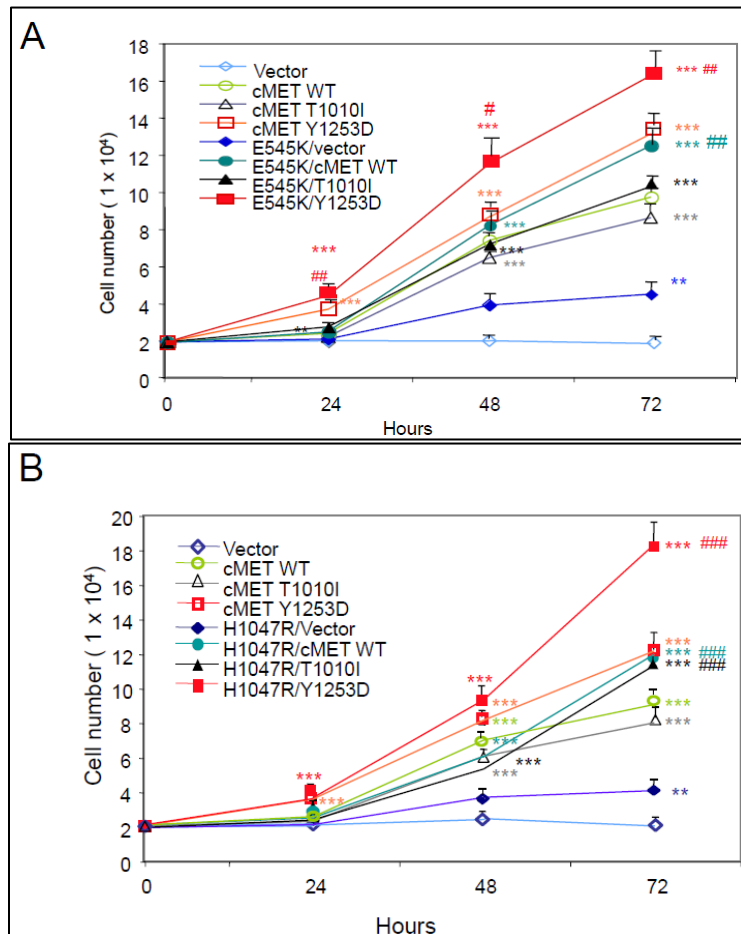
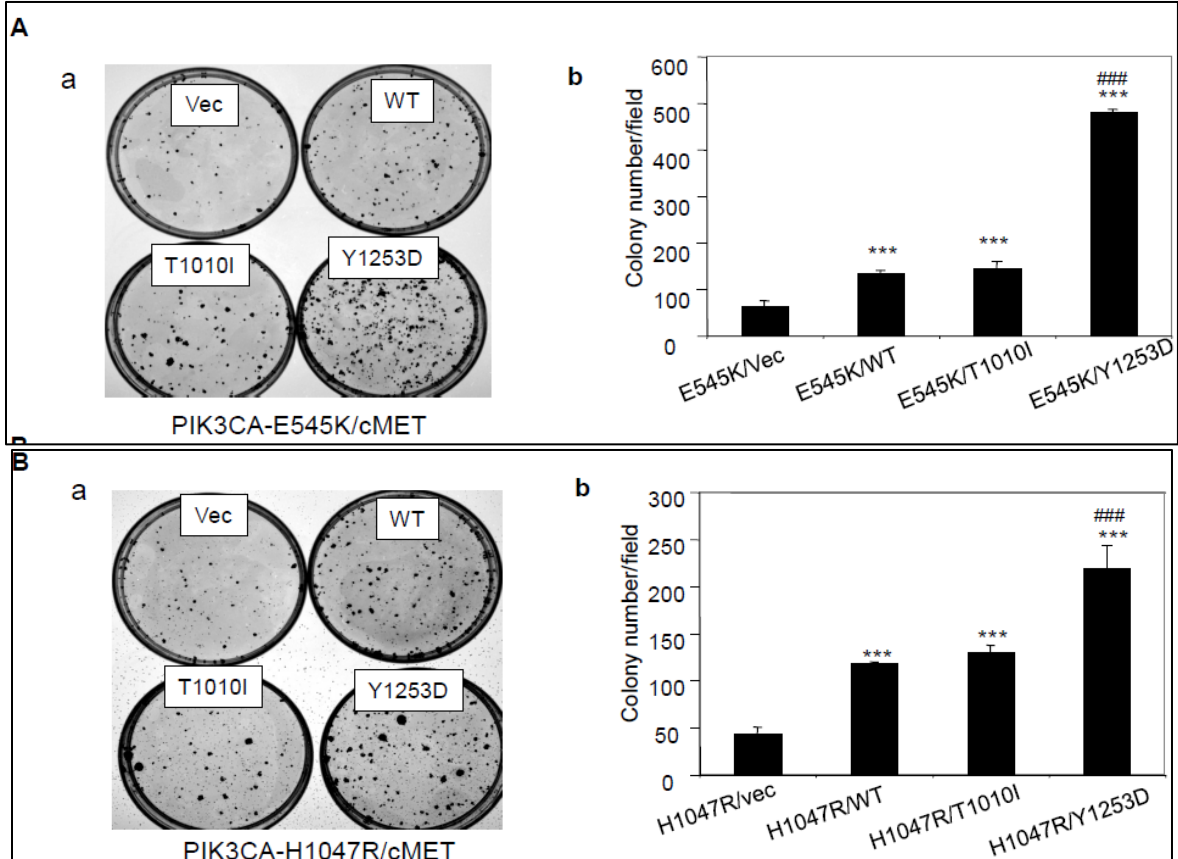


Figure 9. Effect of wild type or mutant PIK3CA/cMETs on Cell Growth

Effect of wild type or mutant PIK3CA/cMETs on growth factor-independent cell growth: MCF-10A

derived cell lines were seeded in 12-well plates at 2×10^4 cells per well in 2.5% horse serum lacking EGF and insulin for 3 days. Cell numbers were counted for each day indicated. Each experiment was done with triplicate wells. The data are mean \pm standard errors of triplicates, representative of two independent experiments **A**. Cells expressing PIK3CA-E545K alone, cMET alone (WT or mutants T1010I, Y1253D) or co-expressing PIK3CA (E545K) and cMET aberrations. (** $P < 0.01$, *** $P < 0.001$ vs Tdv; #, $P < 0.05$, ## $P < 0.01$ vs cMETs alone. ANOVA) **B**. Cells expressing PIK3CA-H1047R alone, cMET alone (WT or mutants T1010I, Y1253D) or co-expressing PIK3CA (H1047R) and cMET aberrations. (** $P < 0.01$, *** $P < 0.001$ vs Tdv; ##, $P < 0.01$, ### $P < 0.001$ vs cMETs alone. ANOVA)

cMET overexpression and its cancer-associated mutations act coordinately with PIK3CA mutations to increase cell survival: To detect whether combination of cMET mutation or overexpression of cMET with PIK3CA mutations affects cell survival, we performed clonogenic assay. Our data showed that, both overexpression of cMET and expression of mutant cMET, in PIK3CA-mutant cells, increased colony formation ($P < 0.001$, respectively). In these PIK3CA-mutant cells, the effect of Y1253D was the strongest, while the T1010I mutation and overexpression of wild type cMET had similar effects ($P > 0.05$) (Figure 10 A, B). Cells expressing only aberrant cMET (wild type or mutants-T1010I, Y1253D) showed smaller and fewer colonies (Figure 10 C) when compared to the PIK3CA, cMET co-aberrant cells. This assay too suggests a possible interaction between aberrant PIK3CA and cMET, since the co-aberrant cells exhibit increased survival.



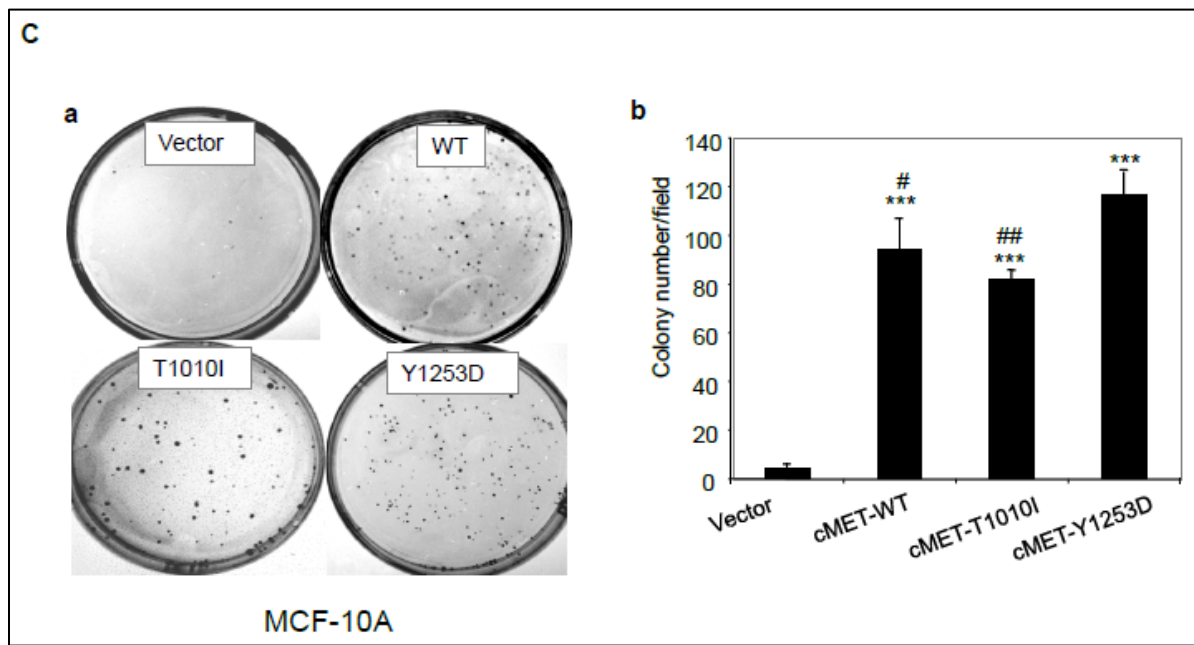


Figure 10. The Effects of PIK3CA/cMET mutations on Colony Formation

The effects of PIK3CA/cMET mutations on colony formation assay: MCF-10A derived cell lines were seeded in triplicate with a density of 1000 cell/60 mm-petri dish. Cells were cultured in 2.5% horse serum, lacking EGF and insulin, supplemented with 40 ng/ml HGF. **A.** PIK3CA-E545K cells expressing wild type cMET or mutant cMETs (T1010I, Y1253D) **B.** PIK3CA-H1047R cells expressing wild type or mutant cMETs (T1010I, Y1253D). **C.** Cells expressing only wild type cMET or mutant cMETs (T1010I, Y1253D). (a) Photos were taken at day 11. (b) The data are mean \pm standard errors of triplicates, representative of two independent experiments (***, $P < 0.001$ vs control cells; ###, $P < 0.001$ vs WT or T1010I cells; #, $P < 0.05$, ##, $P < 0.01$ vs Y1253D. ANOVA).

cMET-T1010I mutation or cMET overexpression, but not cMET-Y1253D, promotes cell proliferation and invasion in matrigel: Previous studies reported that mutant PIK3CA-E545K and PIK3CA-H1047R altered three-dimensional acinar morphogenesis.(131, 137) Here we assessed the effect of cMET overexpression and its mutations on morphogenesis in MCF-10A cells using the three dimensional matrigel system.(138) MCF-10A cells expressing PIK3CA mutants were used as control. Consistent with the previous reports, MCF10A cell lines expressing PIK3CA E545K or PIK3CA H1047R mutations displayed morphological changes with highly proliferative and mildly abnormal structures, when compared to PIK3CA WT cell line or the parental MCF10A cells (Figure 11A, and data not shown).(131, 137) Intriguingly, MCF10A cells expressing cMET-T1010I formed larger acini that invaded into the surrounding matrix (Figure 11B). The MCF10A cells over-expressing wild type cMET showed similar morphological alterations, but milder than cMET-T1010I cells (Figure 11B). In contrast, cells expressing cMET-Y1253D did not show invasion (Figure 11B).

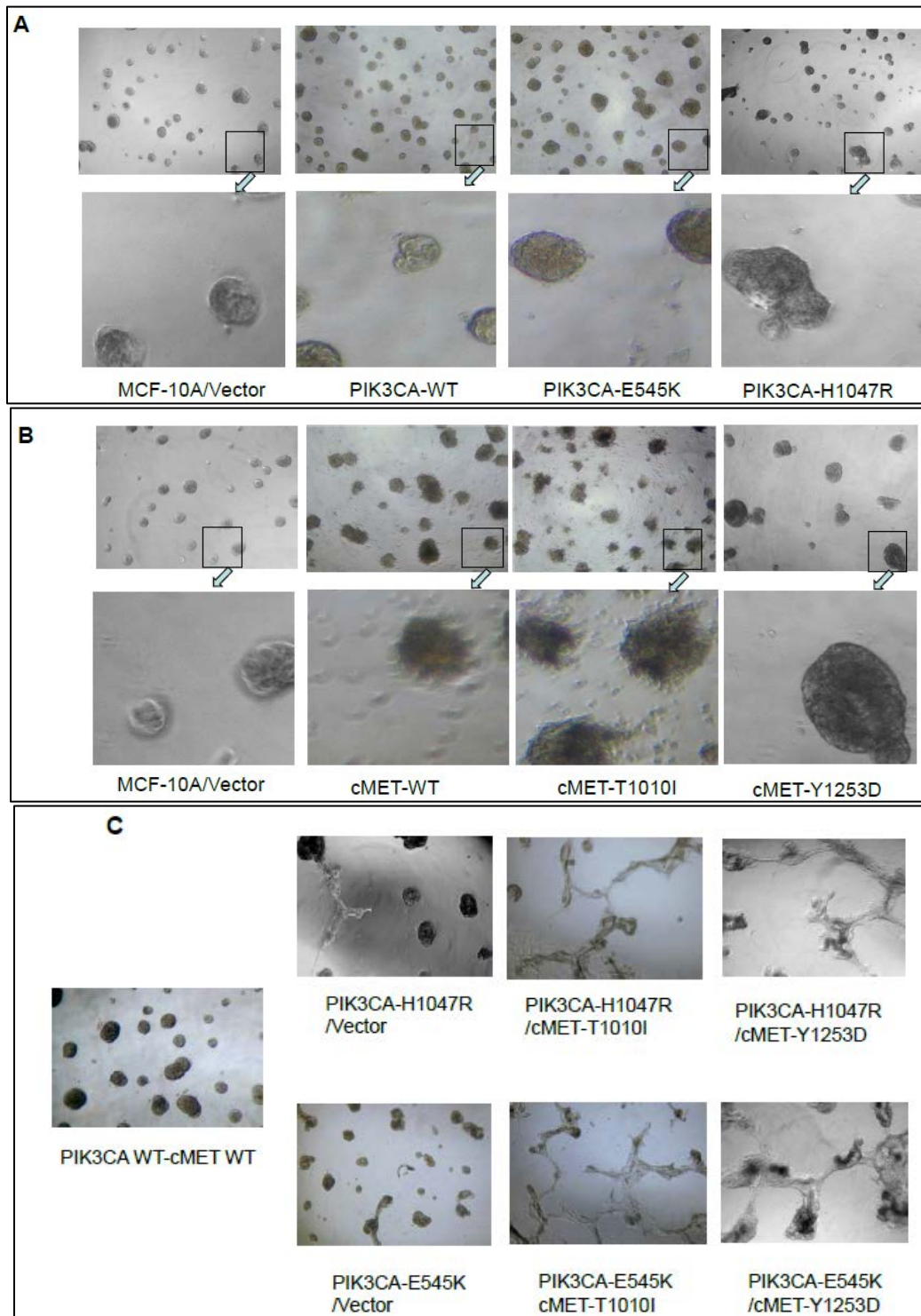


Figure 11. The Effects of cMET or PIK3CA aberrations on Mammary Acinar Morphogenesis

The effects of cMET or PIK3CA aberrations on mammary acinar morphogenesis: MCF10A derived cell lines were cultured on matrigel as described in Materials and Methods. Briefly, 4×10^3 MCF-10A derived cells were resuspended in modified growth medium containing 2% matrigel (BD Biosciences), decreased serum and EGF (2% horse serum, and 5 ng/mL EGF), supplemented with HGF 40 ng/ml. Medium was exchanged every 3 days. Representative bright field images of acini were taken on day 8; original magnification, X40. **A.** MCF-10A derived cells expressing PIK3CAs. **B.** MCF-10A derived cells expressing cMETs. **C.** MCF-10A derived cells expressing wild type PIK3CA/cMET or double mutants.

Co-aberrations in *cMET* /*PIK3CA* (wild type overexpression and double mutations) act in concert to induce alterations in mammary acinar morphogenesis: We further evaluated the effect of *cMET*/*PIK3CA* wild type overexpression and double mutations on mammary acinar morphogenesis. As expected, marked abnormal structures were observed in MCF-10A cells expressing *PIK3CA*-E545K and *cMET* T1010I (*PIK3CA*-E545K/*cMET*-T1010I), or *cMET*-Y1253D (*PIK3CA*-E545K/*cMET*-Y1253D) (Figure 11C). Similar results were detected in *PIK3CA*-H1047R/*cMET*-T1010I and *PIK3CA*-H1047R/*cMET*-Y1253D cells (Figure 11C). The overexpression of wild type *cMET* and *PIK3CA* in MCF-10A cells had a similar but milder effect when compared to the double mutants.

The effects of different *cMET* or *PIK3CA* mutations on cell invasion: To evaluate whether cancer-associated *cMET* mutants or overexpression of wild type *cMET*, and different *PIK3CA* mutations, contribute to cell invasion, we performed a systematic invasion assay by seeding different MCF10A-derived cell lines using invasion chambers, as described in the Methods. We observed that *cMET* mutations (T1010I and Y1253D) significantly increased cell invasion ability ($P < 0.001$), with the T1010I mutant higher than Y1253D ($P < 0.001$). *PIK3CA* mutations (E545K, H1047R) mildly enhanced cell invasion. Intriguingly, the *cMET* T1010I mutation combined with the *PIK3CA* mutation significantly increased the cell invasion ability, when compared to the other MCF-10A cell lines used in this study ($P < 0.001$) (Figure 12). The parental MCF10A cells did not display cell invasiveness, nor did the MCF10A cells with the wild type *cMET* and wild type *PIK3CA*. (Figure 12A, B).

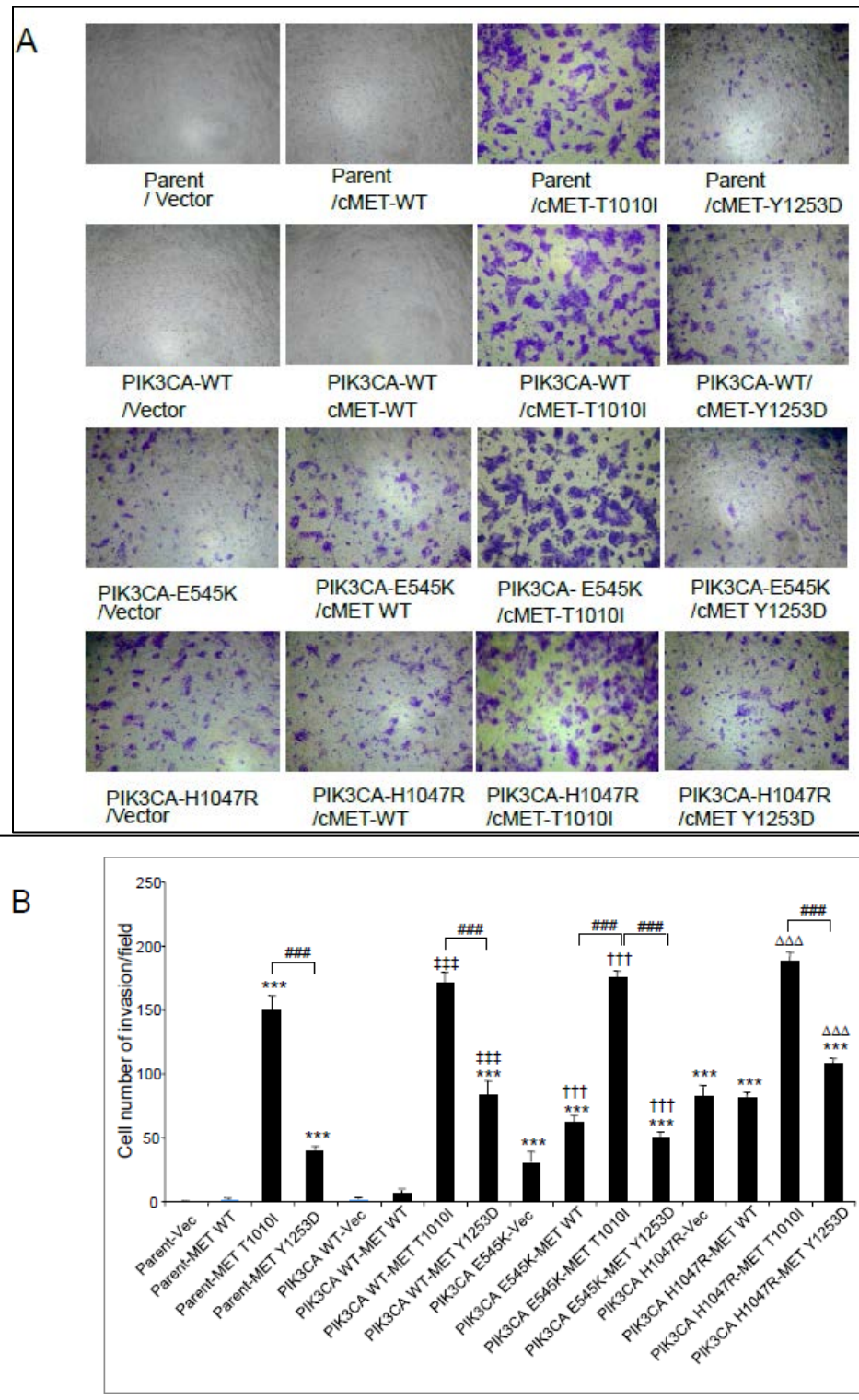


Figure 12. The Effects of cMET and/or PIK3CA overexpression or mutations on Cell Invasion
 The effects of cMET and/or PIK3CA overexpression or mutations on cell invasion: **A**. Cell invasion *in vitro* was analyzed as indicated in Materials and Methods. MCF-10A derived cells invaded through matrigel. The cells were photographed at X100 magnification. **B**. The data are mean \pm standard errors of triplicates, representative of two independent experiments (***, vs parent-vector, $P < 0.0001$; †††, $P < 0.0001$ vs PIK3CA WT-vector; †††, $P < 0.0001$ vs PIK3CA E545K-vector; ΔΔΔ, $P < 0.0001$ vs PIK3CA H1047R-vector).

Effect of *cMET/PIK3CA* mutations on cell signaling: To evaluate the effects of *cMET* and/or *PIK3CA* mutations on cell signaling, we tested the expression level and/or phosphorylation levels of cMET and PI3Kp110 and their downstream targets, including AKT, S6, MAPK and Stat3 with Western blotting. As expected, levels of phosphorylated AKT and S6 were much higher in cells expressing mutant *PIK3CA*-E545K or *PIK3CA*-H1047R, compared to parental MCF-10A cells and the wild type *PIK3CA* cell line (Figure 13). Incubation with HGF did not substantively alter AKT phosphorylation in any of the lines.

Also as expected, endogenous cMET expression in each cell line and exogenous cMET-Flag expression in cMET-transfected cell lines were observed in the absence of HGF. However, Y1253D cMET was expressed at lower levels in all lines. The reason for the decreased levels of Y1253D is not known. Strikingly, levels of exogenous cMET were markedly lower in cells expressing either of the activated *PIK3CA* constructs. This was associated with high levels of phosphorylation of exogenous and wild type cMET. This is an unexpected observation that suggests that the activated *PIK3CA*s increase cMET phosphorylation through an as yet unknown mechanism and lead to degradation of cMET.

40 minutes of incubation with HGF increased phosphorylation of endogenous cMET under all conditions. Further in the presence of *PIK3CA* WT or mutants, phosphorylation of endogenous cMET was increased in the Y1253D construct. Surprisingly, HGF did not increase phosphorylation of exogenous cMET except for wild type cMET in the presence of mutant *PIK3CA*. Intriguingly, this was associated with an increase in endogenous cMET. Unexpectedly, in the presence of HGF in cells expressing exogenous cMETT1010I, neither exogenous nor endogenous cMET was phosphorylated. Indeed, this was associated with a lack of pMAPK in cells expressing cMET T1010I. The results with MAPK phosphorylation were difficult to explain. It appears that under basal conditions that wild type and T1010I MET result in a decrease in pMAPK in parent cells and in the presence of WT *PIK3CA*. This is not seen in the presence of mutant *PIK3CA* potentially due to the increase pcMET noted above. In the presence of HGF pMAPK and pMET with endogenous or endogenous were similar. This suggests that the pMET signal is transmitted successfully to pMAPK.

Together the data is not as expected and suggests complex interactions between *PIK3CA* and MET that warrant extensive further investigation.

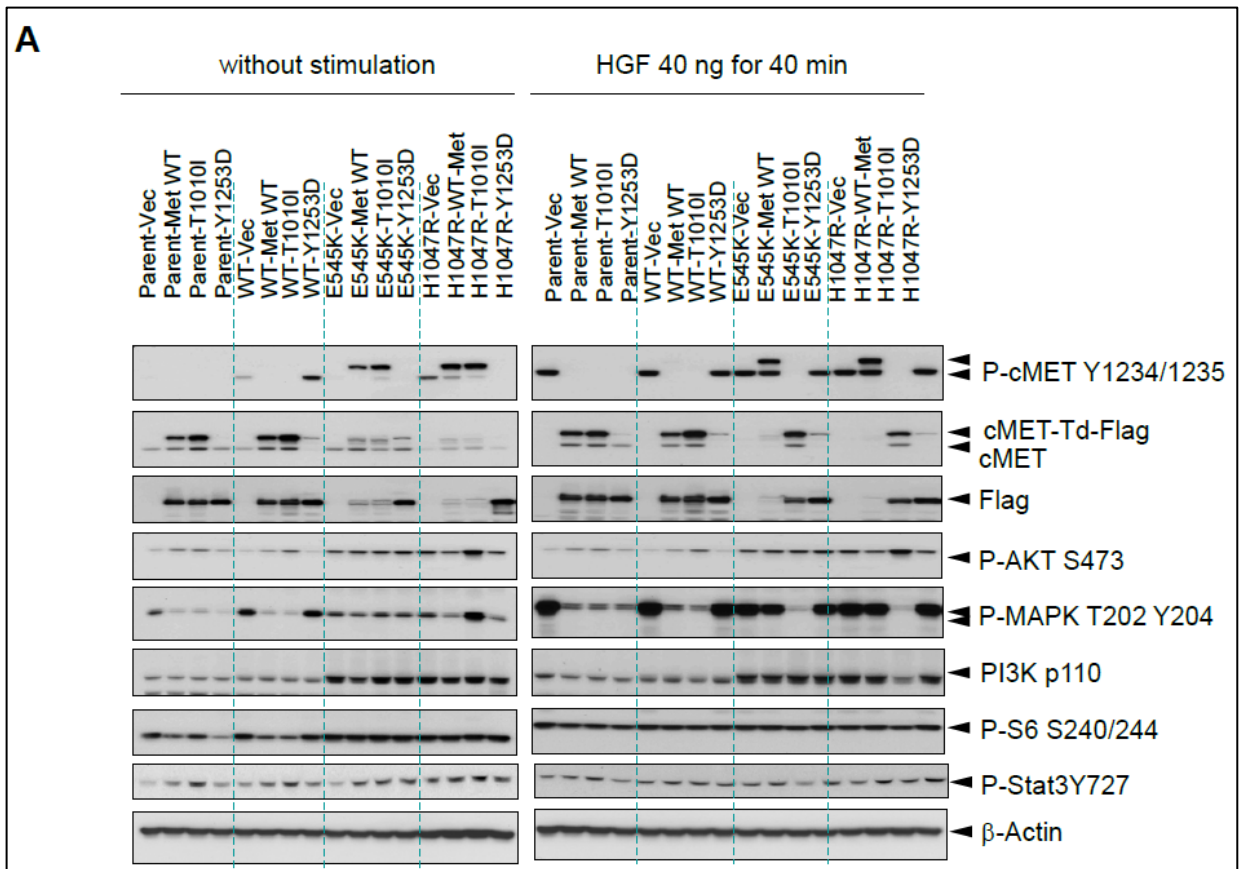


Figure 13. The Effect of mutant and wild type cMET and /or PIK3CA on Cell Signaling

The effect of mutant and wild type cMET and /or PIK3CA on cell signaling: MCF-10A derived cells expressing PIK3CA wild type (WT) or mutants (E545K, H1047R), with or without expression of wild type cMET or mutants (T1010I, Y1253D), were starved over-night, followed by stimulation with HGF, FBS or EGF at indicated doses and time, respectively. And then cell lysates were collected and loaded for Western blot with antibodies, as indicated. β -actin was used as a loading control. **A.** Without stimulation (left panel); stimulated with HGF (right panel).

MODELS	Cell Proliferation Assay
	Effects
MCF-10A-LacZ Vector	
MCF-10A-PIK3CA WT	
MCF-10A- PIK3CA E545K	
MCF-10A- PIK3CA H1047R	
MCF-10A- Tomato Vector	Control
MCF-10A- MET WT	High; significant increase $P < 0.001$ vs control
MCF-10A- MET T1010I	High; significant increase $P < 0.001$ vs control
MCF-10A- MET Y1253D	Highest; significant increase $P < 0.001$ vs control
LacZ vector-Tomato Vector	
LacZ vector-MET WT	
LacZ vector-MET T1010I	
LacZ vector-MET Y1253D	
PIK3CA WT- Tomato Vector	

PIK3CA WT- MET WT	
PIK3CA WT- MET T1010I	
PIK3CA WT- MET Y1253D	
PIK3CA E545K- Tomato Vector	Control (Expression of PIK3CA-E545K only)
PIK3CA E545K- MET WT	High; significant increase P<0.001 vs control; P<0.01 vs MET WT alone
PIK3CA E545K- MET T1010I	High; significant increase P<0.001 vs control
PIK3CA E545K- MET Y1253D	Highest; significant increase P<0.001 vs control; P<0.01 vs MET Y1253D alone
PIK3CA H1047R- Tomato Vector	Control
PIK3CA H1047R- MET WT	High; significant increase P<0.001 vs control; P<0.001 vs MET WT alone
PIK3CA H1047R- MET T1010I	High; significant increase P<0.001 vs control; P<0.001 vs MET T1010I alone
PIK3CA H1047R- MET TY1253D	Highest; significant increase P<0.001 vs control; P<0.001 vs MET Y1253D alone
Conclusion	There could be a possible interaction between aberrant PIK3CA and MET since co-aberrations exhibit increased proliferation
	Colony Formation Assay
MODELS	Effects
MCF-10A-LacZ Vector	
MCF-10A-PIK3CA WT	
MCF-10A- PIK3CA E545K	
MCF-10A- PIK3CA H1047R	
MCF-10A- Tomato Vector	Control
MCF-10A- MET WT	High; significant increase P<0.001 vs control; P<0.05 vs cMET Y1253D only
MCF-10A- MET T1010I	Moderate; significant increase P<0.001 vs control; P<0.01 vs cMET Y1253D only
MCF-10A- MET Y1253D	Highest; significant increase P<0.001 vs control
LacZ vector-Tomato Vector	
LacZ vector-MET WT	
LacZ vector-MET T1010I	
LacZ vector-MET Y1253D	
PIK3CA WT- Tomato Vector	
PIK3CA WT- MET WT	
PIK3CA WT- MET T1010I	
PIK3CA WT- MET Y1253D	
PIK3CA E545K- Tomato Vector	Control Group
PIK3CA E545K- MET WT	High; significant increase P<0.001 vs control
PIK3CA E545K- MET T1010I	High; significant increase P<0.001 vs control
PIK3CA E545K- MET Y1253D	Highest; significant increase P<0.001 vs control, P<0.001 vs WT or T1010I
PIK3CA H1047R- Tomato	Control Group

Vector	
PIK3CA H1047R- MET WT	High; significant increase P<0.001 vs control
PIK3CA H1047R- MET T1010I	High; significant increase P<0.001 vs control
PIK3CA H1047R- MET TY1253D	Highest; significant increase P<0.001 vs control, P<0.001 vs WT or T1010I
Conclusion	There could be a possible interaction between aberrant PIK3CA and MET since co-aberrant cells exhibit increased cell survival
	Mammary Acinar Morphogenesis
MODELS	Effects
MCF-10A-LacZ Vector	Control Group
MCF-10A-PIK3CA WT	No Effect
MCF-10A- PIK3CA E545K	Displayed Highly proliferative and mildly abnormal structures
MCF-10A- PIK3CA H1047R	Displayed Highly proliferative and mildly abnormal structures
MCF-10A- Tomato Vector	control Group
MCF-10A- MET WT	Effect milder than MCF-10A- MET T1010I
MCF-10A- MET T1010I	Formed largest acini that invaded into surrounding matrix
MCF-10A- MET Y1253D	Didn't show invasion
LacZ vector-Tomato Vector	
LacZ vector-MET WT	
LacZ vector-MET T1010I	
LacZ vector-MET Y1253D	
PIK3CA WT- Tomato Vector	
PIK3CA WT- MET WT	Abnormal structures were formed; milder than PIK3CA/MET double mutant cells
PIK3CA WT- MET T1010I	
PIK3CA WT- MET Y1253D	
PIK3CA E545K- Tomato Vector	Control Group
PIK3CA E545K- MET WT	
PIK3CA E545K- MET T1010I	Marked abnormal structures were formed
PIK3CA E545K- MET Y1253D	Marked abnormal structures were formed
PIK3CA H1047R- Tomato Vector	Control Group
PIK3CA H1047R- MET WT	
PIK3CA H1047R- MET T1010I	Marked abnormal structures were formed
PIK3CA H1047R- MET TY1253D	Marked abnormal structures were formed
Conclusion	There could be a possible interaction between aberrant PIK3CA and MET, since co-aberrant cells exhibit markedly abnormal structures
	Cell Invasion
MODELS	Effects

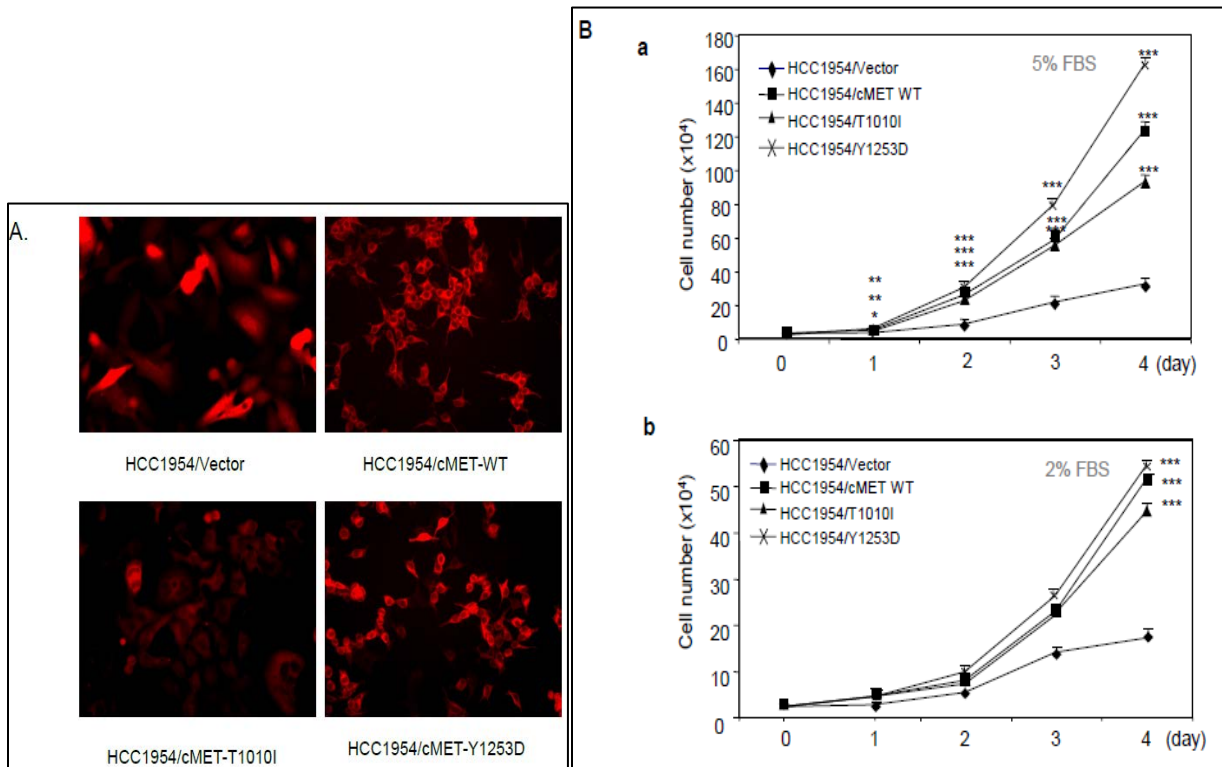
MCF-10A-LacZ Vector	Control Group
MCF-10A-PIK3CA WT	
MCF-10A- PIK3CA E545K	
MCF-10A- PIK3CA H1047R	
MCF-10A- Tomato Vector	Control Group
MCF-10A- MET WT	No Effect
MCF-10A- MET T1010I	High; significant increase P<0.0001 vs control
MCF-10A- MET Y1253D	Mild; significant increase P<0.0001 vs control
LacZ vector-Tomato Vector	
LacZ vector-MET WT	
LacZ vector-MET T1010I	
LacZ vector-MET Y1253D	
PIK3CA WT- Tomato Vector	Insignificant Effect
PIK3CA WT- MET WT	Insignificant Effect
PIK3CA WT- MET T1010I	High; significant increase P<0.0001 vs PIK3CA WT-Tomato Vector
PIK3CA WT- MET Y1253D	Mild; significant increase P<0.0001 vs PIK3CA WT-Tomato Vector
PIK3CA E545K- Tomato Vector	Mild; significant increase P<0.0001 vs control
PIK3CA E545K- MET WT	Mild; significant increase P<0.0001 vs PIK3CA E545K-Tomato Vector
PIK3CA E545K- MET T1010I	Highest; significant increase P<0.0001 vs PIK3CA E545K-Tomato Vector
PIK3CA E545K- MET Y1253D	Mild; significant increase P<0.0001 vs PIK3CA E545K-Tomato Vector
PIK3CA H1047R- Tomato Vector	Mild; significant increase P<0.0001 vs control
PIK3CA H1047R- MET WT	Mild; significant increase P<0.0001 vs control
PIK3CA H1047R- MET T1010I	Highest; significant increase P<0.0001 vs PIK3CA H1047R-Tomato Vector
PIK3CA H1047R- MET TY1253D	Mild; significant increase P<0.0001 vs PIK3CA H1047R-Tomato Vector
Conclusion	There could be a possible interaction between MET-Y1253D and PIK3CA-mutant, since the double mutants exhibit increased invasion when compared to cells expressing MET-Y1253D alone or PIK3CA-mutant alone.

Table 9. Summarizing the Effects of PIK3CA and MET aberrations on mammary epithelial cells
Summarizing the effects of PIK3CA and MET aberrations on mammary epithelial cells. MET WT and PIK3CA WT represent overexpression of Wild Type MET and Wild Type PIK3CA, respectively.

Taken together, our data suggested that cMET overexpression or cancer-associated mutations (T1010I, Y1253D) can act as oncogenes to promote cell growth, focus formation (Y1253D stronger than T1010I), anchorage-independent survival/proliferation and invasion (T1010I stronger than Y1253D). cMET overexpression or mutation, and *PIK3CA* mutation,

act in concert to transform mammary epithelial cells (Table 9).

cMET mutation or overexpression increases cell proliferation in the PIK3CA-mutated breast cancer cell line: To further verify our findings, as described in the Methods, we established four stable cell lines that expressed mutant cMETs (T1010I, Y1253D), wild type cMET or Td Tomato in HCC1954 cells, a breast cancer cell line with mutant PIK3CA at H1047R. The specific expression of infected genes was observed (Figure 14A). To detect the effect of the cMET mutations or the overexpression of the wild type cMET, on cell proliferation, we cultured the cells in low serum medium as indicated. HCC1954 cells, expressing the cMET mutants (T1010I, Y1253D), exhibited significantly higher proliferation ability than the control cells ($P < 0.001$). Interestingly, the HCC1954 cells overexpressing wild type cMET also significantly increased proliferation, even higher than the ones expressing cMET-T1010I. Among these cell lines, the HCC1954 cells expressing the cMET-Y1253D mutation exhibited the highest growth rate (Figure 14B).



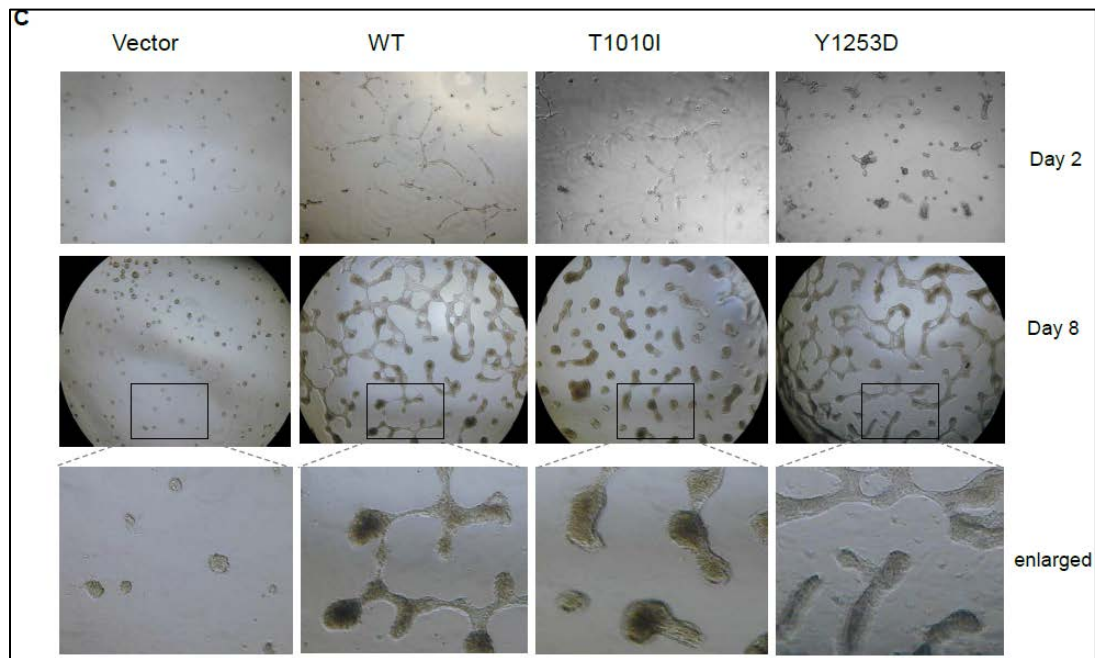


Figure 14. Effects of mutant and wild type cMET on cell proliferation in PIK3CA-mutated breast cancer cells

Effects of mutant and wild type cMET on cell proliferation in PIK3CA-mutated breast cancer cells: We established stable cell lines expressing wild type or mutant cMETs (T1010I, Y1253D) based on the PIK3CA-mutated breast cancer cell line, HCC1954, using the same method that was used to establish MCF-10A derived cells. **A.** Specific protein expressions **B.** Effect of overexpression of wild type cMET or expression of mutant cMETs on cell growth. HCC1954 derived cells were seeded in 12-well plates at 2×10^4 cells per well, in 5% FBS (a) or 2.5% FBS (b) for 4 days. Cell numbers were counted for each day indicated. Each experiment was done with triplicate wells. The data are mean \pm standard errors of triplicates, representative of two independent experiments (*, $P < 0.05$; **, $P < 0.01$; ***, $P < 0.001$ vs control cells, ANOVA). **C.** Effect of overexpression of wild type cMET or expression of mutant cMETs on cell growth in matrigel; original magnification, X40.

cMET mutations or overexpression of wild type cMET induces alteration of mammary acinar morphogenesis in the PIK3CA-mutated breast cancer cell line: We further detected if cMET mutation or overexpression affect cell growth of HCC1954 cells in matrigel. Our data indicated that both expression of mutant cMET (T1010I, Y1253D) and overexpression of wild type cMET induced morphological changes with high proliferation and abnormal structures (Figure 14C).

cMET mutation or overexpression enhances cell survival in the PIK3CA-mutated breast cancer cell line, in basic culture and soft agar: To verify if the combination of cMET overexpression or mutations with PIK3CA mutations contributed to cell survival, we performed clonogenic assay and soft agar assay using HCC1954 cells expressing wild type or mutant cMET-T1010I and cMET-Y1253D. We found that both overexpression of wild type cMET and expression of mutant cMET T1010I or Y1253D significantly increased colony formation when

compared to the control cells ($P < 0.001$, respectively). The effect of Y1253D was the strongest, while the T1010I mutation and overexpression of wild type cMET showed similar effects ($P > 0.05$) (Figure 15A). We further tested the ability of anchorage-independent growth in these cell lines. The control cells did not form colonies under this condition. However, cells expressing mutant cMETs (T1010I, Y1253D) or overexpressing wild type cMET formed colonies in soft agar (Figure 15B). There were significant differences in the effects when compared to the control cells ($P < 0.0001$, respectively). Among these cell lines, the cells expressing cMET-T1010I exhibited higher survival than the ones with cMET-Y1253D ($P < 0.01$) or wild type cMET ($P < 0.05$), in soft agar.

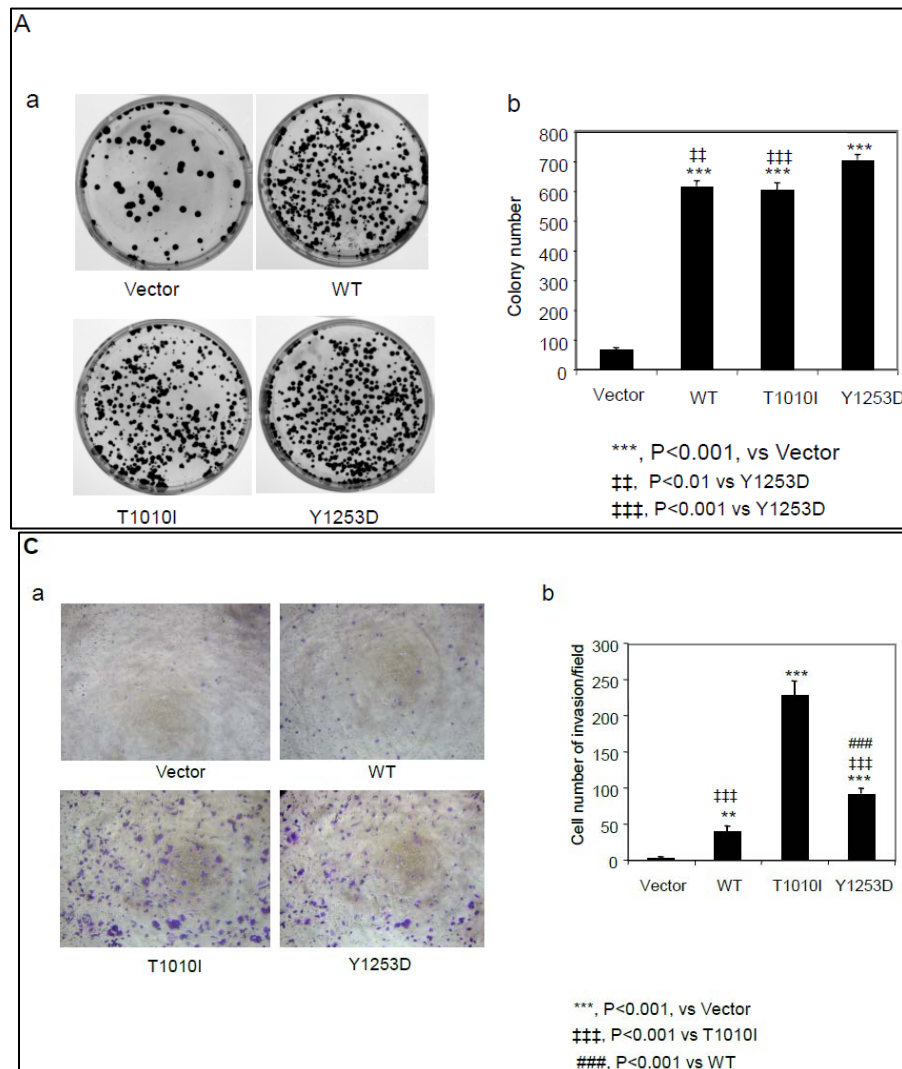


Figure 15. Effects of mutant and wild type cMET on cell survival and anchorage-independent proliferation in PIK3CA-mutated breast cancer cells

Effects of mutant and wild type cMET on cell survival and anchorage-independent proliferation in PIK3CA-mutated breast cancer cells: **A**. Clonogenic assay was analyzed as explained in Material and Methods. HCC1954 derived cells were seeded in triplicates with a density of 1000 cells/60 mm-petri

dish. Cells were cultured in 5% FBS. **A.** Photos were taken at day 10 (a). The data are mean \pm standard errors of triplicates, representative of two independent experiments (***, $P < 0.001$ vs control cells; ††, $P < 0.01$, †††, $P < 0.001$ vs Y1253D cells, ANOVA) (b). **B.** Soft agar assay was analyzed as explained in Material and Methods. 2×10^4 HCC1954 derived cells were suspended in complete growth medium containing 0.3% soft agar and seeded in triplicates on 60-mm dishes precoated with 0.6% agar, in 5% FBS growth medium and incubated at 37°C, 5% CO₂. After 8 days, colonies were photographed and counted in 10 randomly chosen fields and expressed as means of triplicates, representative of three independent experiments (a). The data are mean \pm standard errors of triplicates, representative of two independent experiments (***, $P < 0.001$ vs control cells; †, $P < 0.05$, ††, $P < 0.01$ vs T1010I cells, ANOVA) (b). **C.** *In vitro* cell invasion assay was analyzed as explained in the Materials and Methods. HCC1954 derived cells invaded through the matrigel. The cells were photographed at X100 magnification (a). The data are mean \pm standard errors of triplicates, representative of two independent experiments (**, $P < 0.01$; ***, $P < 0.0001$ vs parent-vector; †††, $P < 0.0001$ vs T1010I cells; ###, $P < 0.0001$ vs cMET-WT).

Cancer-associated mutant cMETs induce invasion of the *PIK3CA*-mutated breast cancer cells: To evaluate whether cancer-associated cMET mutants or overexpression of wild type cMET in *PIK3CA* mutant HCC1954 cells contributed to cell invasion, we performed an invasion assay. Consistent with the finding in MCF10A cells, c-MET mutations (T1010I and Y1253D) significantly increased cell invasion ($P < 0.001$), with HCC1954/cMET- T1010I cells displaying higher invasion than the HCC1954/cMET-Y1253D cells ($P < 0.001$). Overexpression of wild type cMET mildly induced cell invasion ($P < 0.01$) (Figure 15 C).

Effects of expression of mutant *cMETs* or overexpression of wild type *cMET* in *PIK3CA*-mutated breast cancer cells, on tumor progression in hHGF transgenic mice: Our *in vitro* studies demonstrated that the expression of cancer-associated *cMET* mutants (T1010I, Y1253D) or overexpression of wild type cMET induced aggressive phenotypes (with higher proliferation, survival, invasion) in breast cancer cells with *PIK3CA*-H1047R mutation. To detect the properties induced by cMETs *in vivo*, we established tumor xenograft models in human HGF transgenic mice (a gift from Dr. G. F. Vande Woude, Van Andel Research Institute, Grand Rapids, MI)(139) using HCC1954/cMET-WT, HCC1954/cMET-T1010I, HCC1954/cMET-Y1253D, and HCC1954/Td Tomato vector control cells, (see Methods for details). After cell injection, the latent period is 9 days in the cMET-T1010I group, while the cMET-Y1253D and cMET-WT groups had longer latent periods (12 days). Control group showed the longest latent period (Figure 16A). The tumor size in cMET-T1010I and cMET-Y1253D groups was larger than that in the cMET-WT and control groups ($P < 0.05$, respectively). Tumor size of the cMET-WT group was mildly larger than that of the control group (Figure 16A). On day 14, the mice were sacrificed. Xenograft tumors and all organs of each mouse were subjected to double-blind histopathological analysis by a veterinary pathologist. Tumor invasion and metastasis were assessed by H&E staining. All tumors from

the cMET-T1010I group showed invasion to adjacent tissues; 2/5 of the tumors from the Y1253D group showed mild invasion that was similar to the control group. Intriguingly, 3/5 of the tumors from cMET-WT group exhibited marked invasion (Figure 16B), although tumor size was smaller than those of the cMET-Y1253D group.

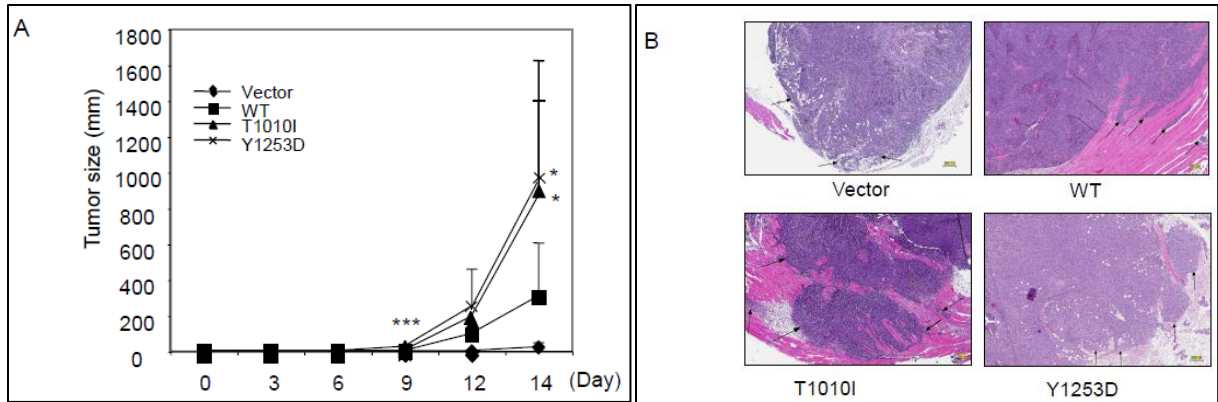


Figure 16. Effects of wild type cMET or its mutants on tumor xenograft formation and progression in hHGF transgenic mice

Effects of wild type cMET or its mutants on tumor xenograft formation and progression in hHGF transgenic mice: A total of 1×10^7 HCC1954 derived cells were injected into the mammary fat pads of hHGF/ SCID transgenic females. Each group consisted of 5 mice. Tumor volume was calculated with the formula ($V = lw^2/2$). Differences in tumor volume among groups at each time point were analyzed using ANOVA (A). On day 14, the mice were sacrificed. Xenograft tumors and all the organs of each mouse were subjected to histopathological analysis by a veterinary pathologist. Tumor invasion to adjacent structures (black arrows) (B).

Effect of the expression of cMET mutations or overexpression of wild type cMET on cell signaling in PIK3CA-mutated breast cancer cells: To evaluate the effects of cMET aberrations on cell signaling in breast cancer cells with the PIK3CA-H1047R mutation, we determined the expression and/or phosphorylation level of multiple molecules of the cMET and PI3K pathways with Western blotting (Figure 17).

As expected, we observed the exogenous cMET expression in each cell line, except control cells. The expression level of exogenous wild type cMET was much higher than the levels of cMET-T1010I or cMET-Y1253D, with cMET-T1010I being lower than cMET-Y1253D. This is surprising given data from others that argues that T1010I stabilizes cMET. Unexpectedly, for as yet unknown reasons, the endogenous cMET level in HCC1954/cMET-Y1253D cells was very low. It is important to note that endogenous cMET levels are near the level of detection and that the apparent decrease may not be significant.

Consistent with the findings in the MCF-10A cell lines, the expression of cMET-T1010I significantly increased phosphorylation of Stat3 with or without stimulation, suggesting

that Stat3 is constitutively active in T1010I cells. Interestingly Src also showed this pattern. Although the overexpression of wild type cMET in HCC1954 cells constitutively increased the phosphorylation of exogenous cMET, elevation of Stat3 phosphorylation was not constitutive, and was inducible with HGF instead. Further pSTAT3 was not detectable in the presence or absence of ligand in cells expressing Y1253D. Interesting, in HCC1954 cells expression of WT cMET did not significantly alter signal transduction to pMAPK. However, cMET T1010I appeared to increase the sensitivity of cells to FBS at least as indicated by pMAPK. Consistent with the unexpected lack of phosphorylation of Y1253D in cells, basal and ligand induced pMAPK was markedly decreased in cells expressing Y1253D cMET. In contrast, expression of wild type or mutant cMET did not significantly affect the PI3K/AKT pathway in HCC1954 cells.

	Cell Proliferation Assay
MODELS	Effects
HCC1954/Tomato Vector	Control
HCC1954/cMET-WT	High; significant increase P<0.001 vs Control
HCC1954/cMET-T1010I	Effect lower than cMET-WT P<0.001 vs Control
HCC1954/cMET-Y1253D	Highest; significant increase P<0.001 vs Control
	Mammary Acinar Morphogenesis
MODELS	Effects
HCC1954/Tomato Vector	Control
HCC1954/cMET-WT	Induced marked abnormal structures
HCC1954/cMET-T1010I	Effect similar to cMET-WT
HCC1954/cMET-Y1253D	Effect similar to cMET-WT
	Clonogenic Assay to test Cell Survival
MODELS	Effects
HCC1954/Tomato Vector	Control
HCC1954/cMET-WT	Significant increase in colony formation; P<0.001 vs Control
HCC1954/cMET-T1010I	Effect similar to cMET-WT; P<0.001 vs Control
HCC1954/cMET-Y1253D	Highest effect (more than cMET T1010I); P<0.001 vs cMET T1010I
	Cell Anchorage Independent Growth
MODELS	Effects
HCC1954/Tomato Vector	Control
HCC1954/cMET-WT	Significant increase in colony formation; P<0.0001 vs Control

HCC1954/cMET-T1010I	Highest effect; P<0.0001 vs Control
HCC1954/cMET-Y1253D	Significant increase in colony formation; P<0.0001 vs Control
MODELS	Cell Invasion
	Effects
HCC1954/Tomato Vector	Control
HCC1954/cMET-WT	Mildly increased cell invasion; P<0.01 vs Control and T1010I
HCC1954/cMET-T1010I	Highest effect; P<0.001 vs Control
HCC1954/cMET-Y1253D	Significantly increased cell invasion; P<0.001 vs Control, T1010I and WT
MODELS	Tumor progression in hHGF transgenic mice
	Latent Period of tumor formation
HCC1954/Tomato Vector	longest latent period
HCC1954/cMET-WT	long latent period (12 days)
HCC1954/cMET-T1010I	shortest latent period (9days)
HCC1954/cMET-Y1253D	long latent period (12 days)
MODELS	Tumor size
HCC1954/Tomato Vector	Control
HCC1954/cMET-WT	Mildly larger than Control; Insignificant
HCC1954/cMET-T1010I	Significantly larger than Control and cMET WT; P<0.05
HCC1954/cMET-Y1253D	Significantly larger than Control and cMET WT; P<0.05
MODELS	Tumor Invasion
HCC1954/Tomato Vector	Control
HCC1954/cMET-WT	Marked invasion by 3/5th of tumors
HCC1954/cMET-T1010I	All tumors showed invasion
HCC1954/cMET-Y1253D	Mild invasion by 2/5th tumors; insignificant

Table 10. Summarizing the Effects of MET aberrations on PIK3CA mutant-HCC1954 cells
Summarizing the effects of *MET* aberrations on *PIK3CA* mutant-HCC1954 cells, and tumor xenograft formation and progression in hHGF transgenic mice. **MET WT represents overexpression of Wild Type MET.**

Taken together, our data from both mammary epithelial cells and *PIK3CA* mutant breast cancer cells, *in vitro* and *in vivo*, suggested that cancer-associated cMET mutations or cMET overexpression alone, or acting coordinately with breast cancer associated *PI3KCA* mutations, promoted cell growth, survival and invasion similar to what would be expected of

oncogenes (Table 10). These findings led us to investigate if deregulation or mutations of cMET affect the response of *PIK3CA* mutant cells to PI3K-targeting drugs.

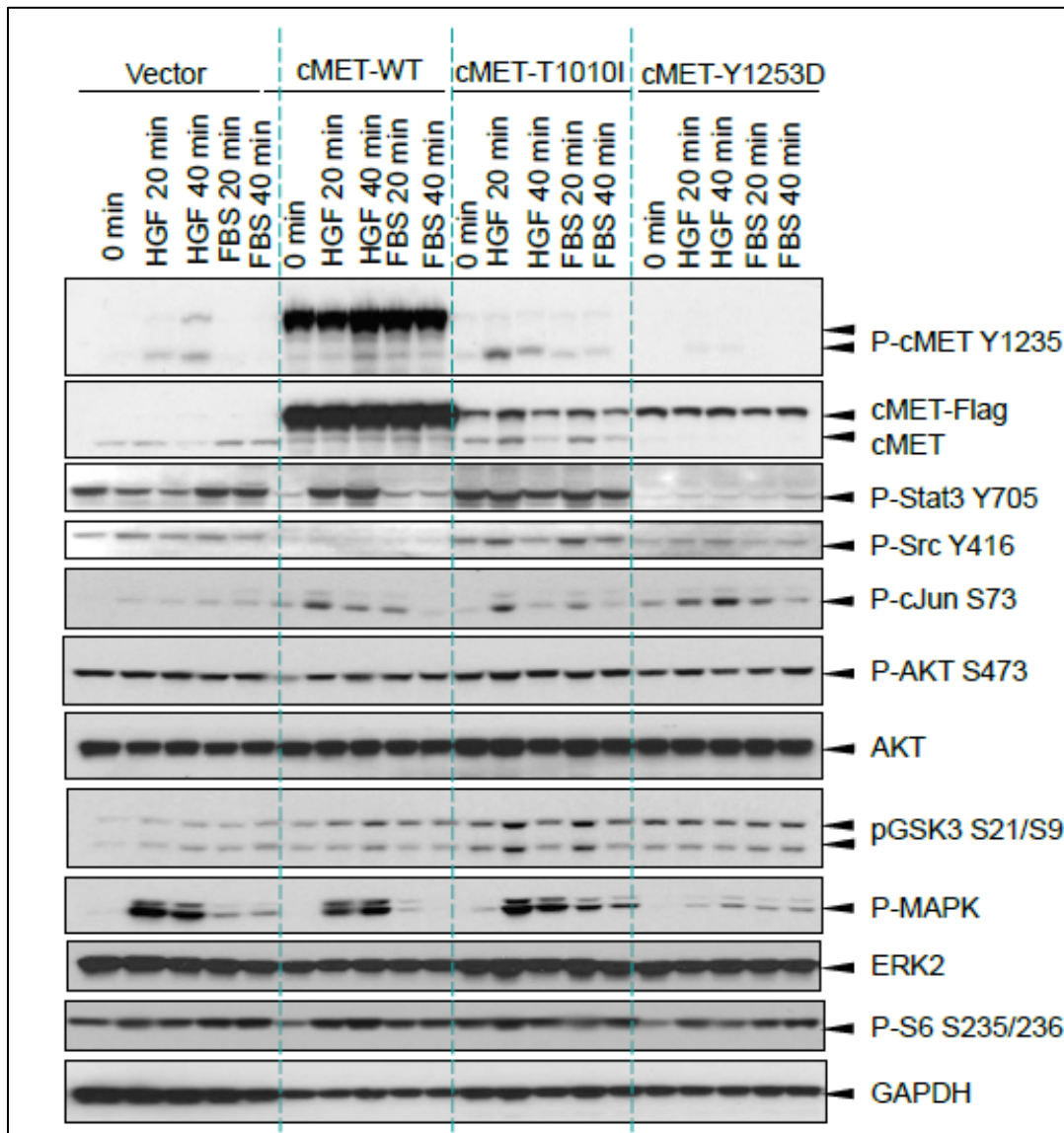


Figure 17. Effect of wild type or mutant cMET on Cell Signaling in *PIK3CA*-mutated breast cancer cells
 The effect of wild type or mutant cMET on cell signaling in *PIK3CA*-mutated breast cancer cells: HCC1954 derived cells as indicated were starved overnight, followed by stimulation with HGF or FBS at indicated doses and time, respectively. Thereafter, the cell lysates were collected and loaded for Western blot with antibodies as indicated. GAPDH was used as a loading control.

Expression of mutant cMET decreases sensitivity to PI3K inhibitor in *PIK3CA*-mutated breast cancer cell: We determined whether HCC1954 cells expressing cMET mutants were more resistant to PI3K inhibitor than control or cMET-WT cells. After 72 hours of exposure to varying concentrations of GDC941 or GDC980 in low serum medium (2% FBS), cells expressing the cMET mutants (T1010I or Y1253D) had higher viability compared to controls, showing decreased sensitivity to GDC941 (GI₅₀: 0.75 μ M and

0.375 μ M respectively) (Figure 18A) and GDC980 (GI50: 0.375 μ M and 0.125 μ M, respectively) (Figure 18B).

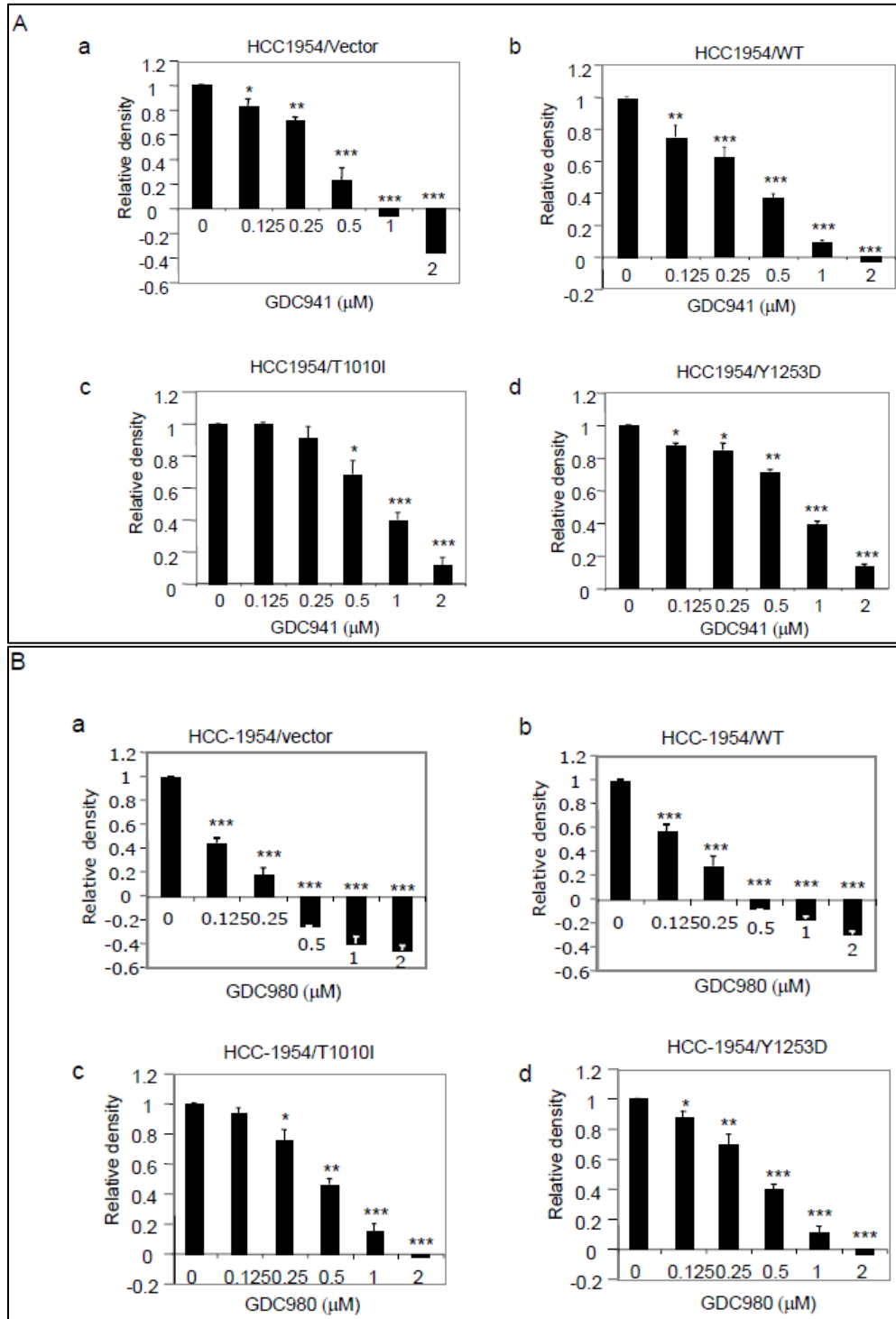


Figure 18. Effects of wild type or mutant cMETs on cell response to PI3K inhibitors in PIK3CA-mutated breast cancer cells

Effects of wild type or mutant cMETs on cell response to PI3K inhibitors in PIK3CA-mutated breast cancer cells: HCC1954 derived cells were seeded in 96-well plates (2,000 cells per well) in complete growth medium and were allowed to attach for 24 hours. The medium was changed to low serum medium (2% FBS). Cells were incubated overnight at 37°C, followed by the addition of serial dilutions of

drugs with variable combinations for 72 hours. Growth inhibition was determined using the CellTiter-Blue and fluorescence was recorded at 560_{Ex}/590_{Em}. Each experiment was repeated at least three times. Results of cell viability were calculated on the basis of percentage change versus vehicle-treated control. **A.** The inhibition effect of GDC941 on HCC1954 derived cells (*, P < 0.05; **, P < 0.01; ***, P < 0.001 vs vehicle) (a-d). **B.** The inhibition effect of GDC980 on HCC1954 derived cells breast cancer cells (*, P < 0.05; **, P < 0.01; ***, P < 0.001 vs vehicle) (a-d).

Effects of targeting PIK3CA and c-MET on cell signaling: First we examined the specificity of targeting compounds. We treated HCC1954/cMET-T1010I, the most aggressive cell line among the cell lines used, with GDC941 (PI3K inhibitor), GDC980 (PI3K/mTor inhibitor), Onartuzumab (cMET monoclonal antibody) and ARQ 197 (a small-molecule inhibitor of cMET as a control of the cMET antibody), followed by stimulation with or without 10% FBS or HGF. Phosphorylation and expression of molecules of cMET and PI3K pathways were evaluated with Western blot (Figure 19). Our data showed that Onartuzumab and ARQ197 inhibited phosphorylation of cMET specifically. GDC941 and GDC980 inhibited the PI3K pathway, as indicated by decreased phosphorylation of AKT, mTOR and S6. Unexpectedly, GDC941 and GDC980 also decreased phosphorylation of cMET. We also noticed that FBS could be used as an inducer for the phosphorylation of the cMET pathway as well as the PI3K pathway, although HGF was more effective than FBS for inducing the phosphorylation of cMET.

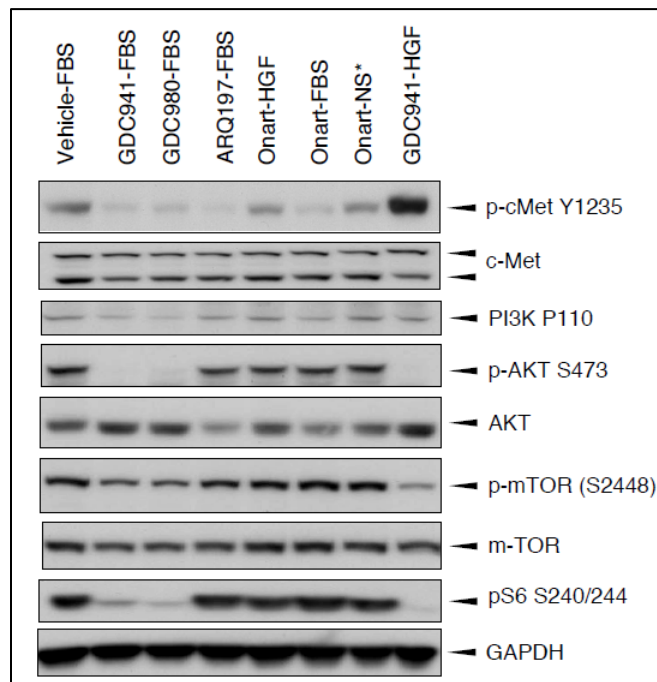
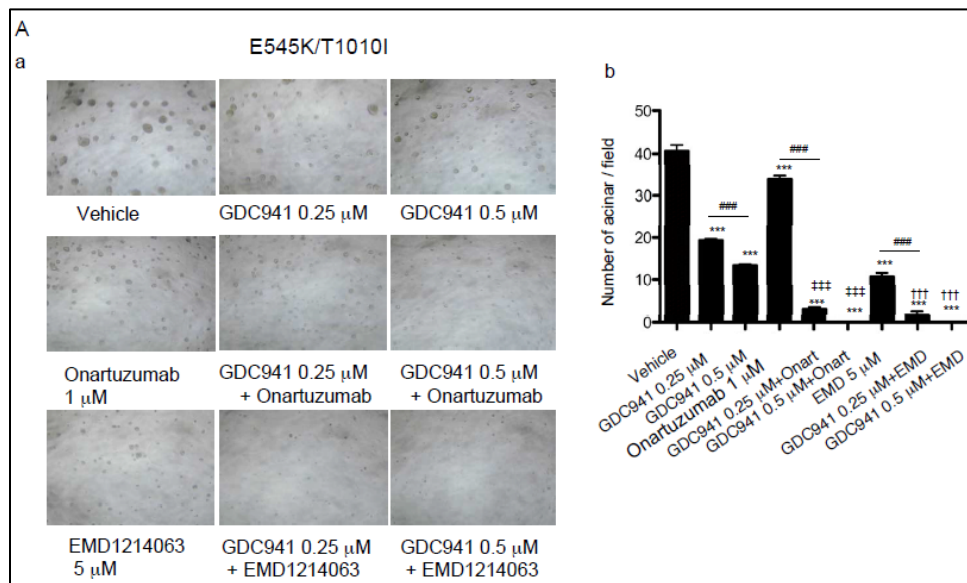
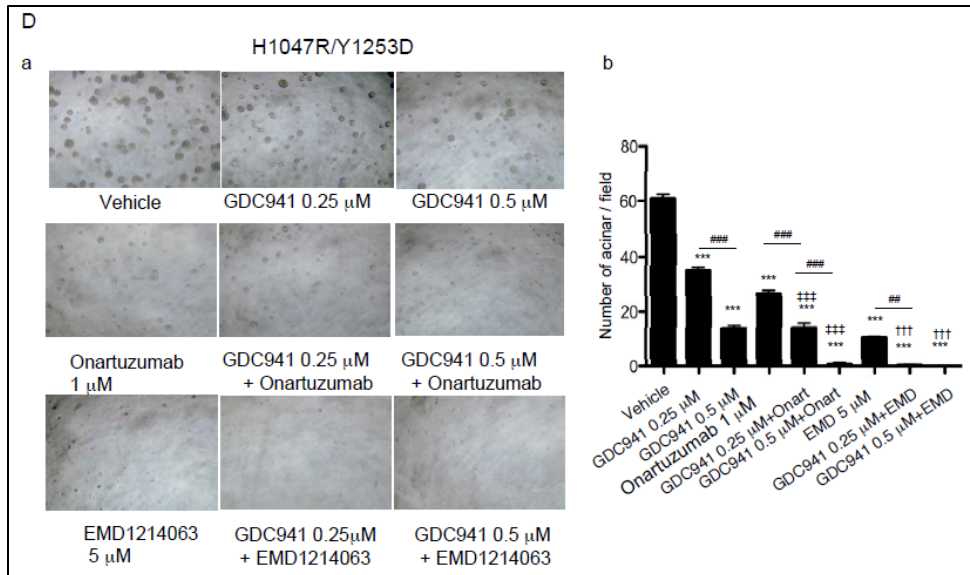
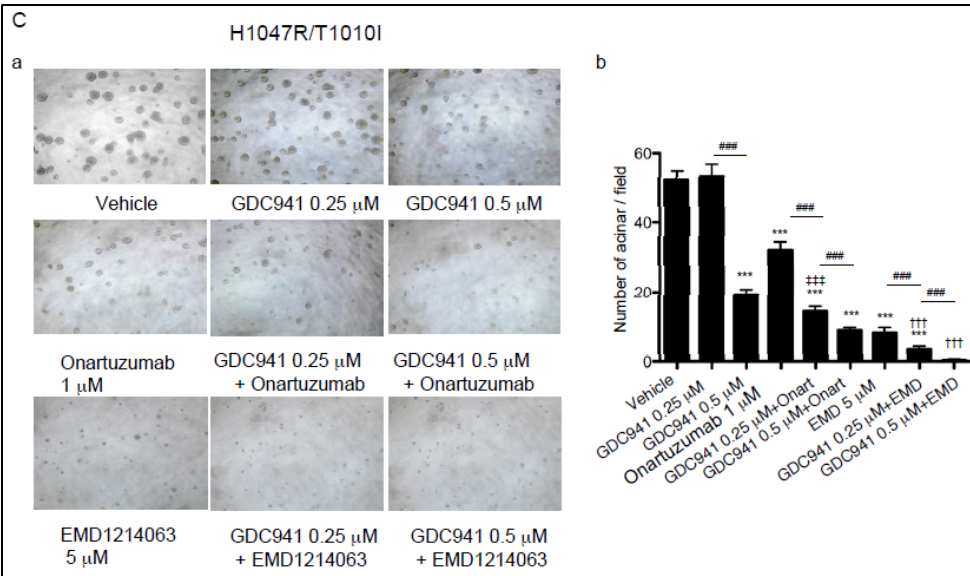
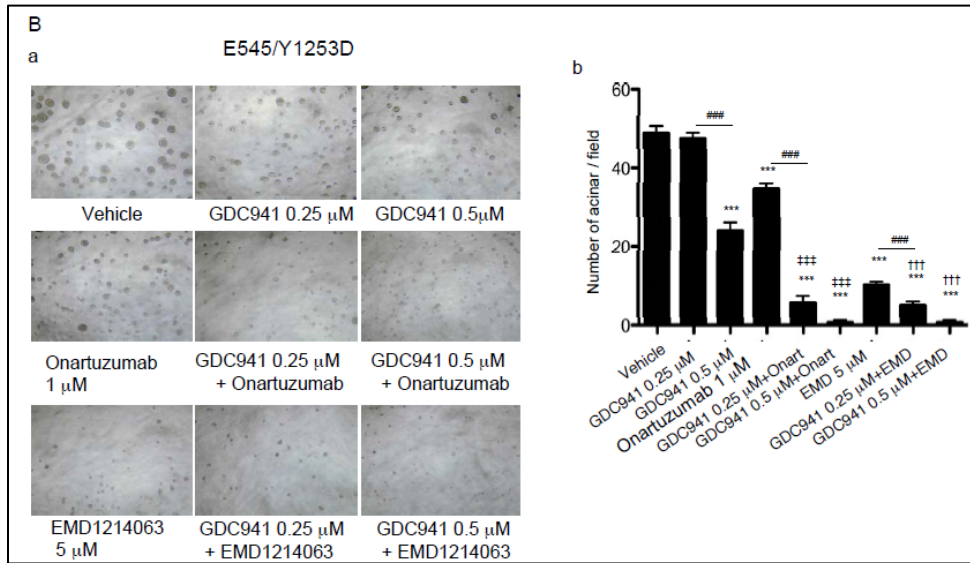


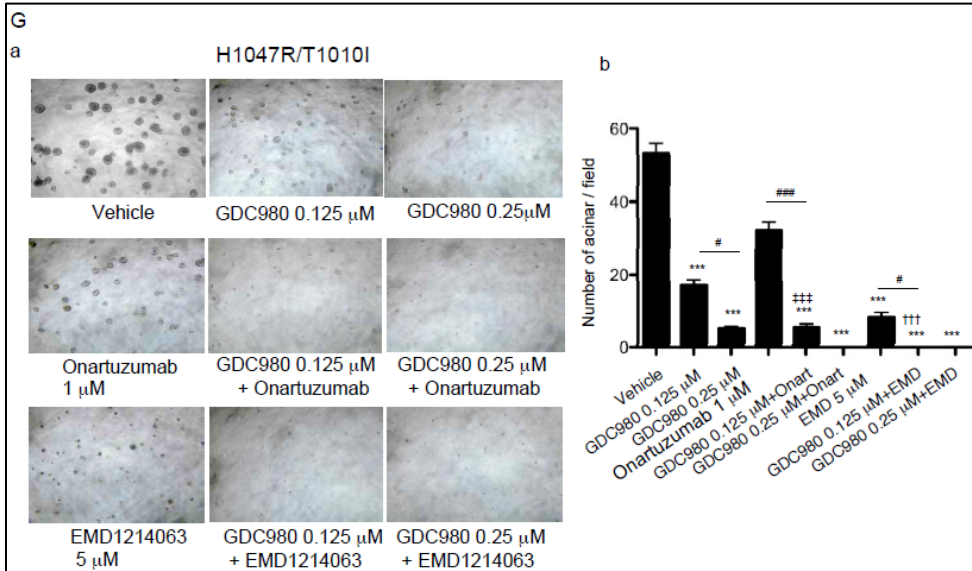
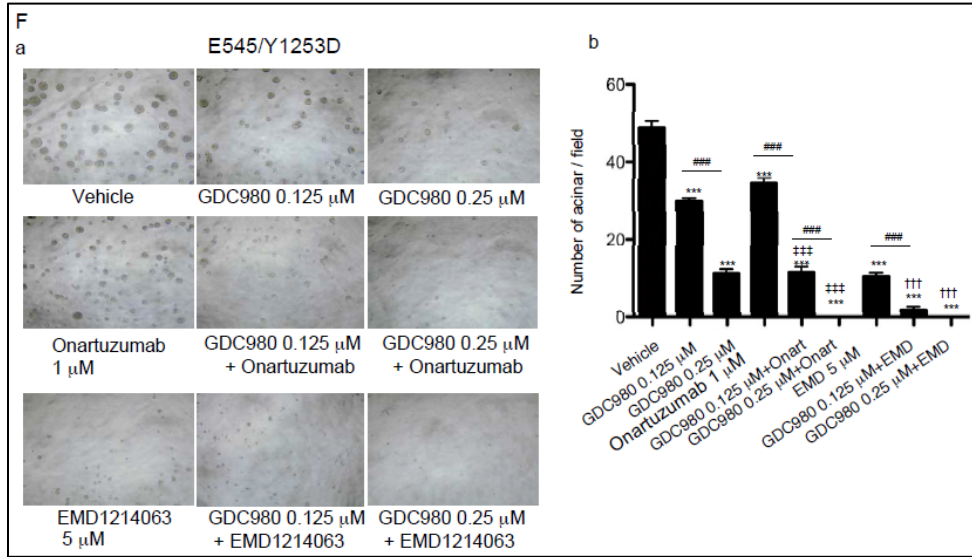
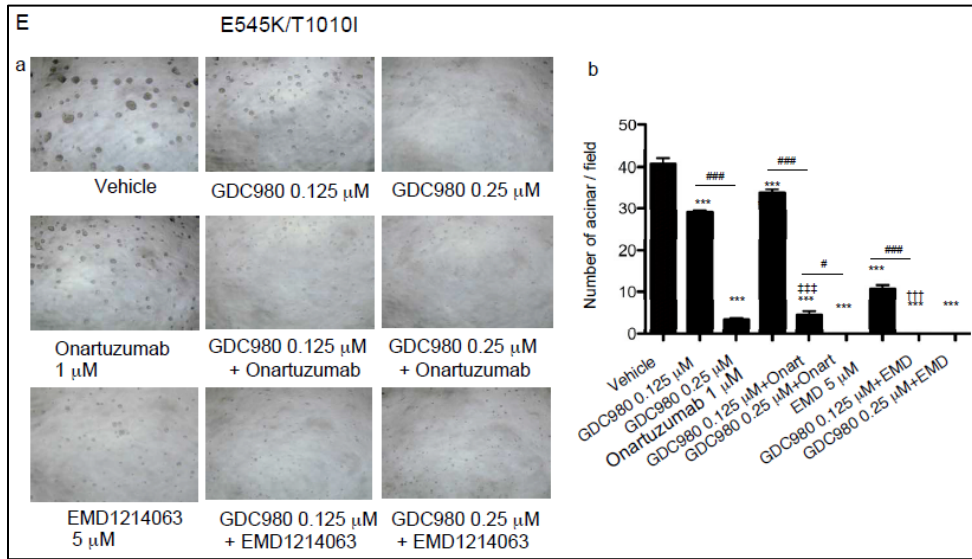
Figure 19. Effects of targeting cMET or PI3K on cell signaling in PIK3CA-mutated breast cancer cell
The effects of targeting cMET or PI3K on cell signaling in PIK3CA-mutated breast cancer cells: Expressing mutant cMET-T1010I conferred HCC1954 cells with the highest survival and invasion ability among the cMET expression cells used in this study. We used this cell line to test the specificity and

activity of inhibitors of cMET or PI3K. HCC1954/cMET-T1010I cells were starved overnight, followed by treatment with drugs as indicated for 6 hours and then stimulated with 10% FBS or HGF (40ng/ml) or left unstimulated (NS) respectively. And then cell lysates were collected and loaded for Western blot with antibodies, as indicated. GAPDH was used as a loading control.

Combination of targeting cMET and PI3K, inhibits cell proliferation in three-dimensional culture in cMET/PIK3CA double mutant mammary epithelial cells: To determine whether targeting cMET and/or PI3K could reverse cell proliferation induced by cMET/PIK3CA double mutants, we treated MCF10A expressing cMET/PIK3CA double mutant cells with Onartuzumab and/or GDC941 and GDC980 using a three-dimensional culture system. The results exhibited that PI3K inhibitor (GDC941) (Figure 20 A-D) or PI3K/mTOR inhibitor (GDC980) (Figure 20 E-H) dose- dependently inhibited the cell growth in 3D culture. Onartuzumab (1 uM) alone mildly inhibited cell growth in 3D culture. Moreover, combination of Onartuzumab and GDC941 or GDC980 significantly increased the inhibitory effects ($P < 0.05-0.001$, respectively as indicated) (Figure 20).







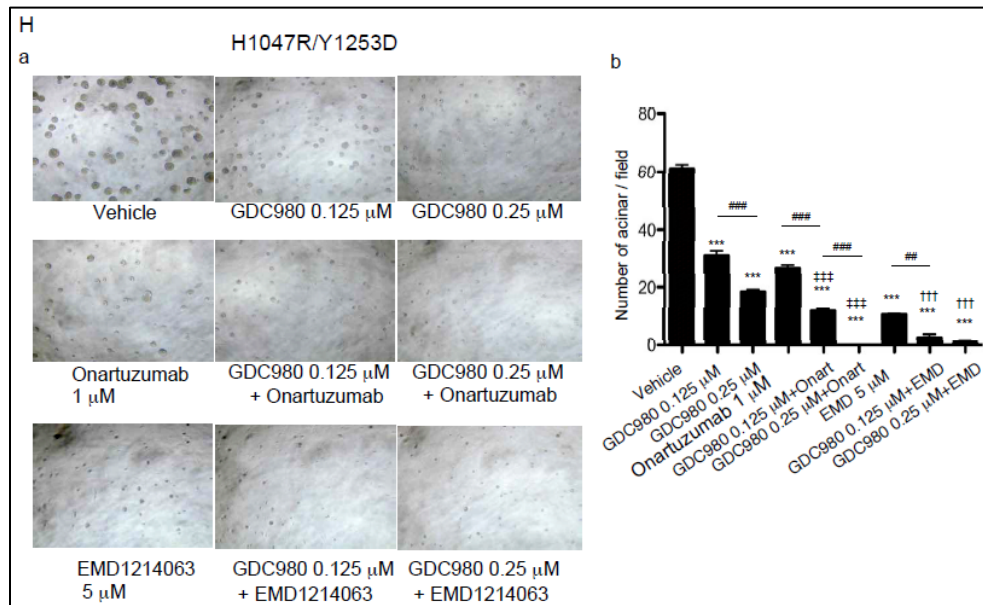


Figure 20. Effects of combinations of PI3K inhibitors with cMET antibody, onartuzumab, or cMET inhibitor, EMD1214063, on Cell Proliferation

Effects of combinations of PI3K inhibitors with cMET antibody, Onartuzumab, or cMET inhibitor, EMD1214063, on cell proliferation in matrigel: MCF10A derived cell lines were cultured on matrigel as described in Materials and Methods. Briefly, 4×10^3 cells were resuspended in modified growth medium lacking EGF, supplemented with hHGF 40 ng/ml, 2.5 % horse serum, 2% growth factor decreased matrigel and variable drugs as indicated. Medium was exchanged every 3 days. E545K/T1010I, E545/Y1253D, H1047R/T1010I and H1047R/Y1253D double mutant cells were treated with GDC941, Onartuzumab, EMD1214063 or variable combinations (A-D), or they were treated with GDC980, Onartuzumab, EMD1214063 or variable combinations (E-H). Photographs (X40) of representative fields were taken on day 7 (a). The data are mean \pm standard errors of triplicates, representative of two independent experiments (b) (***, $P < 0.0001$ vs vehicle; #, $P < 0.05$; ##, $P < 0.01$; ###, $P < 0.001$; †, $P < 0.05$; ††, $P < 0.01$; †††, $P < 0.001$, vs without Onartuzumab addition; †, $P < 0.05$; ††, $P < 0.01$; †††, $P < 0.001$ vs without EMD1214063 addition).

Combination of targeting cMET and PI3K reverses the cell invasion ability induced by cMET/PIK3CA double mutant in mammary epithelial cells: Our data showed that the that the cMET/PIK3CA double mutation enhanced cell invasion compared to the PIK3CA mutation alone, especially the cMET T1010I mutation markedly induced cell invasion (Figure 12). To determine whether targeting PI3K using selective inhibitors (GDC941 and GDC980) and blocking cMET with a specific antibody (Onartuzumab) could reverse the phenotype, we treated the cMET-T1010I/PIK3CA-E545K expressing mammary epithelial cells (Figure 21) with PI3K inhibitor (GDC941) or PI3K/mTOR inhibitor (GDC980), which inhibited the cell invasion in a dose dependent manner in both cell lines. Treatment with Onartuzumab (1.5 μ M) alone, mildly inhibited cell invasion. However, combination with GDC941 or GDC980 significantly increased the inhibitory effects ($P < 0.01-0.001$, respectively as indicated) (Figure 21 A-B). We further verified the findings in HCC1954 cells expressing cMET-T1010I with the same methods, and the results were consistent (Figure 22 A-D).

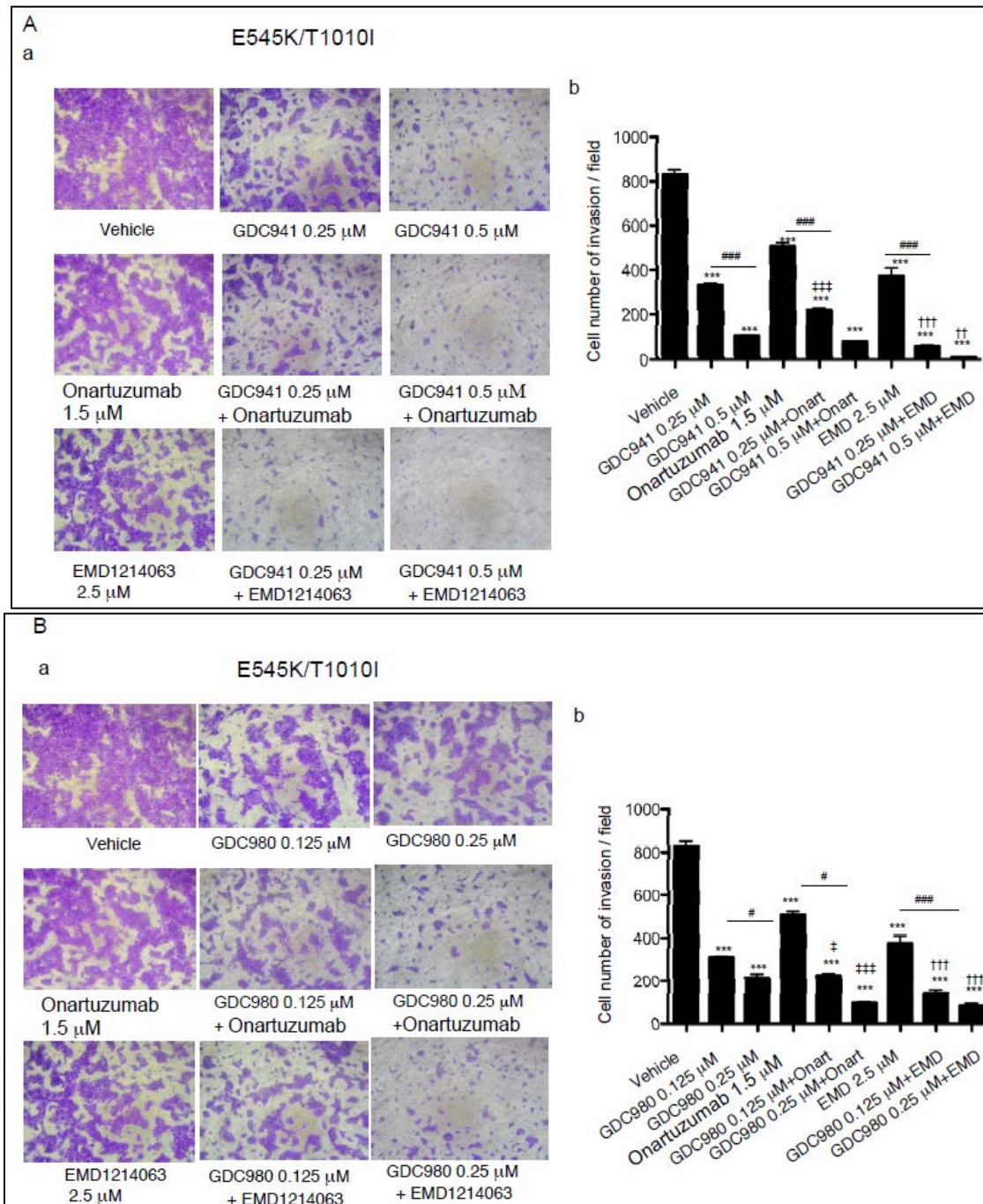
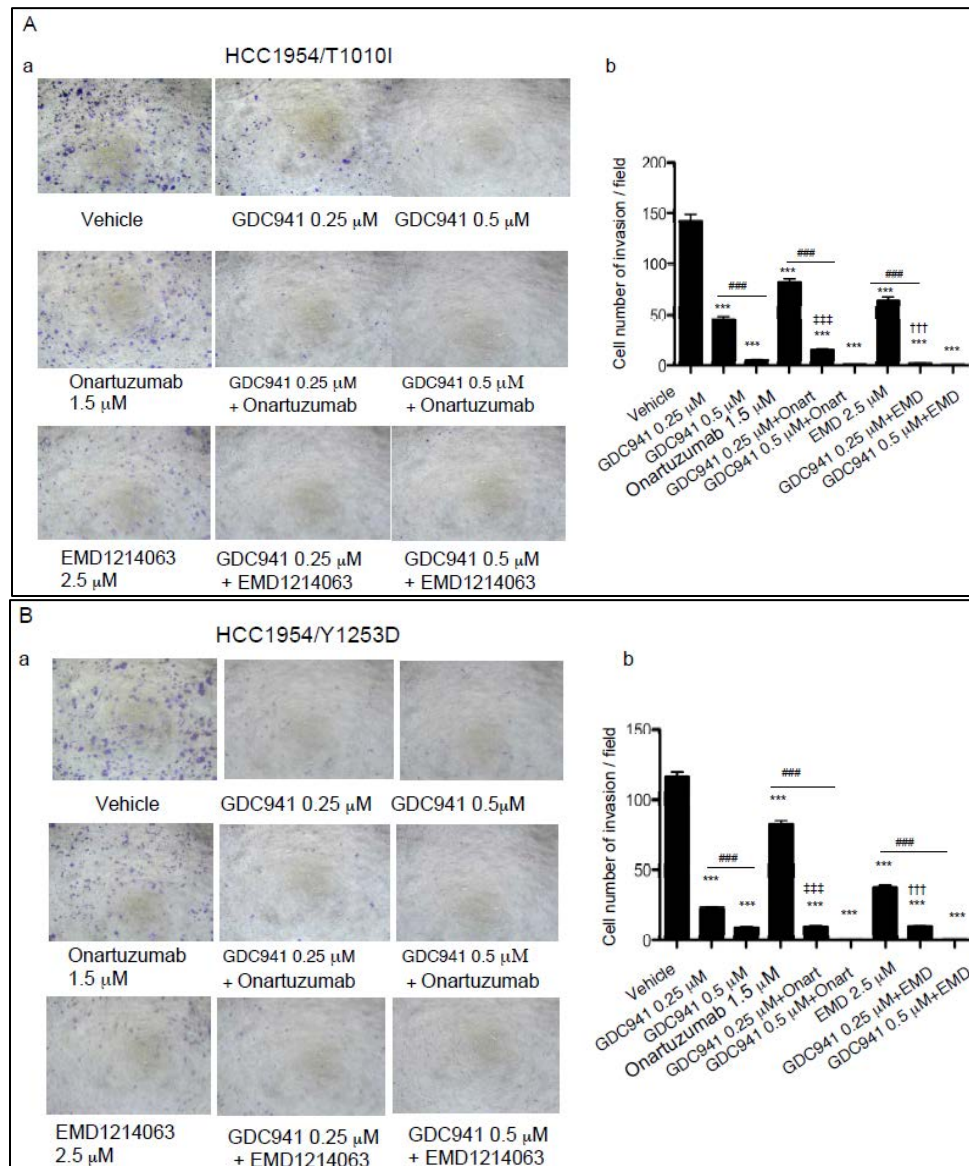


Figure 21. Effects of combinations of PI3K inhibitors with cMET antibody, onartuzumab, or cmet inhibitor, EMD1214063, on Cell Invasion

Effects of combinations of PI3K inhibitors with cMET antibody, Onartuzumab, or cMET inhibitor, EMD1214063, on cell invasion: Cell invasion was analyzed as explained in Materials and Methods. Stating briefly, MCF-10A derived E545K/T1010I cells were starved for 20 hours in serum-free DMEM F12 lacking EGF. A total of 1×10^5 cells were inoculated into the upper chamber, with fibronectin as inducer. Onartuzumab (1.5 μ M) or EMD-1214063 (2.5 μ M), alone or combined, with GDC941 (A) or GDC980 (B) was added to both the upper and lower chambers. To test the effect of Onartuzumab or its combinations, HGF (50 ng/ml) was also added. Invasive cells were photographed and counted in 10 random fields (a). The data are mean \pm standard errors of triplicates, representative of two independent experiments (***, $P < 0.001$ vs vehicle; ###, $P < 0.001$; †, $P < 0.05$; ††, $P < 0.01$; †††, $P < 0.001$, vs without Onartuzumab addition; †, $P < 0.05$; ††, $P < 0.01$; †††, $P < 0.001$ vs without EMD1214063 addition).

Combination of the cMET inhibitor, EMD 1214063, with PI3K inhibitors, reverses the phenotype induced by cMET/PIK3CA double mutation: To further verify the findings that targeting cMET and PI3K synergistically inhibited cell growth on 3D or cell invasion, we used EMD 1214063, a cMET inhibitor, instead of the cMET antibody. We found that EMD 1214063 (2.5 μ M) alone mildly inhibited cell growth on 3D culture. However, combination with GDC941 or GDC980 significantly enhanced this inhibitory effect ($P < 0.05-0.001$, respectively as indicated) (Figure 21A- B). Consistently, EMD 1214063 (2.5 μ M) alone mildly inhibited the cell invasion of *PIK3CA*-mutated breast cancer cells expressing *cMET* mutants, while combination with GDC941 or GDC980 significantly inhibited the cell invasion ($P < 0.05-0.001$, respectively as indicated) (Figure 22A-D).



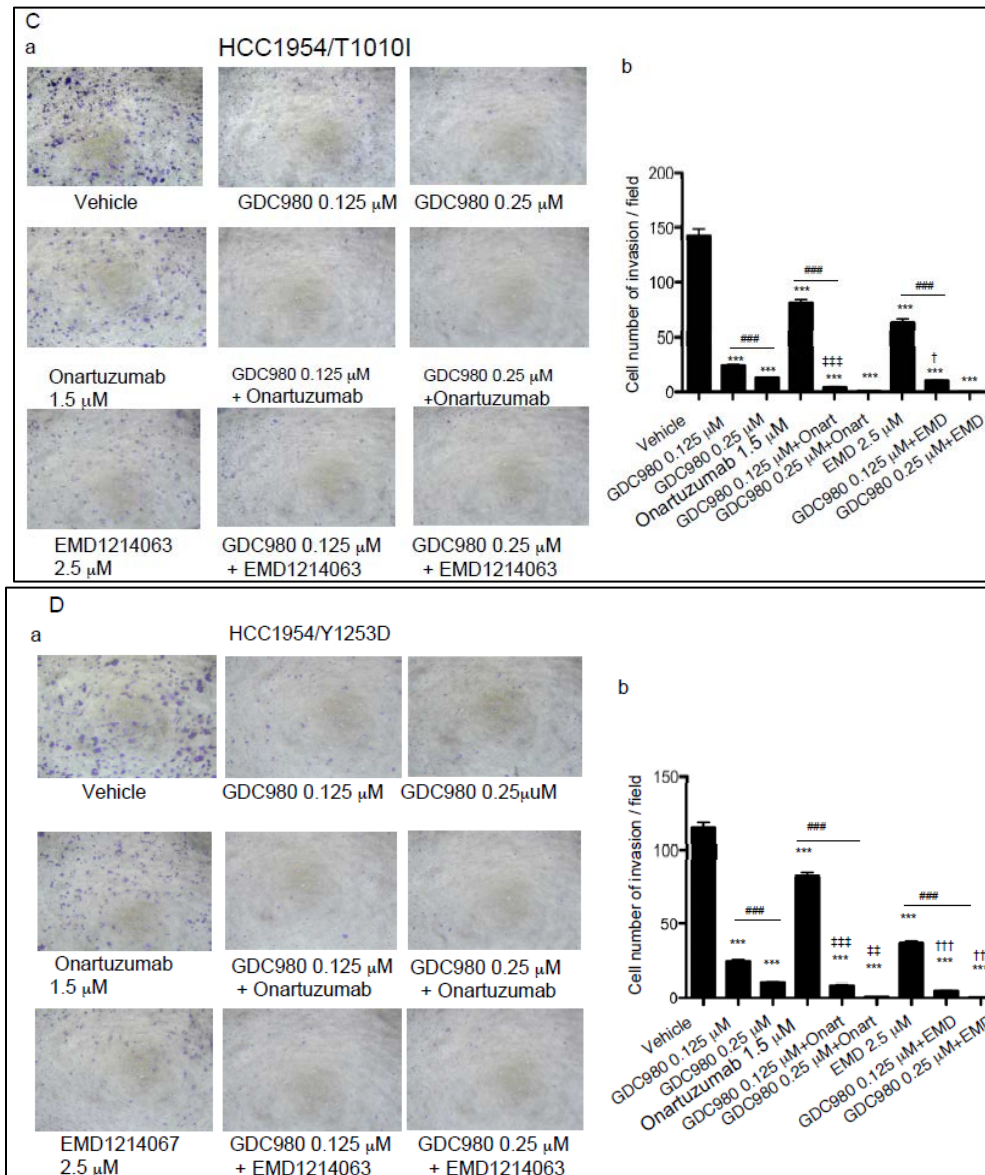


Figure 22. Effects of combinations of PI3K inhibitors with cMET antibody, onartuzumab, or cMET inhibitor, EMD1214063, on Cell Invasion of HCC1954 cells

Effects of combinations of PI3K inhibitors with cMET antibody, Onartuzumab, or cMET inhibitor, EMD1214063, on cell invasion of PIK3CA-mutated breast cancer cells expressing cMET mutants: HCC1954 derived cells expressing mutant cMETs were used to verify the effect of Onartuzumab or EMD-1214063, alone or in combination with PI3K inhibitors, on cell invasion using the same method that was used in Figure 16. HCC1954/T1010I or HCC1954/Y1253D cells treated with GDC941 and variable combinations (A, B). HCC1954/T1010I or HCC1954/Y1253D cells treated with GDC980 and variable combinations (C, D). Invasive cells were photographed and counted in 10 random fields (a). The data are mean \pm standard errors of triplicates, representative of two independent experiments (***, $P < 0.001$ vs vehicle; ###, $P < 0.001$; †, $P < 0.05$; ††, $P < 0.01$; †††, $P < 0.001$, vs without Onartuzumab addition; †, $P < 0.05$; ††, $P < 0.01$; †††, $P < 0.001$ vs without EMD1214063 addition).

MODELS	Sensitivity to GDC941	Sensitivity to GDC980	
HCC1954/Tomato Vector	sensitivite to 0.5µM ; P<0.001 vs vehicle	sensitivite to 0.125µM ; P<0.001 vs vehicle	
HCC1954/cMET-WT	sensitivite to 0.5µM ; P<0.001 vs vehicle	sensitivite to 0.125µM ; P<0.001 vs vehicle	
HCC1954/cMET-T1010I	decreased sensitivity (GI50: 0.75µM)	decreased sensitivity (GI50: 0.375µM)	
HCC1954/cMET-Y1253D	decreased sensitivity (GI50: 0.375µM)	decreased sensitivity (GI50: 0.125µM)	
Models	Drug Classification	Drug	Effect of the drugs on the cell invasion of HCC1954/T1010I cell line
HCC1954/T1010I	Control	Vehicle	Control
	MET Inhibitor	Onartuzumab (1.5µM)	reduced invasiveness ***
	PI3K Inhibitor	GDC941 (0.25 µM)	reduced invasiveness ***
	PI3K/mTOR Inhibitor	GDC980 (0.125 µM)	reduced invasiveness ***
	MET Inhibitor	EMD1214063 (2.5 µM)	reduced invasiveness ***
	PI3K Inhibitor + MET Inhibitor	GDC941 (0.25 µM) and Onartuzumab (1.5µM)	More effective compared to single agent treatment ###
	PI3K Inhibitor + MET Inhibitor	GDC941 (0.25 µM) and EMD (2.5 µM)	More effective compared to single agent treatment ###
	PI3K Inhibitor + MET Inhibitor	GDC980 (0.125 µM) and Onartuzumab (1.5µM)	More effective compared to single agent treatment ###
	PI3K Inhibitor + MET Inhibitor	GDC980 (0.125 µM) and EMD (2.5 µM)	More effective compared to single agent treatment; #
Models	Drug Classification	Drug	Effect of the drugs on the cell invasion of HCC1954/Y1253D cell line
HCC1954/Y1253D	Control	Vehicle	Control
	MET Inhibitor	Onartuzumab (1.5µM)	reduced invasiveness ***
	PI3K Inhibitor	GDC941 (0.25 µM)	reduced invasiveness ***
	PI3K/mTOR Inhibitor	GDC980 (0.125 µM)	reduced invasiveness ***
	MET Inhibitor	EMD1214063 (2.5 µM)	reduced invasiveness ***
	PI3K Inhibitor + MET Inhibitor	GDC941 (0.25 µM) and Onartuzumab (1.5µM)	More effective compared to single agent treatment ###
	PI3K Inhibitor + MET Inhibitor	GDC941 (0.25 µM) and EMD (2.5 µM)	More effective compared to single agent treatment ###
	PI3K Inhibitor + MET Inhibitor	GDC980 (0.125 µM) and Onartuzumab	More effective compared to single agent treatment ###

		(1.5µM)	
	PI3K Inhibitor + MET Inhibitor	GDC980 (0.125 µM) and EMD (2.5 µM)	More effective compared to single agent treatment ###
*** P<0.001 vs vehicle			
### P<0.001 vs single agent			
# P<0.001 vs without GDC941; P<0.05 vs without EMD			

Table 11. Summarizing the Effects of selective PI3K pathway inhibitors and MET inhibitors on MET aberrant HCC1954 cells

Summarizing the effects of selective PI3K pathway inhibitors and MET inhibitors on MET aberrant HCC1954 cells. **MET WT** represents overexpression of Wild Type **MET**.

Models	Drug Classification	Drug	Effect of drugs on the cell invasion ability of MCF10A cells with E545K/T1010I
E545K/T1010I	Control	Vehicle	Control
	MET Inhibitor	Onartuzumab (1.5 µM)	mildly inhibited cell invasion **
	PI3K Inhibitor	GDC941 (0.25 µM)	mildly inhibited cell invasion **
	PI3K/mTOR Inhibitor	GDC980 (0.125 µM)	mildly inhibited cell invasion **
	MET Inhibitor	EMD1214063 (2.5 µM)	mildly inhibited cell invasion **
	PI3K Inhibitor + MET Inhibitor	GDC941 (0.25 µM) and Onartuzumab (1.5 µM)	increased inhibition compared to single agent ###
	PI3K Inhibitor + MET Inhibitor	GDC941 (0.25 µM) and EMD (2.5 µM)	increased inhibition compared to single agent ###
	PI3K Inhibitor + MET Inhibitor	GDC980 (0.125 µM) and Onartuzumab (1.5 µM)	increased inhibition compared to single agent #
	PI3K Inhibitor + MET Inhibitor	GDC980 (0.125 µM) and EMD (2.5 µM)	increased inhibition compared to single agent ###
** P<0.001 vs vehicle			
### P<0.001 vs single agent			
# P<0.001 vs Onartuzumab, P<0.05 vs GDC980			
Models	Drug Classification	Drug	Growth inhibitory effect of the drugs on MCF10A models grown in a 3D culture
E545K/T1010I	Control	Vehicle	Control
	MET Inhibitor	Onartuzumab (1 µM)	inhibited cell growth ***

	PI3K Inhibitor	GDC941 (0.25 μ M)	inhibited cell growth ***
	PI3K/mTOR Inhibitor	GDC980 (0.125 μ M)	inhibited cell growth ***
	MET Inhibitor	EMD1214063 (5 μ M)	inhibited cell growth ***
	PI3K Inhibitor + MET Inhibitor	GDC941 (0.25 μ M) and Onartuzumab (1 μ M)	More effective compared to single agent treatment ###
	PI3K Inhibitor + MET Inhibitor	GDC941 (0.25 μ M) and EMD (5 μ M)	More effective compared to single agent treatment ###
	PI3K Inhibitor + MET Inhibitor	GDC980 (0.125 μ M) and Onartuzumab (1 μ M)	More effective compared to single agent treatment ###
	PI3K Inhibitor + MET Inhibitor	GDC980 (0.125 μ M) and EMD (5 μ M)	More effective compared to single agent treatment ###
	Control	Vehicle	Control
	MET Inhibitor	Onartuzumab (1 μ M)	inhibited cell growth ***
	PI3K Inhibitor	GDC941 (0.5 μ M)	inhibited cell growth ***
	PI3K/mTOR Inhibitor	GDC980 (0.125 μ M)	inhibited cell growth ***
	MET Inhibitor	EMD1214063 (5 μ M)	inhibited cell growth ***
	PI3K Inhibitor + MET Inhibitor	GDC941 (0.25 μ M) and Onartuzumab (1 μ M)	More effective compared to single agent treatment ###
	PI3K Inhibitor + MET Inhibitor	GDC941 (0.25 μ M) and EMD (5 μ M)	More effective compared to single agent treatment ###
	PI3K Inhibitor + MET Inhibitor	GDC980 (0.125 μ M) and Onartuzumab (1 μ M)	More effective compared to single agent treatment ###
	PI3K Inhibitor + MET Inhibitor	GDC980 (0.125 μ M) and EMD (5 μ M)	More effective compared to single agent treatment ###
E545K/Y1253D	Control	Vehicle	Control
	MET Inhibitor	Onartuzumab (1 μ M)	inhibited cell growth ***
	PI3K Inhibitor	GDC941 (0.5 μ M)	inhibited cell growth ***
	PI3K/mTOR Inhibitor	GDC980 (0.125 μ M)	inhibited cell growth ***
	MET Inhibitor	EMD1214063 (5 μ M)	inhibited cell growth ***
	PI3K Inhibitor + MET Inhibitor	GDC941 (0.25 μ M) and Onartuzumab (1 μ M)	More effective compared to single agent treatment ###
	PI3K Inhibitor + MET Inhibitor	GDC941 (0.25 μ M) and EMD (5 μ M)	More effective compared to single agent treatment ###
	PI3K Inhibitor + MET Inhibitor	GDC980 (0.125 μ M) and Onartuzumab (1 μ M)	More effective compared to single agent treatment ###
	PI3K Inhibitor + MET Inhibitor	GDC980 (0.125 μ M) and EMD (5 μ M)	More effective compared to single agent treatment #
H1047R/T1010I	Control	Vehicle	Control
	MET Inhibitor	Onartuzumab (1 μ M)	inhibited cell growth ***
	PI3K Inhibitor	GDC941 (0.5 μ M)	inhibited cell growth ***
	PI3K/mTOR Inhibitor	GDC980 (0.125 μ M)	inhibited cell growth ***
	MET Inhibitor	EMD1214063 (5 μ M)	inhibited cell growth ***
	PI3K Inhibitor + MET Inhibitor	GDC941 (0.25 μ M) and Onartuzumab (1 μ M)	More effective compared to single agent treatment ###
	PI3K Inhibitor + MET Inhibitor	GDC941 (0.25 μ M) and EMD (5 μ M)	More effective compared to single agent treatment ###
	PI3K Inhibitor + MET Inhibitor	GDC980 (0.125 μ M) and Onartuzumab (1 μ M)	More effective compared to single agent treatment ###
	PI3K Inhibitor + MET Inhibitor	GDC980 (0.125 μ M) and EMD (5 μ M)	More effective compared to single agent treatment #
H1047R/Y1253D	Control	Vehicle	Control
	MET Inhibitor	Onartuzumab (1 μ M)	inhibited cell growth ***

	PI3K Inhibitor	GDC941 (0.25 μ M)	inhibited cell growth ***
	PI3K/mTOR Inhibitor	GDC980 (0.125 μ M)	inhibited cell growth ***
	MET Inhibitor	EMD1214063 (5 μ M)	inhibited cell growth ***
	PI3K Inhibitor + MET Inhibitor	GDC941 (0.25 μ M) and Onartuzumab (1 μ M)	More effective compared to single agent treatment ###
	PI3K Inhibitor + MET Inhibitor	GDC941 (0.25 μ M) and EMD (5 μ M)	More effective compared to single agent treatment ##
	PI3K Inhibitor + MET Inhibitor	GDC980 (0.125 μ M) and Onartuzumab (1 μ M)	More effective compared to single agent treatment ###
	PI3K Inhibitor + MET Inhibitor	GDC980 (0.125 μ M) and EMD (5 μ M)	More effective compared to single agent treatment ###
*** P<0.0001 vs vehicle			
### P<0.001 vs single agent			
# P<0.05 vs only EMD; P<0.001 vs only GDC 980			
## P<0.01 vs only EMD; P<0.001 vs only GDC 941			

Table 12. Summarizing the Effects of selective PI3K pathway inhibitors and MET inhibitors on MET and/or PIK3CA aberrant MCF -10Acells

Summarizing the effects of selective PI3K pathway inhibitors and MET inhibitors on MET and/or PIK3CA aberrant MCF -10Acells.

DISCUSSION

More than 25% of breast cancers harbor somatic mutations in the *PIK3CA*-encoded p110 α catalytic subunit of PI3K.(125-128) There are several reports of high frequency *PIK3CA* missense mutations observed at the amino acid residues E545K and H1047R. These mutations occur in the helical region (E545K and E542K) or the kinase domain (H1047R) of p110 α ; H1047R is the most common mutation (>50% of cases).(129) Several experimental models have demonstrated that these tumor-associated *PIK3CA* mutations lead to constitutive p110 α activation and oncogenic transformation,(129-133) making the *PIK3CA* oncogene a target for cancer therapy. Zhao and colleagues have reported that the helical and kinase domain mutations in *PIK3CA* trigger gain of function through different mechanisms.(141) They carried out a genetic and biochemical analysis of the hot-spot mutations E545K and H1047R, and have shown that gain of function induced by E545K is independent of binding to p85 but requires interaction with RAS-GTP.(141) In contrast, the kinase domain mutation H1047R is active in the absence of RAS-GTP binding but is highly dependent on the interaction with p85. Additionally, their data and conclusions are in broad agreement with the crystal structure

publication of the p110 α -p85 complex.(142) Considering the fact that helical and kinase domain mutations of *PIK3CA* alter function through different mechanisms, we decided to evaluate both E545K as well as H1047R in our study.

High levels of HGF and/or MET correlate with poor prognosis in breast cancers, and *MET* activation is caused by the presence of activating mutations. Missense germ-line mutations in the tyrosine kinase (TK) were initially described in patients with hereditary papillary renal carcinoma.(44) Sporadic and germline mutations have been detected in multiple solid tumors. However, only some of these mutant alleles have been proven to cause malignant transformation as a result of constitutive receptor activation posing a potential for therapeutic targeting or altering response to therapy targeting other molecules.(45) Oncogenic somatic and germline mutations have been found to be predominantly located in the non-kinase domain, mainly in regions encoding the extracellular semaphorin domain (E168D, L229F, S323G, and N375S) and the intracellular juxtamembrane domain (R988C, T1010I, S1058P, and exon-14 deletions).(45) The juxtamembrane domain regulates ligand-dependent MET internalization by Y1003 phosphorylation in response to HGF binding leading to MET ubiquitination and degradation(33) and when a mutation/SNP occurs, it can result in MET accumulation at the cell surface and persistent HGF-stimulation leading to tumorigenesis.(46) Transgenic expression of the MET receptor in mammary epithelium was sufficient to induce tumors with features of basal breast cancer,(59) and this study investigates the malignant transforming role of *MET* T1010I and Y1253D, and *MET* amplification in breast cancers.

Multiplexed mutational analysis of over 1000 primary untreated breast cancers completed at our institution demonstrated that 16% of breast cancers with activated *PIK3CA* mutations (22% of all breast cancers) exhibited co-mutations/SNPs in *MET* suggesting concurrent selection of PI3K and MET pathway aberrations. Thus, 4-5% of breast cancer patients (8,000-10,000 new patients a year in the US) are likely to demonstrate concurrent mutations. However, when PI3K pathway aberrations (*PIK3CA* and *AKT* mutation/amplification, PTEN and INPP4B loss) and MET aberrations (MET protein and RNA overexpression, and gene amplification) were assessed, our analysis indicated that at least 10% of breast cancers (20,000 cases per year) exhibit concurrent aberrations. Further, our data suggests that the incidence of PI3K and MET pathway aberrations, and particularly concurrent aberrations, varies by breast cancer subtype. *MET* amplification or mutation may be selected by PI3K pathway targeted therapy or vice versa. The frequency of *MET* aberrations and PI3K pathway aberrations in patients entering trials (i.e., patients with

metastatic disease that have PI3K pathway or MET receptor aberrations) is unknown. It is thus critical to ascertain the biological role of concurrent aberrations in *PIK3CA* and *MET* and their response to selected therapeutics targeting each pathway in breast cancer.

The purpose of this study was to determine the effect of *MET* mutations/SNPs (T1010I and Y1253D) and *MET* overexpression, on the activity of *PIK3CA* mutations (E545K and H1047R) in mammary epithelial cells (MCF 10A) and breast cancer cells (HCC1954).

As summarized on table 9, we found that cell proliferation and cell survival was enhanced in MCF 10A^{E545K} or MCF 10A^{H1047R} cells that overexpressed WT (wild type) *MET* or expressed *MET* T1010I or *MET* Y1253D, when compared to the MCF 10A^{E545K} or MCF 10A^{H1047R} cells that lacked exogenous *MET* expression ($P < 0.001$). Assays determining the effect of these co-aberrations on the morphology of mammary epithelial cells showed that, MCF 10A^{E545K & Y1253D}, MCF 10A^{E545K & T1010I}, and MCF 10A^{H1047R & T1010I} cells formed markedly abnormal structures at an early stage. The cell proliferation assay, colony formation assay and the morphogenesis assay suggest a possible interaction between aberrant *PIK3CA* and *MET*, as the co-aberrant cells exhibit increased proliferation, cell survival and form markedly abnormal structures, respectively. We also performed *in vitro* invasion assays using MCF 10A cells and showed that the *PIK3CA* mutations (E545K, H1047R) enhanced cell invasion. However, *MET* T1010I along with the *PIK3CA* mutations significantly increased cell invasiveness ($P < 0.001$). The presence of *MET* Y1253D also increased cell invasiveness, albeit with lesser intensity when compared to *MET* T1010I ($P < 0.001$). The two *MET* aberrations, Y1253D and T1010I, seem to be having different effects on breast epithelial cells, wherein, the overexpression of *MET* wild type alone did not influence cell invasion. We speculate that the T1010I and Y1253D aberrations, located on different exons, could be displaying their effects through different mechanisms. We also note here that the effects of *MET*-T1010I do not require the presence of a *PIK3CA* mutant. However, there seems to be some interaction between *MET*-Y1253D and the *PIK3CA* mutants, as the presence of both these aberrations leads to significantly increased cell invasion.

A recent study by Meyer and colleagues revealed that expression of the *PIK3CA*-H1047R mutant in mammary epithelial cells is sufficient to induce tumor formation in transgenic mice.(143, 144) The authors postulate that *PIK3CA*-H1047R may (a) transform multi-potent progenitor cells to allow both luminal and basal differentiation, (b) induce de-differentiation of luminal cells to multi-potent progenitors, which then give rise to both lineages,

or (c) do both.(143, 144) Isakoff et al. have reported the ability of the two *PIK3CA* mutations, E545K and H1047R, to transform the MCF-10A cells by inducing anchorage-independent proliferation in soft agar, growth factor-independent proliferation on monolayer cell culture and abnormal mammary acinar morphogenesis in three-dimensional basement membrane cultures.(131) Our study is unique for showing that, co-existence of the MET aberrations (WT overexpression or the expression of the mutations T1010I/Y1253D) with the *PIK3CA* mutations enhances the oncogenic effects of the *PIK3CA* mutations in the MCF 10A cells. Given the high frequency of overlapping aberrations in cancers, it is pertinent to evaluate the effects of co-aberrations in breast cancers. Studies have drawn an association between ERBB2 overexpression and *PIK3CA* mutation in human breast tumors.(145) However, this is the first study to report the effects of *PIK3CA* and MET co-aberrations in breast epithelial/cancer cells. An MMTV-driven, *PIK3CA*-H1047R transgenic mouse model by Liu et al., reports *MET* amplification in recurrent mammary tumors (after *PIK3CA* inactivation)(60). We have gone further to establish and understand the synergistic effects of the MET and *PIK3CA* co-aberrations in breast epithelial as well as breast cancer cells. Our results suggest that *MET* aberrations act in concert with *PIK3CA* mutations to render enhanced tumorigenic properties in mammary epithelial cells.

HCC1954 is a breast cancer cell line with the *PIK3CA*^{H1047R} mutation. Overexpression of WT MET or expression of the *MET* mutants (T1010I/ Y1253D) in these cells significantly increased ($P < 0.001$; control cells: HCC1954^{empty vector}) cell proliferation and colony formation, in addition to inducing abnormal morphological structures. The presence of these MET aberrations in HCC1954 cells also lead to colony formation in soft agar ($P < 0.0001$). The inability of the control cells (HCC1954^{empty vector}) to form colonies under similar conditions reflects that, the introduction of MET aberrations in these cells helps in their anchorage-independent growth. The HCC1954^{T1010I} and HCC1954^{Y1253D} cells also demonstrated marked invasiveness, much like the MCF 10A cells, where T1010I induced maximum cell invasiveness (Table 10).

In the past years, a number of studies have reported MET-receptor overexpression in breast cancer cells(146), a BRCA1-p53 breast cancer mouse model,(147) and tumor tissue from breast cancer patients.(37, 104, 105, 148, 149) We have contributed novel information by reporting the oncogenic role of MET overexpression in breast cancer cells, in cooperation with the *PIK3CA*-H1047R aberration. Ponzio and colleagues have illustrated that MMTV-driven-MET mutant mouse models produce tumors resembling human basal breast cancer.(59) Their

study used mice that were transgenic for oncogenic variants of the MET receptor- M1248T, Y1003F/M1248T. Graveel et al. showed that MET M1248T, D1226N, and Y1228C knock-in lines, in the FVB/N background, developed a high incidence of mammary carcinomas with diverse histopathologies suggesting that activation of MET is able to initiate neoplasia in multiple mammary cell types and that *MET* mutations may uniquely influence cellular differentiation in the mammary gland during tumorigenic growth.(150) Thus, they advocate the need to assess other MET mutations. We here have assessed the oncogenic role of MET-T1010I and MET-Y1253D.

The T1010I SNP has been reported in hereditary renal papillary cancer, large-cell lung cancer cell line Hop-92 and in a patient with breast cancer.(53, 55, 151) Though previous reports suggest that T1010I might be a germline mutation and could have oncogenic properties, views on these findings are not consistent. Schmidt et al. showed that the T1010I mutation is a SNP and lacks the ability to transform NH3T3 cells.(55) Contrary to these results, our study demonstrates that T1010I has marked functional consequences in concert with the *PIK3CA* mutations to render or enhance oncogenic properties in mammary epithelial cells and breast cancer cells. Interestingly, our data showed a difference between the effects of the somatic *MET* mutation, Y1253D, and the possible SNP, T1010I, in both these cell lines. Y1253D had a significantly increased influence on cell proliferation and cell survival, when compared to wild type MET and MET-T1010I. On the other hand, the T1010I SNP induced maximum invasiveness in these cells when compared to wild type MET and Y1253D. We speculate that these aberrations (T1010I and Y1253D) located on different exons could be displaying their effects through different mechanisms. However, further experimentation is needed in order to elucidate this phenomenon.

Having confirmed the role of these co-aberrations in transforming the mammary-epithelial cells, we analyzed their effect on cell signaling. Many of the results were unexpected and suggest a much more complex interaction between the PI3K pathway and the MET pathway than previously described. Further the interactions with the mutant *PIK3CA* and the mutant *MET* constructs in each of the model systems studied could not be predicted from prior knowledge. Thus these models of coexpression of *PIK3CA* and *MET* mutants have the potential to provide new information on these important signaling pathways.

Intriguingly, overexpression of WT *MET* or T1010I in MCF 10A^{E545K} or MCF 10A^{H1047R} cells constitutively enhanced *MET* phosphorylation even without exogenous stimulation. It is pertinent to note that HGF stimulation abolished this phosphorylation of *MET* in MCF 10A^{E545K}

or MCF 10A^{H1047R} cells that expressed T1010I. This is completely unexpected and warrants further exploration. Our cell signaling data consistently shows that the level of endogenous MET or exogenous MET-Flag decreases with increase in phosphorylated MET. In fact, it was difficult to detect total MET or MET-Flag in the presence of markedly increased phosphorylated MET. These findings are in sync with reports that have shown that MET is degraded after phosphorylation.(152) On HGF/SF stimulation, phosphorylated MET is able to recruit the E3 ubiquitin ligase casitas B-lineage lymphoma (CBL), promoting receptor ubiquitination.(152) This could also explain what happens in the cells expressing T1010I. We speculate that if exogenous MET isn't being actively degraded, then this may free the machinery to degrade the wild type MET.

Although, elevated MET and phospho-MET protein levels have been associated with poor outcome in human breast cancer, the role of the MET receptor tyrosine kinase in the induction and development of breast cancer is poorly understood.(144) Deregulation of the HGF-MET signaling axis has been reported in a number of human cancers, inclusive of breast cancers.(47) Several transgenic mouse models have highlighted the susceptibility of the mammary epithelium to be transformed by an enhanced MET/HGF signal.(59) Our findings show that coexistence of the *PIK3CA* mutations with MET-T1010I, in MCF 10A cells, constitutively enhances MET phosphorylation even without stimulation; and HGF is capable of abolishing this phosphorylation. Though we do not have an explanation as yet to this phenomenon, we think it would be worthwhile to explore it further and understand its significance in transforming the mammary epithelial cells.

Meyer and colleagues demonstrated that WAP/MMTV driven *PIK3CA*-H1047R transgenic mouse models developed tumors that showed very low rates of apoptosis and higher levels of phosphorylated AKT than mammary tumors from another model (MMTV-NeuNT), suggesting that *PIK3CA*-H1047R prevents cell death by increased PI3K/AKT pathway activation.(143) In another study, Liu et al., developed an MMTV driven *PIK3CA*-H1047R transgenic mouse model and showed that transgene activation led to MET amplification and increased phospho-AKT levels in the mammary epithelial cells of these mice and formed mammary tumors of varying histologic subtypes.(60) We are the first to report that the presence of the T1010I mutation enhanced the levels of phospho-AKT induced by *PIK3CA*-E545K/H1047R in MCF 10A^{E545K} or MCF 10A^{H1047R} cells. Conceivably, T1010I could be enhancing the tumorigenic properties of the *PIK3CA*-mutant MCF 10A cells by increasing PI3K/AKT pathway activation.

Multiple reports have suggested that constitutively active Stat3 is an important aspect of a diverse group of malignancies.(153) Stat3 is constitutively activated in more than 50% of primary breast tumors and tumor-derived cell lines.(154) Numerous reports of p-Stat3 overexpressing tumors and potent evidences of Stat3 targeted studies have provided a strong rationale for the development of selective Stat3 inhibitors.(155) Consistent with these findings, the expression of MET-T1010I in HCC1954 cells significantly increased phosphorylation of Stat3 with or without stimulation, suggesting that Stat3 is constitutively active in these cells. However, in HCC1954^{WT MET} cells, elevation of phospho-Stat3 was not constitutive, and was induced by HGF. This phenomenon can be explained by Src-dependent phosphorylation regulated by PI3K signaling. Previous studies of EGFR activation by G protein-coupled receptors demonstrated that the TNF-alpha converting enzyme (TACE), a disintegrin and metalloproteinase-17, undergoes a Src-dependent phosphorylation that regulates the release of the EGFR ligand amphiregulin. Further investigation showed the PI3K as the intermediate between c-Src and TACE. (156)

To summarize (Table 10), the presence of aberrations in *PIK3CA* and/or *MET* promotes cell proliferation, cell survival, cell invasiveness, and abnormal morphological structures in MCF 10A cells and HCC1954 cells. In some assays, the co-aberrations significantly increased the oncogenic properties in these cell lines, while in others a single aberration alone was enough to contribute to the observed effects. These findings led us to investigate the sensitivity of the breast epithelial/cancer cells (with *PIK3CA* and *MET* aberrations) to selective PI3K pathway and MET receptor inhibitors, when given alone or in combination. We used the following drugs to generate our *in vitro* pathway targeting data: GDC941 (PI3K inhibitor), GDC980 (PI3K/mTOR inhibitor), onartuzumab (Met-MAbTM) (monoclonal antibody), and EMD1214063 (MET tyrosine kinase inhibitor).

Amplified MET signaling promotes cancer cell survival by activating both the PI3K/Akt/mTORC1 and the Ras/MEK/ERK pathways.(157) In a recent report by Donev et al., an HGF-stimulated, gefitinib (EGFR inhibitor) resistant, xenograft model for lung cancer was shown to be resistant to PI103 (a dual inhibitor of class I PI3K and mTORC1) alone but was highly sensitive to combined treatment with PI103 and gefitinib.(62) Their results suggest that enhanced MET receptor signaling, following HGF treatment, in lung cancer cells results in resistance to the inhibition of the PI3K/Akt/mTORC1 pathway by PI103.(62) Yuen et al. have shown that *MET* amplification in HCC827-GR5 cells (lung cancer cell line) generates a

negative-feedback loop from the PI3K/Akt/mTORC1 pathway to the Ras/MEK/ERK pathway, and that combined inhibition of these pathways, by PI103 and PD184352 (a specific MEK1/2 inhibitor), synergistically induces the apoptotic pathway in these cells.(158) Their results suggest that, *MET* amplification and signaling may be a biomarker for determining the sensitivity of lung cancers to PI3K/Akt/mTORC1 inhibitors, and that a combinatorial inhibition of these pathways will be more effective in lung cancers with *MET* amplification. As a corollary, we investigated the effect of *MET* co-aberrations on the response of *PIK3CA* mutant-breast epithelial/cancer cells to the PI3K inhibitors.

We tested the growth inhibitory effect of the PI3K and *MET* targeting drugs on MCF 10A cells (with co-aberrations in *PIK3CA* and *MET*), grown in a 3D culture. Cells treated with onartuzumab (1 μ M) showed slight growth inhibition in 3D culture. However, the addition of a PI3K inhibitor [GDC941 (0.25 μ M) or GDC980 (0.125 μ M)], to the onartuzumab treatment, significantly increased the growth inhibitory effect in these cells (Figure 14 A-H; $P < 0.05$ - 0.001 , respectively). To prove the converse, we treated these double mutant MCF 10A cells with the PI3K inhibitors alone [GDC941 (0.25 μ M) or GDC980 (0.125 μ M)], and found that the growth inhibition significantly increased with the addition of the *MET* inhibitor EMD1214063 (2.5 μ M), [PI3K inhibitor vs. (PI3K inhibitor with *MET* inhibitor); $P < 0.0001$]. These drugs had similar inhibitory effects on the invasiveness of MCF 10A^{E545K & T1010I}, HCC 1954^{T1010I} and HCC 1954^{Y1253D} cells. 1.5 μ M of onartuzumab slightly reduced the invasiveness of the above mentioned cells. However, the addition of a PI3K inhibitor [GDC941 (0.25 μ M) or GDC980 (0.125 μ M)], to the onartuzumab treatment, significantly reduced the invasiveness of these cells [onartuzumab vs (onartuzumab with PI3K inhibitor) $P < 0.001$]. To prove the converse, we treated these cells with the PI3K inhibitor alone [GDC941 (0.25 μ M) or GDC980 (0.125 μ M)], and found that the cell invasiveness significantly reduced with the addition of the *MET* inhibitor EMD1214063 (2.5 μ M), [PI3K inhibitor vs. (PI3K inhibitor with *MET* inhibitor); $P < 0.0001$] (Tables 11 and 12).

Our results suggest that concurrent aberrations in *PIK3CA* and *MET* render mammary epithelial cells and breast cancer cells resistant to therapies targeting each individual pathway (PI3K and *MET* signaling pathway), and that combination therapy targeting both these pathways provides evidence for improved treatment efficacy. Unexpectedly, our cell signaling data showed that HCC 1954^{T1010I} cells (the most aggressive cells among our cell lines) treated with GDC941 or GDC980 led to decreased phosphorylation of *MET*. This suggests that there could be a cross-talk between the PI3K and the *MET* pathway. This crosstalk is supported by evidence presented by Maulik and colleagues, who have reported that HGF-stimulated

activation of the MET pathway targets the PI3K pathway via GAB2 in small cell lung cancer cells lines (SCLC).(159)

Gene amplification and protein over-expression of MET contribute towards EGFR inhibitor resistance, both in NSCLC cell lines and in patients.(43) Engelman et al. have found that MET amplification causes gefitinib resistance by driving ERBB3 (HER3)–dependent activation of PI3K, a pathway thought to be specific to EGFR/ERBB family receptors.(43) Thus, they propose that MET amplification may promote drug resistance in other ERBB-driven cancers as well.(43) We here have shown that the presence of MET amplification or *MET* mutations in *PIK3CA* mutant breast epithelial/cancer cells contributes to PI3K inhibitor resistance, and that therapy targeting both these pathways helps circumvent this resistance.

Muellner et al. identified a novel mechanism of resistance to PI3K inhibitors in breast cancer cell lines by activating NOTCH signaling and induction of c-MYC.(134) In other words, activated Notch signaling overrode the dependency of cells on PI3K pathway for proliferation.(134) Preliminary data presented on a public peer-reviewed grant application claims that the authors have demonstrated the ability of the HGF-MET signaling to preserve Notch expression/activation in breast cancer cells, which protects the cells from GSI (Gamma secretase inhibitors, blocks Notch activation)-induced death.(160) They postulate a new signaling mechanism linking HGF/c-Met and Notch with respect to cell survival.(160) In addition, they have shown that HGF promotes the expression of Notch ligands on breast cancer cells that activate Notch on adjacent endothelial cells, to promote angiogenesis.(160) The Muellner et al. report and the preliminary studies reported in the application, together, help us to postulate that the HGF-MET signaling preserves Notch activation, which in turn contributes to PI3K inhibitor resistance in breast cancer cells.

Additionally, Yuen et al. have shown that *MET* amplification in a lung cancer cell line generates a negative-feedback loop from the PI3K/Akt/mTORC1 pathway to the Ras/MEK/ERK pathway, resulting in PI3K inhibitor resistance.(158) It is conceivable that the Ras/MEK/ERK pathway could mediate the crosstalk between the MET and the PI3K pathway in *MET/PIK3CA* co-aberrant breast cancer cells, however, this phenomenon remains to be studied.

Our cell signaling data on the mammary epithelial cells and the breast cancer cells provide us clues to the mechanisms associated with the effects of the *PIK3CA* and *MET* co-

aberrations, but it is pertinent to perform experiments that provide a holistic picture. In order to tease apart the signaling pathways involved, and to assist establishing mechanistic explanations, we are currently performing an RPPA analysis. Recent data from our laboratory has demonstrated significant correlations between RPPA and IHC in snap frozen primary breast tumors and has established reliability of RPPA in functional proteomic “fingerprinting”. Compared to IHC or ELISA, RPPA is more sensitive, reduces variability and avoids observer dependency(106). Using RPPA, we wish to comprehensively analyze the signals induced during the crosstalk between the MET and PI3K pathway. As mentioned above, we suspect the role of other pathways such as Notch and Ras/MEK/ERK to mediate this crosstalk. An RPPA analysis would assist elucidating these aspects.

In order to study the effects of these co-aberrations in an *in vivo* environment, we carried out the initial experiments by establishing tumor xenograft models in transgenic mice, hHGF Tg SCID females,(139) using HCC954^{WT MET}, HCC954^{T1010I}, HCC954^{Y1253D}, and HCC954^{Td vector} cells (Figure 16). Cells with the T1010I and Y1253D mutations displayed enlarged tumors compared to the controls; moreover, all the tumors from the T1010I group were markedly invasive. These initial results corroborate with our *in vitro* findings and help strengthen our hypothesis.

Currently, we are in the process of developing a tetracycline dependent transgenic mouse model with concurrent aberrations in *PIK3CA* and *MET*. With the help of this model, in an *in vivo* environment, we intend to understand the effects of the co-aberrations in the pathogenesis of breast cancer and also assess the effectiveness of the proposed MET/PI3K combinatorial therapy.

Most deaths due to breast cancer are attributable to drug resistance, where curative therapies cannot be identified. As tumors invariably acquire resistance to single agent treatments, the ability to anticipate PI3K inhibitor resistance has enormous clinical value.(134) Genetic and adaptive resistances are major obstacles in translating therapeutic efficacy into curative cancer therapy due to the evolutionary nature of cancer and the instable genome of some cancers. Hence, in order to improve cancer therapy, designing multidrug combinations to circumvent resistance, is of paramount importance. A thorough understanding of the “wiring diagram” of breast cancer cells and the mechanisms of resistance to PI3K targeted therapy, has the potential to benefit a significant number of patients with breast cancer.

We have proposed that tumors with concurrent aberrations in *MET* and *PIK3CA* could be more aggressive, and resistant to therapies targeting each pathway, and that combinatorial therapy could circumvent this resistance.

CHAPTER 5: DISCUSSION

The PI3K/Akt/mTOR pathway is mutationally activated in more tumors than any other pathway making it a highly attractive therapeutic target. Indeed, more drugs are in or about to enter clinical trials targeting this pathway than any other. We and others have demonstrated that the PI3K pathway aberrations correlate with resistance to receptor targeted therapies.(23-26) Thus, it is critically important to identify mechanisms of resistance to the PI3K pathway inhibitors.

In vitro studies have shown that the HGF/MET signaling pathway can confer resistance against induction of apoptosis by various DNA damaging-agents (radiation and cytotoxic agents such as anthracyclines and taxanes).(113) Moreover, the pathway is also involved in promoting cell survival by enhancing DNA repair.(114) Studies also suggest that overexpression of HGF and MET contributes to resistance, both inherent and treatment-acquired, to endocrine therapy and to trastuzumab treatment.(13, 14) The anti-apoptotic prosurvival effect of the HGF/MET signaling pathway makes MET inhibition a potential therapeutic approach for breast cancers that are resistant and refractory to conventional therapies. Since MET participates in the acquisition of resistance, a subset of breast cancers may benefit from the combination of MET inhibitors as a first line therapy with traditional treatments. However, approaches to identify these patients are not available. Additionally, pre-clinical data suggests that MET inhibition impairs tumor cell proliferation, survival, motility, and invasion as well as angiogenesis.(116, 117) Several small molecule MET kinase inhibitors and, antibodies against HGF and MET are in various stages of development as potential cancer therapies.(15-17)

In lung cancer cells, HGF induces EGFR-TKI resistance by activating MET with restoration of downstream MAPK-ERK1/2 and PI3K signaling. Indeed, transient blockade of the PI3K pathway with PI-103 (PI3K inhibitor) and gefitinib overcame HGF-mediated resistance to EGFR-TKIs by inducing apoptosis in EGFR mutant lung cancer cell lines.(62) The effects may be bidirectional, as in collaborative studies, we have shown that *MET* amplification can induce resistance to PI3K pathway inhibition in breast cancer murine model systems.(60) Thus, crosstalk between MET and the PI3K pathway may mediate cross-resistance to targeted therapies.

In this thesis we tested the hypothesis that concurrent aberrations in *PI3K* and *MET* will render breast cancers resistant to therapies targeting each pathway, and that combination therapy targeting the PI3K and MET pathway will optimize therapy-effect by preventing the acquisition of resistance.

In order to test this hypothesis, we first studied protein expression levels of total cMET and p-cMET by breast cancer subtype, and their correlation with patient outcome.(1) Both HGF expression and cMET expression have been shown to correlate with poor prognosis in breast cancer. These clinical outcomes are a consequence of multiple phenotypic properties that are imparted to tumor cells by HGF/cMET activation. HGF/cMET signaling enhances the transition from pre-invasive DCIS to invasive carcinoma(37). The pathway also promotes cell motility and angiogenesis(109, 110). Hence, it was pertinent to analyze cMET and phospho-cMET protein levels in breast cancer samples. Our RPPA analysis of 257 breast cancer samples demonstrated elevated levels of total cMET and p-cMET in nearly 70% and 50% of breast cancers, respectively. This finding is in line with previous reports that suggest the role of MET activation in the pathogenesis of cancer. Our results show that elevated levels of total cMET and p-cMET are seen across breast cancer subtypes. Survival analysis revealed that total cMET and p-cMET levels are significant prognostic factors for both RFS and OS. Analysis of survival outcomes among various tumor subtypes showed that high cMET levels is an indication of a poor prognosis for hormone receptor-positive breast cancer and high p-cMET levels correlate with poor prognosis for HER2-positive breast cancers. HGF/cMET receptor signals synergize with HER2 and promote the breakdown of cell-cell junctions and enhance cell invasiveness (112). This cross talk is possibly responsible for the poor prognosis seen in HER2-positive breast cancers with high levels of p-cMET (RFS: P = 0.019 and OS: P = 0.014). To the best of our knowledge, this is the first study to investigate the significance of differential expression of cMET and p-cMET across breast cancer subtypes (HR-positive, HER2-positive and TNBC), and to report p-cMET levels as a prognostic factor in breast cancer.(1)

We then looked at the frequency of *MET* and *PIK3CA* copy number abnormalities in breast cancer tumors, and their associations with patient outcome.(2) The hypothesis of this thesis is that concurrent aberrations in *PI3K* and *MET* alter the behavior of tumors and could change the response to therapy in breast cancer. Therefore, before analyzing the effect of the aberrations on tumorigenesis and targeted therapy, we evaluated patient tumor samples to determine the frequency of *MET* and *PIK3CA* copy number aberrations in breast cancer patients, and their associations with patient outcome. Molecular inversion probe arrays on 971

early breast cancer tumors suggested that 82 (8.44%) and 134 (13.8%) tumors had increased *MET* or *PIK3CA* copy number, respectively, and 25.6% of the tumors with a *MET* copy number elevation had a concurrent *PIK3CA* copy number elevation. Upon assessing breast cancer subtypes, 28% of triple receptor-negative breast cancers had a high *PIK3CA* copy number, suggesting that gene amplification in conjunction with loss of PTEN and INPP4B may contribute to the PI3K pathway activation observed in this subtype. This result is in line with a previous study, which reported that, of the 209 invasive breast tumors tested, 28 had *PIK3CA* amplification (13.4%).(123) As indicated above, 26% of the *MET*-amplified tumors also had *PIK3CA* amplification, which is a higher frequency than predicted by chance, thereby indicating that co-aberrations in the PI3K and MET pathways occur at a sufficient frequency to warrant extensive preclinical and mechanistic evaluation and to potentially warrant altered management approaches for patients. These findings were published prior to the recent TCGA publication(57) on human breast tumors. Our findings differ from the TCGA results, possibly due to the elimination of dbSNPs in their report.

We also found that patients with either a *MET* or *PIK3CA* high copy number tended to have clinical features associated with a poor prognosis (larger tumor size, higher tumor grade, and hormone receptor negativity). Both *MET* and *PIK3CA* high copy numbers were more likely to occur in patients with triple negative disease ($P=0.019$ and <0.001 , respectively). At a median follow-up of 7.4 years, there were 252 cases of disease recurrence. The 5-year RFS rates were 63.5%, and 83.1% for *MET* high copy number and *MET* normal/low copy number, respectively ($P=0.06$) and 73.1%, and 82.3% for *PIK3CA* high copy number and *PIK3CA* normal/low copy number, respectively ($P=0.15$). Patients with elevation in both *MET* and *PIK3CA* copy numbers had worse RFS than any other group (Refer Figure 5C).

Our study concludes that co-amplification is frequent, and a high copy number of *MET* or *PIK3CA* is associated with poorer prognostic features and the triple receptor-negative disease. Two interesting findings need to be highlighted: the higher proportion of triple-negative disease with this aberration, and the prognostic value of copy number in breast cancer, especially in patients with hormone receptor-positive disease. This is important as we continue to need new therapeutic targets in triple receptor-negative breast cancer. In this population, *MET* receptor inhibition could prevent cell proliferation, survival and invasion. Conversely, in our search for mechanisms of resistance to endocrine therapy, *MET* signaling should also be investigated. *MET* amplification or mutation may be selected by PI3K pathway targeted therapy or vice versa. However, the frequency of *MET* mutations and PI3K pathway

aberrations in patients entering trials (i.e., patients with metastatic disease that have PI3K pathway or MET receptor aberrations) remains to be investigated. Thus, it is critical to ascertain the role of concurrent mutations in *PIK3CA* and *MET*, in the response of breast cancer cells to select therapeutics targeting the PI3K and MET pathway.

Lastly, we studied the effects of co-mutations/SNPs in *MET* and *MET* overexpression found in breast cancers, on the activity of the two most common breast cancer *PIK3CA* mutations (E545K and H1047R) *in vitro*. The purpose of this section of our study is to determine the effect of *MET* SNPs/mutations (T1010I and Y1253D) and *MET* overexpression, on the activity of *PIK3CA* mutations (E545K and H1047R) in mammary epithelial cells (MCF 10A) and breast cancer cells (HCC1954).

We found that *MET* aberrations (T1010I or Y1253D) and/or *PIK3CA* mutations (E545K or H1047R) promote cell proliferation, cell survival, cell invasiveness, and abnormal morphological structures in MCF 10A cells and HCC1954 cells (Table 9 and Table 10). Several studies have shown the oncogenic effects of the *PIK3CA* mutations in breast epithelial and cancer cells. However, we are the first to show that the presence of *MET* aberrations enhances the tumorigenic effects induced by the *PIK3CA* mutations in breast epithelial and breast cancer cells.

Interestingly, our data demonstrated a difference between the effects of the somatic *MET* mutation- Y1253D, and the possible germline *MET* mutation- T1010I, in both these cell lines. While Y1253D had the highest influence on cell proliferation and cell survival, the T1010I mutation induced maximum invasiveness in these cells. Though previous reports suggest that T1010I might be a germline mutation and could have oncogenic properties, views on these findings are not consistent. Schmidt et al. suggest that the T1010I is a SNP and showed that it lacks the ability to transform NH3T3 cells.(55) Contrary to these results, our study demonstrates this sequence change has differential effects from the WT construct particularly in concert with *PIK3CA* mutations to render or enhance oncogenic properties in mammary epithelial cells and breast cancer cells.

After analyzing the effect of these co-aberrations on cell signaling in mammary epithelial/cancer cells, our results suggest that phosphorylation of: MET, Akt, Stat-3, cJun and Src, could play an important role in the oncogenic effects of the co-aberrations. Our findings show that coexistence of the *PIK3CA* mutations with MET-T1010I, in MCF 10A cells,

constitutively enhances MET phosphorylation even without addition of exogenous growth factors; and HGF is capable of abolishing this phosphorylation. Though we do not have an explanation as yet for the reason why HGF decreases phosphorylation, we think it would be worthwhile to explore it further and understand its role in transforming the mammary epithelial cells. It is possible that phosphorylation results in receptor degradation resulting in an apparent decrease in phosphorylated receptor. Previous reports have shown that PIK3CA-H1047R prevents cell death in mammary tumors by increased PI3K/AKT pathway activation, indicated by higher levels of phosphorylated AKT.(60, 143) Our study is unique in showing that the presence of the T1010I mutation enhanced the levels of phospho-AKT induced by PIK3CA-E545K/H1047R in MCF10A^{E545K} or MCF10A^{H1047R} cells. Conceivably, T1010I could be enhancing the tumorigenic properties of the PIK3CA-mutant MCF10A cells by increasing PI3K/AKT pathway activation.

Consistent with previous studies that have found constitutively active Stat3 in more than 50% of primary breast tumors and tumor-derived cell lines,(154) the expression of MET-T1010I in HCC1954 cells significantly increased the phosphorylation of Stat3 with or without exogenous ligand, suggesting that Stat3 is constitutively activate in these cells.

In a recent report, Donev and colleagues demonstrated that, enhanced MET receptor signaling following HGF treatment in lung cancer cells results in resistance to the inhibition of the PI3K/Akt/mTORC1 pathway by PI103 (a dual inhibitor of class I PI3K and mTORC1), and that combined treatment with PI103 and gefitinib (EGFR inhibitor) overcame this resistance.(62) Since enhanced HGF-MET signaling is associated with the resistance of lung cancer cells to PI3K inhibitors, we investigated the effect of MET co-aberrations on the response of PIK3CA mutant-breast epithelial/cancer cells to the PI3K inhibitors.

We tested the interaction of PI3K (GDC941 or GDC 980) and MET (onartuzumab or EMD 1214063) targeting drugs on MCF-10A and HCC1954 cells having concurrent aberrations in *MET* and *PIK3CA*. Our results suggest that combinatorial therapy with MET and PI3K inhibitors had a significantly higher inhibitory effect on the tumorigenicity of MCF-10A and HCC1954 cells that had concurrent aberrations in *MET* and *PIK3CA*. Thus we propose that tumors with concurrent aberrations in *MET* and *PIK3CA* could be more aggressive, and resistant to therapies targeting each pathway, and that combinatorial therapy could circumvent this resistance.

FUTURE DIRECTIONS: Our data demonstrated a difference between the effects of the somatic *MET* mutation- Y1253D, and the possible germline *MET* mutation, T1010I, in the MCF 10A and HCC1954 cells. While Y1253D had the highest influence on cell proliferation and cell survival, the T1010I mutation induced maximum invasiveness in both these cell lines. The T1010I mutation was previously identified in a tumor biopsy of hereditary renal papillary cancer and a papillary renal cancer cell line, ACHN.(44) Schmidt et al. proposed T1010I to be a SNP and showed that it lacks the ability to transform NH3T3 cells.(55) However, Lee et al. showed that this mutation was more active than the wild-type *MET* in an athymic nude mice tumorigenesis assay, suggesting that it may contribute to tumorigenesis.(53) They screened 30 breast cancer samples and found one tumor with the T1010I missense mutation in the intracellular juxtamembrane domain of the MET receptor.(53) In fact, this mutation was shown to be present in the DNA from a tumor cell-negative lymph node of the same individual, suggesting that T1010I could be a germline mutation.(53) Though some reports suggest that T1010I might be a germline mutation and could have oncogenic properties, views on these findings are not consistent. Contrary to the previous studies that have reported that T1010I lacks the ability to induce tumorigenicity, our study demonstrates that it works in concert with the PIK3CA mutations to render or enhance oncogenic properties in mammary epithelial cells and breast cancer cells. However, it remains to be explored if T1010I is indeed a germline mutation. We intend to analyze the frequency and origin of this mutation in a large cohort of breast cancer patients. If T1010I is closely associated with the pathogenesis of breast cancer and turns out to be germline, it has the potential to be used as a predictive marker for screening, much like BRCA1 and BRCA2.

Further studies including comprehensive analysis of large cohorts of breast cancers (i.e. TCGA- The Cancer Genome Atlas) are on-going in our group for analyzing the frequencies of mutations, copy number, and methylation, as well as, translational changes in PI3K pathway-related genes and *MET* (alone and in combination) to determine the frequency of co-aberrations in the pathways across multiple modalities.(2)

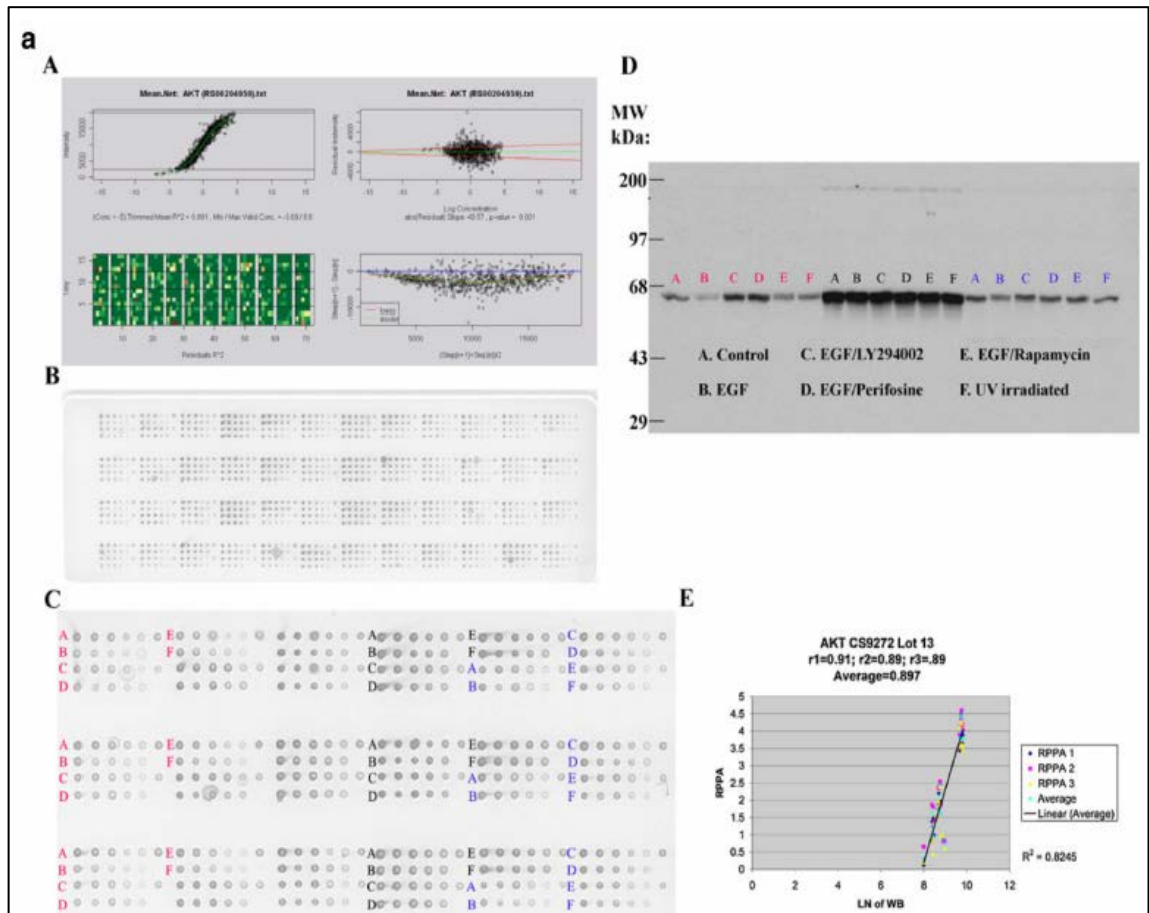
In order to study the effects of these co-aberrations in an *in vivo* environment, we carried out a preliminary experiment by establishing tumor xenograft models in transgenic mice, named hHGF Tg SCID females,(139) using HCC954^{WT MET}, HCC954^{T1010I}, HCC954^{Y1253D}, and HCC954^{Td vector} cells (Figure 16). Consistent with our *in vitro* results, the presence of the T1010I and Y1253D mutations displayed enlarged tumors compared to the controls, moreover, all the tumors from the T1010I group were markedly invasive.

The generation of transgenic animals is essential for the *in vivo* study of gene function during development, organogenesis and aging.(161) It also permits the evaluation of therapeutic strategies in models of human disease, as well as the investigation of disease progression in a manner not possible in human subjects.(161) Currently, we are in the process of developing a tetracycline dependent transgenic mouse model with concurrent aberrations in *PIK3CA* and *MET*. With the help of this model, in an *in vivo* environment, we intend to understand the effects of the co-mutations in the pathogenesis of breast cancer and also assess the effectiveness of the proposed MET/PI3K combinatorial therapy. The tetracycline dependency of this model will help us achieve an off/off transition of the transgenes, which will help us comprehensively analyze the signals induced during the crosstalk between MET and PI3K. Moreover, as indicated in Chapter 4, we suspect the role of other pathways such as Notch and Ras/MEK/ERK to mediate this crosstalk between PI3K and MET. An RPPA analysis would enlighten our knowledge on these aspects.

We propose that tumors with concurrent aberrations in *MET* and *PIK3CA* could be more aggressive, and resistant to therapies targeting each pathway, and that combinatorial therapy could circumvent this resistance. In order to test the synergistic effect of PI3K and MET inhibitors on breast cancer patients with concurrent aberrations in *PIK3CA* and *MET*, we are in the process of acquiring an IND (Investigational New Drug application) approval for the clinical trial, the protocol for which has been written and approved by Genentech.

RPPA analysis, animal studies and clinical trials, together with the *in vitro* data generated in this study, would elucidate the oncogenic signals induced by the MET/PIK3CA co-aberrations during breast cancer pathogenesis, and help us assess the efficacy/feasibility of our proposed combinatorial treatment.

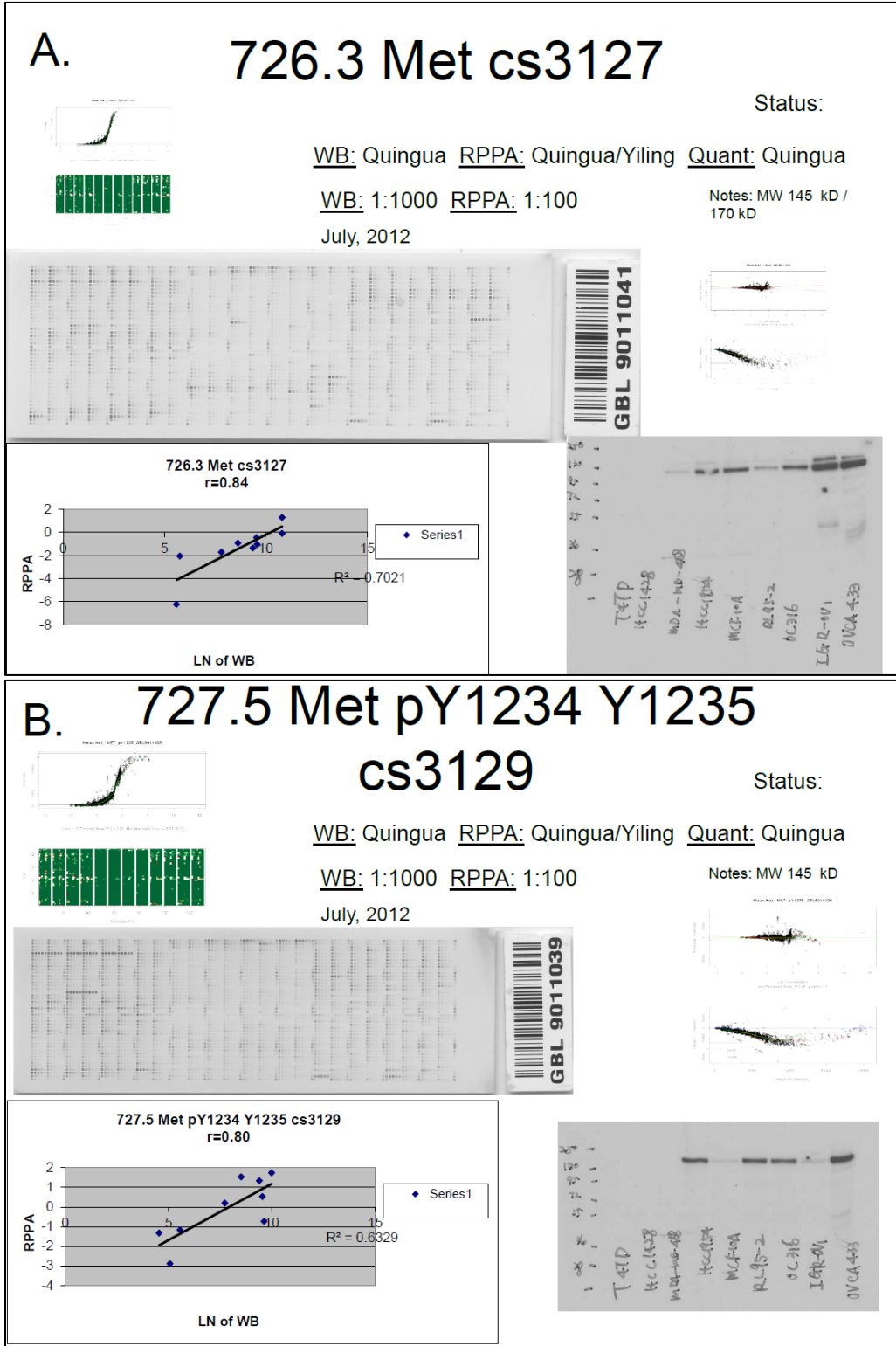
APPENDIX 1



Appendix 1.(99) a Akt and **b** Aktp473 antibody validation for reverse phase protein array (RPPA).MDAMB468 (*red*), ZR75-1 (*black*) and T47D (*blue*) cells were left untreated followed by no stimulation (control) or by stimulation with epidermal growth factor (EGF) or were treated with LY294002 (phosphatidylinositol-3-kinase (PI3K) inhibitor), perifosine (Akt inhibitor), rapamycin (mTOR inhibitor), or ultraviolet (UV) irradiation and then stimulated with epidermal growth factor (EGF) in the case of treatment with the three inhibitors. Lysates were then probed with antibody to total Akt (**a**) or to phosphorylated Akt at serine 473 (Aktp473, **b**) by RPPA in triplicate (*panels A–C*) and by western blotting (*panel D*) and the derived signals for total Akt and for Aktp473 were quantified and correlated (*panel E* in **a** and **b**). For RPPA, each lysate was arrayed in five serial 2-fold dilutions on nitrocellulose slides (with increasing dilution from *left to right* on each slide for each lysate as shown in *panel B*). A control spot (a mixed cell line lysate) was placed at the end of each sample lysate’s five serial 2-fold dilution series to give six spots. Four samples are arrayed in this fashion in each grid of 24 spots on the nitrocellulose slides shown. The correlation coefficients between signals derived using RPPA and western blotting for Akt and Aktp473 were 0.897 and 0.93, respectively (*panel E* in **a** and **b**). These correlation coefficients were based on 18 data points as shown and indicate valid antibodies for RPPA. *Panel A* in **a** and **b** demonstrates the process of curve fitting for RPPA that is applied by the R package SuperCurve (version 1.01). In the *upper left of panel A*, estimated protein concentration (*x*-axis) is plotted against signal intensity (*y*-axis). In the *upper right of panel A*, residuals from model fitting (*y*-axis) are plotted against estimated protein concentration (*x*-axis).

Ideally, the residuals should be symmetrical about the horizontal 0 line and should not increase with increasing concentration. In the *lower left of panel A* is an image plot of squared residuals from model fitting. This plot shows that the squared residuals are largely homogeneous. In the *lower right of panel A*, the intensity differences of adjacent dilution steps are plotted (*y*-axis) against the averaged intensities of adjacent dilution steps (*x*-axis). If this curve is flat and close to the horizontal line, the dilutions were unsuccessful and the data are not reliable.

APPENDIX 2



Appendix 2. The Method described in Appendix 1 was used to validate (A) primary MET and (B) p-MET antibodies (Cell Signalling Technology, Danvers, MA) for use in RPPA. The following values were obtained after the validation--: MET $r = 0.84$; p-MET $r = 0.80$

BIBLIOGRAPHY

1. Raghav KP, Wang W, Liu S, Chavez-MacGregor M, Meng X, Hortobagyi GN, Mills GB, Meric-Bernstam F, Blumenschein GR, Jr., Gonzalez-Angulo AM. cMET and phospho-cMET protein levels in breast cancers and survival outcomes. *Clin Cancer Res.* 2012;18(8):2269-77. Epub 2012/03/01. doi: 10.1158/1078-0432.ccr-11-2830. PubMed PMID: 22374333.
2. Gonzalez-Angulo AM, Chen H, Karuturi MS, Chavez-MacGregor M, Tsavachidis S, Meric-Bernstam F, Do KA, Hortobagyi GN, Thompson PA, Mills GB, Bondy ML, Blumenschein GR, Jr. Frequency of mesenchymal-epithelial transition factor gene (MET) and the catalytic subunit of phosphoinositide-3-kinase (PIK3CA) copy number elevation and correlation with outcome in patients with early stage breast cancer. *Cancer.* 2013;119(1):7-15. Epub 2012/06/28. doi: 10.1002/cncr.27608. PubMed PMID: 22736407; PubMed Central PMCID: PMC3461089.
3. Jemal A, Siegel R, Xu J, Ward E. Cancer statistics, 2010. *CA Cancer J Clin.* 2010;60(5):277-300. Epub 2010/07/09. doi: 10.3322/caac.20073. PubMed PMID: 20610543.
4. Siegel R, Naishadham D, Jemal A. Cancer statistics, 2012. *CA Cancer J Clin.* 2012;62(1):10-29. Epub 2012/01/13. doi: 10.3322/caac.20138. PubMed PMID: 22237781.
5. Polyak K. Heterogeneity in breast cancer. *J Clin Invest.* 2011;121(10):3786-8. Epub 2011/10/04. doi: 10.1172/jci60534. PubMed PMID: 21965334; PubMed Central PMCID: PMC3195489.
6. Irvin WJ, Jr., Carey LA. What is triple-negative breast cancer? *Eur J Cancer.* 2008;44(18):2799-805. Epub 2008/11/15. doi: 10.1016/j.ejca.2008.09.034. PubMed PMID: 19008097.
7. Livasy CA, Karaca G, Nanda R, Tretiakova MS, Olopade OI, Moore DT, Perou CM. Phenotypic evaluation of the basal-like subtype of invasive breast carcinoma. *Mod Pathol.* 2006;19(2):264-71. Epub 2005/12/13. doi: 10.1038/modpathol.3800528. PubMed PMID: 16341146.

8. Fulford LG, Easton DF, Reis-Filho JS, Sofronis A, Gillett CE, Lakhani SR, Hanby A. Specific morphological features predictive for the basal phenotype in grade 3 invasive ductal carcinoma of breast. *Histopathology*. 2006;49(1):22-34. Epub 2006/07/18. doi: 10.1111/j.1365-2559.2006.02453.x. PubMed PMID: 16842243.
9. Reis-Filho JS, Milanezi F, Steele D, Savage K, Simpson PT, Nesland JM, Pereira EM, Lakhani SR, Schmitt FC. Metaplastic breast carcinomas are basal-like tumours. *Histopathology*. 2006;49(1):10-21. Epub 2006/07/18. doi: 10.1111/j.1365-2559.2006.02467.x. PubMed PMID: 16842242.
10. Beatty JD, Atwood M, Tickman R, Reiner M. Metaplastic breast cancer: clinical significance. *Am J Surg*. 2006;191(5):657-64. Epub 2006/05/02. doi: 10.1016/j.amjsurg.2006.01.038. PubMed PMID: 16647355.
11. Jacquemier J, Padovani L, Rabayrol L, Lakhani SR, Penault-Llorca F, Denoux Y, Fiche M, Figueiro P, Maisongrosse V, Ledoussal V, Martinez Penuela J, Udvarhelyi N, El Makdissi G, Ginestier C, Geneix J, Charafe-Jauffret E, Xerri L, Eisinger F, Birnbaum D, Sobol H. Typical medullary breast carcinomas have a basal/myoepithelial phenotype. *J Pathol*. 2005;207(3):260-8. Epub 2005/09/17. doi: 10.1002/path.1845. PubMed PMID: 16167361.
12. Britschgi A, Andraos R, Brinkhaus H, Klebba I, Romanet V, Muller U, Murakami M, Radimerski T, Bentires-Alj M. JAK2/STAT5 Inhibition Circumvents Resistance to PI3K/mTOR Blockade: A Rationale for Cotargeting These Pathways in Metastatic Breast Cancer. *Cancer Cell*. 2012;22(6):796-811. Epub 2012/12/15. doi: 10.1016/j.ccr.2012.10.023. PubMed PMID: 23238015.
13. Hiscox S, Jordan NJ, Jiang W, Harper M, McClelland R, Smith C, Nicholson RI. Chronic exposure to fulvestrant promotes overexpression of the c-Met receptor in breast cancer cells: implications for tumour-stroma interactions. *Endocr Relat Cancer*. 2006;13(4):1085-99. Epub 2006/12/13. doi: 10.1016/j.erc.1.01270. PubMed PMID: 17158755.

14. Shattuck DL, Miller JK, Carraway KL, 3rd, Sweeney C. Met receptor contributes to trastuzumab resistance of Her2-overexpressing breast cancer cells. *Cancer Res.* 2008;68(5):1471-7. Epub 2008/03/05. doi: 68/5/1471 [pii]
10.1158/0008-5472.CAN-07-5962. PubMed PMID: 18316611.
15. Stella GM, Benvenuti S, Comoglio PM. Targeting the MET oncogene in cancer and metastases. *Expert Opin Investig Drugs.*19(11):1381-94. Epub 2010/09/28. doi: 10.1517/13543784.2010.522988. PubMed PMID: 20868306.
16. Liu X, Yao W, Newton RC, Scherle PA. Targeting the c-MET signaling pathway for cancer therapy. *Expert Opin Investig Drugs.* 2008;17(7):997-1011. Epub 2008/06/14. doi: 10.1517/13543784.17.7.997. PubMed PMID: 18549337.
17. Cecchi F, Rabe DC, Bottaro DP. Targeting the HGF/Met signalling pathway in cancer. *Eur J Cancer.*46(7):1260-70. Epub 2010/03/23. doi: S0959-8049(10)00155-3 [pii]
10.1016/j.ejca.2010.02.028. PubMed PMID: 20303741.
18. Hennessy BT, Smith DL, Ram PT, Lu Y, Mills GB. Exploiting the PI3K/AKT pathway for cancer drug discovery. *Nat Rev Drug Discov.* 2005;4(12):988-1004. Epub 2005/12/13. doi: 10.1038/nrd1902. PubMed PMID: 16341064.
19. Meric-Bernstam F, Gonzalez-Angulo AM. Targeting the mTOR signaling network for cancer therapy. *J Clin Oncol.* 2009;27(13):2278-87. Epub 2009/04/01. doi: 10.1200/jco.2008.20.0766. PubMed PMID: 19332717; PubMed Central PMCID: PMC2738634.
20. Saal LH, Johansson P, Holm K, Gruvberger-Saal SK, She QB, Maurer M, Koujak S, Ferrando AA, Malmstrom P, Memeo L, Isola J, Bendahl PO, Rosen N, Hibshoosh H, Ringner M, Borg A, Parsons R. Poor prognosis in carcinoma is associated with a gene expression signature of aberrant PTEN tumor suppressor pathway activity. *Proc Natl Acad Sci U S A.* 2007;104(18):7564-9. Epub 2007/04/25. doi: 10.1073/pnas.0702507104. PubMed PMID: 17452630; PubMed Central PMCID: PMC1855070.

21. Stemke-Hale K, Gonzalez-Angulo AM, Lluch A, Neve RM, Kuo WL, Davies M, Carey M, Hu Z, Guan Y, Sahin A, Symmans WF, Pusztai L, Nolden LK, Horlings H, Berns K, Hung MC, van de Vijver MJ, Valero V, Gray JW, Bernardis R, Mills GB, Hennessy BT. An integrative genomic and proteomic analysis of PIK3CA, PTEN, and AKT mutations in breast cancer. *Cancer Res.* 2008;68(15):6084-91. Epub 2008/08/05. doi: 10.1158/0008-5472.can-07-6854. PubMed PMID: 18676830; PubMed Central PMCID: PMC2680495.
22. Agarwal R, Carey M, Hennessy B, Mills GB. PI3K pathway-directed therapeutic strategies in cancer. *Curr Opin Investig Drugs.* 2010;11(6):615-28. Epub 2010/05/25. PubMed PMID: 20496256.
23. Berns K, Horlings HM, Hennessy BT, Madiredjo M, Hijmans EM, Beelen K, Linn SC, Gonzalez-Angulo AM, Stemke-Hale K, Hauptmann M, Beijersbergen RL, Mills GB, van de Vijver MJ, Bernardis R. A functional genetic approach identifies the PI3K pathway as a major determinant of trastuzumab resistance in breast cancer. *Cancer Cell.* 2007;12(4):395-402. Epub 2007/10/16. doi: 10.1016/j.ccr.2007.08.030. PubMed PMID: 17936563.
24. Miller TW, Perez-Torres M, Narasanna A, Guix M, Stal O, Perez-Tenorio G, Gonzalez-Angulo AM, Hennessy BT, Mills GB, Kennedy JP, Lindsley CW, Arteaga CL. Loss of Phosphatase and Tensin homologue deleted on chromosome 10 engages ErbB3 and insulin-like growth factor-I receptor signaling to promote antiestrogen resistance in breast cancer. *Cancer Res.* 2009;69(10):4192-201. Epub 2009/05/14. doi: 10.1158/0008-5472.can-09-0042. PubMed PMID: 19435893; PubMed Central PMCID: PMC2724871.
25. Nagata Y, Lan KH, Zhou X, Tan M, Esteva FJ, Sahin AA, Klos KS, Li P, Monia BP, Nguyen NT, Hortobagyi GN, Hung MC, Yu D. PTEN activation contributes to tumor inhibition by trastuzumab, and loss of PTEN predicts trastuzumab resistance in patients. *Cancer Cell.* 2004;6(2):117-27. Epub 2004/08/25. doi: 10.1016/j.ccr.2004.06.022. PubMed PMID: 15324695.

26. Perez-Tenorio G, Stal O. Activation of AKT/PKB in breast cancer predicts a worse outcome among endocrine treated patients. *Br J Cancer*. 2002;86(4):540-5. Epub 2002/03/01. doi: 10.1038/sj.bjc.6600126. PubMed PMID: 11870534; PubMed Central PMCID: PMC2375266.
27. McAuliffe PF, Meric-Bernstam F, Mills GB, Gonzalez-Angulo AM. Deciphering the role of PI3K/Akt/mTOR pathway in breast cancer biology and pathogenesis. *Clin Breast Cancer*. 2010;10 Suppl 3:S59-65. Epub 2010/12/01. doi: 10.3816/CBC.2010.s.013. PubMed PMID: 21115423.
28. Bottaro DP, Rubin JS, Faletto DL, Chan AM, Kmieciak TE, Vande Woude GF, Aaronson SA. Identification of the hepatocyte growth factor receptor as the c-met proto-oncogene product. *Science*. 1991;251(4995):802-4. Epub 1991/02/15. PubMed PMID: 1846706.
29. Gherardi E, Stoker M. Hepatocytes and scatter factor. *Nature*. 1990;346(6281):228. Epub 1990/07/19. doi: 10.1038/346228b0. PubMed PMID: 2142751.
30. Ma PC, Maulik G, Christensen J, Salgia R. c-Met: structure, functions and potential for therapeutic inhibition. *Cancer Metastasis Rev*. 2003;22(4):309-25. Epub 2003/07/30. PubMed PMID: 12884908.
31. Miyazawa K, Tsubouchi H, Naka D, Takahashi K, Okigaki M, Arakaki N, Nakayama H, Hirono S, Sakiyama O, et al. Molecular cloning and sequence analysis of cDNA for human hepatocyte growth factor. *Biochem Biophys Res Commun*. 1989;163(2):967-73. Epub 1989/09/15. PubMed PMID: 2528952.
32. Nakamura T, Nishizawa T, Hagiya M, Seki T, Shimonishi M, Sugimura A, Tashiro K, Shimizu S. Molecular cloning and expression of human hepatocyte growth factor. *Nature*. 1989;342(6248):440-3. Epub 1989/11/23. doi: 10.1038/342440a0. PubMed PMID: 2531289.
33. Stoker M, Gherardi E, Perryman M, Gray J. Scatter factor is a fibroblast-derived modulator of epithelial cell mobility. *Nature*. 1987;327(6119):239-42. Epub 1987/05/21. doi: 10.1038/327239a0. PubMed PMID: 2952888.

34. Weidner KM, Arakaki N, Hartmann G, Vandekerckhove J, Weingart S, Rieder H, Fonatsch C, Tsubouchi H, Hishida T, Daikuhara Y, et al. Evidence for the identity of human scatter factor and human hepatocyte growth factor. *Proc Natl Acad Sci U S A*. 1991;88(16):7001-5. Epub 1991/08/15. PubMed PMID: 1831266; PubMed Central PMCID: PMC52221.
35. Zarnegar R, Michalopoulos G. Purification and biological characterization of human hepatopoietin A, a polypeptide growth factor for hepatocytes. *Cancer Res*. 1989;49(12):3314-20. Epub 1989/06/15. PubMed PMID: 2524251.
36. Boix L, Rosa JL, Ventura F, Castells A, Bruix J, Rodes J, Bartrons R. c-met mRNA overexpression in human hepatocellular carcinoma. *Hepatology*. 1994;19(1):88-91. Epub 1994/01/01. PubMed PMID: 8276372.
37. Edakuni G, Sasatomi E, Satoh T, Tokunaga O, Miyazaki K. Expression of the hepatocyte growth factor/c-Met pathway is increased at the cancer front in breast carcinoma. *Pathol Int*. 2001;51(3):172-8. Epub 2001/05/01. PubMed PMID: 11328532.
38. Ichimura E, Maeshima A, Nakajima T, Nakamura T. Expression of c-met/HGF receptor in human non-small cell lung carcinomas in vitro and in vivo and its prognostic significance. *Jpn J Cancer Res*. 1996;87(10):1063-9. Epub 1996/10/01. PubMed PMID: 8957065.
39. Ayhan A, Ertunc D, Tok EC. Expression of the c-Met in advanced epithelial ovarian cancer and its prognostic significance. *Int J Gynecol Cancer*. 2005;15(4):618-23. Epub 2005/07/15. doi: 10.1111/j.1525-1438.2005.00117.x. PubMed PMID: 16014115.
40. Danilkovitch-Miagkova A, Zbar B. Dysregulation of Met receptor tyrosine kinase activity in invasive tumors. *J Clin Invest*. 2002;109(7):863-7. Epub 2002/04/03. doi: 10.1172/jci15418. PubMed PMID: 11927612; PubMed Central PMCID: PMC150937.
41. Parr C, Watkins G, Mansel RE, Jiang WG. The hepatocyte growth factor regulatory factors in human breast cancer. *Clin Cancer Res*. 2004;10(1 Pt 1):202-11. Epub 2004/01/22. PubMed PMID: 14734471.

42. Yamashita J, Ogawa M, Yamashita S, Nomura K, Kuramoto M, Saishoji T, Shin S. Immunoreactive hepatocyte growth factor is a strong and independent predictor of recurrence and survival in human breast cancer. *Cancer Res.* 1994;54(7):1630-3. Epub 1994/04/01. PubMed PMID: 8137271.
43. Engelman JA, Zejnullahu K, Mitsudomi T, Song Y, Hyland C, Park JO, Lindeman N, Gale CM, Zhao X, Christensen J, Kosaka T, Holmes AJ, Rogers AM, Cappuzzo F, Mok T, Lee C, Johnson BE, Cantley LC, Janne PA. MET amplification leads to gefitinib resistance in lung cancer by activating ERBB3 signaling. *Science.* 2007;316(5827):1039-43. Epub 2007/04/28. doi: 10.1126/science.1141478. PubMed PMID: 17463250.
44. Schmidt L, Duh FM, Chen F, Kishida T, Glenn G, Choyke P, Scherer SW, Zhuang Z, Lubensky I, Dean M, Allikmets R, Chidambaram A, Bergerheim UR, Feltis JT, Casadevall C, Zamarron A, Bernues M, Richard S, Lips CJ, Walther MM, Tsui LC, Geil L, Orcutt ML, Stackhouse T, Lipan J, Slife L, Brauch H, Decker J, Niehans G, Hughson MD, Moch H, Storkel S, Lerman MI, Linehan WM, Zbar B. Germline and somatic mutations in the tyrosine kinase domain of the MET proto-oncogene in papillary renal carcinomas. *Nat Genet.* 1997;16(1):68-73. Epub 1997/05/01. doi: 10.1038/ng0597-68. PubMed PMID: 9140397.
45. Ma PC, Jagadeeswaran R, Jagadeesh S, Tretiakova MS, Nallasura V, Fox EA, Hansen M, Schaefer E, Naoki K, Lader A, Richards W, Sugarbaker D, Husain AN, Christensen JG, Salgia R. Functional expression and mutations of c-Met and its therapeutic inhibition with SU11274 and small interfering RNA in non-small cell lung cancer. *Cancer Res.* 2005;65(4):1479-88. Epub 2005/03/01. doi: 10.1158/0008-5472.can-04-2650. PubMed PMID: 15735036.
46. Peschard P, Park M. From Tpr-Met to Met, tumorigenesis and tubes. *Oncogene.* 2007;26(9):1276-85. Epub 2007/02/27. doi: 10.1038/sj.onc.1210201. PubMed PMID: 17322912.

47. Blumenschein GR, Jr., Mills GB, Gonzalez-Angulo AM. Targeting the hepatocyte growth factor-cMET axis in cancer therapy. *J Clin Oncol.* 2012;30(26):3287-96. Epub 2012/08/08. doi: 10.1200/jco.2011.40.3774. PubMed PMID: 22869872; PubMed Central PMCID: PMC3434988.
48. Aebbersold DM, Landt O, Berthou S, Gruber G, Beer KT, Greiner RH, Zimmer Y. Prevalence and clinical impact of Met Y1253D-activating point mutation in radiotherapy-treated squamous cell cancer of the oropharynx. *Oncogene.* 2003;22(52):8519-23. Epub 2003/11/25. doi: 10.1038/sj.onc.1206968. PubMed PMID: 14627992.
49. Di Renzo MF, Olivero M, Martone T, Maffe A, Maggiora P, Stefani AD, Valente G, Giordano S, Cortesina G, Comoglio PM. Somatic mutations of the MET oncogene are selected during metastatic spread of human HNSC carcinomas. *Oncogene.* 2000;19(12):1547-55. Epub 2000/03/29. doi: 10.1038/sj.onc.1203455. PubMed PMID: 10734314.
50. Lorenzato A, Olivero M, Patane S, Rosso E, Oliaro A, Comoglio PM, Di Renzo MF. Novel somatic mutations of the MET oncogene in human carcinoma metastases activating cell motility and invasion. *Cancer Res.* 2002;62(23):7025-30. Epub 2002/12/04. PubMed PMID: 12460923.
51. Schmid F, Burock S, Klockmeier K, Schlag PM, Stein U. SNPs in the coding region of the metastasis-inducing gene MACC1 and clinical outcome in colorectal cancer. *Mol Cancer.* 2012;11:49. Epub 2012/07/31. doi: 10.1186/1476-4598-11-49. PubMed PMID: 22838389; PubMed Central PMCID: PMC3480947.
52. Wasenius VM, Hemmer S, Karjalainen-Lindsberg ML, Nupponen NN, Franssila K, Joensuu H. MET receptor tyrosine kinase sequence alterations in differentiated thyroid carcinoma. *Am J Surg Pathol.* 2005;29(4):544-9. Epub 2005/03/16. PubMed PMID: 15767811.
53. Lee JH, Han SU, Cho H, Jennings B, Gerrard B, Dean M, Schmidt L, Zbar B, Vande Woude GF. A novel germ line juxtamembrane Met mutation in human gastric cancer.

Oncogene. 2000;19(43):4947-53. Epub 2000/10/24. doi: 10.1038/sj.onc.1203874. PubMed PMID: 11042681.

54. Tyner JW, Fletcher LB, Wang EQ, Yang WF, Rutenberg-Schoenberg ML, Beadling C, Mori M, Heinrich MC, Deininger MW, Druker BJ, Loriaux MM. MET receptor sequence variants R970C and T992I lack transforming capacity. *Cancer Res.* 2010;70(15):6233-7. Epub 2010/07/31. doi: 10.1158/0008-5472.can-10-0429. PubMed PMID: 20670955; PubMed Central PMCID: PMC2913476.

55. Schmidt L, Junker K, Nakaigawa N, Kinjerski T, Weirich G, Miller M, Lubensky I, Neumann HP, Brauch H, Decker J, Vocke C, Brown JA, Jenkins R, Richard S, Bergerheim U, Gerrard B, Dean M, Linehan WM, Zbar B. Novel mutations of the MET proto-oncogene in papillary renal carcinomas. *Oncogene.* 1999;18(14):2343-50. Epub 1999/05/18. doi: 10.1038/sj.onc.1202547. PubMed PMID: 10327054.

56. Hennessy BT, Timms KM, Carey MS, Gutin A, Meyer LA, Flake DD, 2nd, Abkevich V, Potter J, Pruss D, Glenn P, Li Y, Li J, Gonzalez-Angulo AM, McCune KS, Markman M, Broaddus RR, Lanchbury JS, Lu KH, Mills GB. Somatic mutations in BRCA1 and BRCA2 could expand the number of patients that benefit from poly (ADP ribose) polymerase inhibitors in ovarian cancer. *J Clin Oncol.* 2010;28(22):3570-6. Epub 2010/07/08. doi: 10.1200/jco.2009.27.2997. PubMed PMID: 20606085; PubMed Central PMCID: PMC2917312.

57. Comprehensive molecular portraits of human breast tumours. *Nature.* 2012;490(7418):61-70. Epub 2012/09/25. doi: 10.1038/nature11412. PubMed PMID: 23000897; PubMed Central PMCID: PMC3465532.

58. NCBI. Reference SNP Cluster Report: rs56391007. Available from: http://www.ncbi.nlm.nih.gov/projects/SNP/snp_ref.cgi?rs=56391007.

59. Ponzio MG, Lesurf R, Petkiewicz S, O'Malley FP, Pinnaduwage D, Andrulis IL, Bull SB, Chughtai N, Zuo D, Souleimanova M, Germain D, Omeroglu A, Cardiff RD, Hallett M, Park M. Met induces mammary tumors with diverse histologies and is associated with poor outcome

and human basal breast cancer. *Proc Natl Acad Sci U S A*. 2009;106(31):12903-8. Epub 2009/07/21. doi: 10.1073/pnas.0810402106. PubMed PMID: 19617568; PubMed Central PMCID: PMC2722321.

60. Liu P, Cheng H, Santiago S, Raeder M, Zhang F, Isabella A, Yang J, Semaan DJ, Chen C, Fox EA, Gray NS, Monahan J, Schlegel R, Beroukhim R, Mills GB, Zhao JJ. Oncogenic PIK3CA-driven mammary tumors frequently recur via PI3K pathway-dependent and PI3K pathway-independent mechanisms. *Nat Med*. 2011;17(9):1116-20. Epub 2011/08/09. doi: 10.1038/nm.2402. PubMed PMID: 21822287; PubMed Central PMCID: PMC3169724.

61. NIH. ClinicalTrials.Gov. Available from: www.clinicaltrials.gov.

62. Donev IS, Wang W, Yamada T, Li Q, Takeuchi S, Matsumoto K, Yamori T, Nishioka Y, Sone S, Yano S. Transient PI3K inhibition induces apoptosis and overcomes HGF-mediated resistance to EGFR-TKIs in EGFR mutant lung cancer. *Clin Cancer Res*. 2011;17(8):2260-9. Epub 2011/01/12. doi: 10.1158/1078-0432.ccr-10-1993. PubMed PMID: 21220474.

63. Gherardi E, Youles ME, Miguel RN, Blundell TL, Iamele L, Gough J, Bandyopadhyay A, Hartmann G, Butler PJ. Functional map and domain structure of MET, the product of the c-met protooncogene and receptor for hepatocyte growth factor/scatter factor. *Proceedings of the National Academy of Sciences of the United States of America*. 2003;100(21):12039-44. Epub 2003/10/07. doi: 10.1073/pnas.2034936100. PubMed PMID: 14528000; PubMed Central PMCID: PMC218709.

64. Lokker NA, Mark MR, Luis EA, Bennett GL, Robbins KA, Baker JB, Godowski PJ. Structure-function analysis of hepatocyte growth factor: identification of variants that lack mitogenic activity yet retain high affinity receptor binding. *The EMBO journal*. 1992;11(7):2503-10. Epub 1992/07/01. PubMed PMID: 1321034; PubMed Central PMCID: PMC556725.

65. Gherardi E, Sandin S, Petoukhov MV, Finch J, Youles ME, Ofverstedt LG, Miguel RN, Blundell TL, Vande Woude GF, Skoglund U, Svergun DI. Structural basis of hepatocyte growth

factor/scatter factor and MET signalling. *Proceedings of the National Academy of Sciences of the United States of America*. 2006;103(11):4046-51. Epub 2006/03/16. doi: 10.1073/pnas.0509040103. PubMed PMID: 16537482; PubMed Central PMCID: PMC1449643.

66. Zhang YW, Vande Woude GF. HGF/SF-met signaling in the control of branching morphogenesis and invasion. *Journal of cellular biochemistry*. 2003;88(2):408-17. Epub 2003/01/10. doi: 10.1002/jcb.10358. PubMed PMID: 12520544.

67. Rosario M, Birchmeier W. How to make tubes: signaling by the Met receptor tyrosine kinase. *Trends in cell biology*. 2003;13(6):328-35. Epub 2003/06/07. PubMed PMID: 12791299.

68. Corso S, Comoglio PM, Giordano S. Cancer therapy: can the challenge be MET? *Trends in molecular medicine*. 2005;11(6):284-92. Epub 2005/06/14. doi: 10.1016/j.molmed.2005.04.005. PubMed PMID: 15949770.

69. Stamos J, Lazarus RA, Yao X, Kirchhofer D, Wiesmann C. Crystal structure of the HGF beta-chain in complex with the Sema domain of the Met receptor. *The EMBO journal*. 2004;23(12):2325-35. Epub 2004/05/29. doi: 10.1038/sj.emboj.7600243. PubMed PMID: 15167892; PubMed Central PMCID: PMC423285.

70. Boccaccio C, Comoglio PM. Invasive growth: a MET-driven genetic programme for cancer and stem cells. *Nature reviews Cancer*. 2006;6(8):637-45. Epub 2006/07/25. doi: 10.1038/nrc1912. PubMed PMID: 16862193.

71. Trusolino L, Bertotti A, Comoglio PM. A signaling adapter function for alpha6beta4 integrin in the control of HGF-dependent invasive growth. *Cell*. 2001;107(5):643-54. Epub 2001/12/06. PubMed PMID: 11733063.

72. Basile JR, Afkhami T, Gutkind JS. Semaphorin 4D/plexin-B1 induces endothelial cell migration through the activation of PYK2, Src, and the phosphatidylinositol 3-kinase-Akt pathway. *Molecular and cellular biology*. 2005;25(16):6889-98. Epub 2005/08/02. doi:

10.1128/MCB.25.16.6889-6898.2005. PubMed PMID: 16055703; PubMed Central PMCID: PMC1190270.

73. Gomez-Quiroz LE, Factor VM, Kaposi-Novak P, Coulouarn C, Conner EA, Thorgeirsson SS. Hepatocyte-specific c-Met deletion disrupts redox homeostasis and sensitizes to Fas-mediated apoptosis. *The Journal of biological chemistry*. 2008;283(21):14581-9. Epub 2008/03/20. doi: 10.1074/jbc.M707733200. PubMed PMID: 18348981; PubMed Central PMCID: PMC2386934.

74. Puri N, Salgia R. Synergism of EGFR and c-Met pathways, cross-talk and inhibition, in non-small cell lung cancer. *Journal of carcinogenesis*. 2008;7:9. Epub 2009/02/26. PubMed PMID: 19240370; PubMed Central PMCID: PMC2669728.

75. Shattuck DL, Miller JK, Carraway KL, 3rd, Sweeney C. Met receptor contributes to trastuzumab resistance of Her2-overexpressing breast cancer cells. *Cancer research*. 2008;68(5):1471-7. Epub 2008/03/05. doi: 10.1158/0008-5472.CAN-07-5962. PubMed PMID: 18316611.

76. Bauer TW, Somcio RJ, Fan F, Liu W, Johnson M, Lesslie DP, Evans DB, Gallick GE, Ellis LM. Regulatory role of c-Met in insulin-like growth factor-I receptor-mediated migration and invasion of human pancreatic carcinoma cells. *Molecular cancer therapeutics*. 2006;5(7):1676-82. Epub 2006/08/08. doi: 10.1158/1535-7163.MCT-05-0175. PubMed PMID: 16891453.

77. Smolen GA, Sordella R, Muir B, Mohapatra G, Barmettler A, Archibald H, Kim WJ, Okimoto RA, Bell DW, Sgroi DC, Christensen JG, Settleman J, Haber DA. Amplification of MET may identify a subset of cancers with extreme sensitivity to the selective tyrosine kinase inhibitor PHA-665752. *Proceedings of the National Academy of Sciences of the United States of America*. 2006;103(7):2316-21. Epub 2006/02/08. doi: 10.1073/pnas.0508776103. PubMed PMID: 16461907; PubMed Central PMCID: PMC1413705.

78. Lengyel E, Prechtel D, Resau JH, Gauger K, Welk A, Lindemann K, Salanti G, Richter T, Knudsen B, Vande Woude GF, Harbeck N. C-Met overexpression in node-positive breast cancer identifies patients with poor clinical outcome independent of Her2/neu. *International journal of cancer Journal international du cancer*. 2005;113(4):678-82. Epub 2004/09/30. doi: 10.1002/ijc.20598. PubMed PMID: 15455388.
79. Christensen JG, Burrows J, Salgia R. c-Met as a target for human cancer and characterization of inhibitors for therapeutic intervention. *Cancer letters*. 2005;225(1):1-26. Epub 2005/06/01. doi: 10.1016/j.canlet.2004.09.044. PubMed PMID: 15922853.
80. Soman NR, Correa P, Ruiz BA, Wogan GN. The TPR-MET oncogenic rearrangement is present and expressed in human gastric carcinoma and precursor lesions. *Proceedings of the National Academy of Sciences of the United States of America*. 1991;88(11):4892-6. Epub 1991/06/01. PubMed PMID: 2052572; PubMed Central PMCID: PMC51773.
81. Danilkovitch-Miagkova A, Zbar B. Dysregulation of Met receptor tyrosine kinase activity in invasive tumors. *The Journal of clinical investigation*. 2002;109(7):863-7. Epub 2002/04/03. doi: 10.1172/JCI15418. PubMed PMID: 11927612; PubMed Central PMCID: PMC150937.
82. Ichimura E, Maeshima A, Nakajima T, Nakamura T. Expression of c-met/HGF receptor in human non-small cell lung carcinomas in vitro and in vivo and its prognostic significance. *Japanese journal of cancer research : Gann*. 1996;87(10):1063-9. Epub 1996/10/01. PubMed PMID: 8957065.
83. Cipriani NA, Abidoye OO, Vokes E, Salgia R. MET as a target for treatment of chest tumors. *Lung cancer*. 2009;63(2):169-79. Epub 2008/08/02. doi: 10.1016/j.lungcan.2008.06.011. PubMed PMID: 18672314; PubMed Central PMCID: PMC2659375.
84. Garcia S, Dalès J-P, Charafe-Jauffret E, Carpentier-Meunier S, Andrac-Meyer L, Jacquemier J, Andonian C, Lavaut M-N, Allasia C, Bonnier P, Charpin C. Poor prognosis in breast carcinomas correlates with increased expression of targetable CD146 and c-Met and

with proteomic basal-like phenotype. *Human Pathology*. 2007;38(6):830-41. doi: 10.1016/j.humpath.2006.11.015.

85. Ma PC, Jagadeeswaran R, Jagadeesh S, Tretiakova MS, Nallasura V, Fox EA, Hansen M, Schaefer E, Naoki K, Lader A, Richards W, Sugarbaker D, Husain AN, Christensen JG, Salgia R. Functional expression and mutations of c-Met and its therapeutic inhibition with SU11274 and small interfering RNA in non-small cell lung cancer. *Cancer research*. 2005;65(4):1479-88. Epub 2005/03/01. doi: 10.1158/0008-5472.CAN-04-2650. PubMed PMID: 15735036.

86. Olivero M, Rizzo M, Madeddu R, Casadio C, Pennacchietti S, Nicotra MR, Prat M, Maggi G, Arena N, Natali PG, Comoglio PM, Di Renzo MF. Overexpression and activation of hepatocyte growth factor/scatter factor in human non-small-cell lung carcinomas. *British journal of cancer*. 1996;74(12):1862-8. Epub 1996/12/01. PubMed PMID: 8980383; PubMed Central PMCID: PMC2074802.

87. Takanami I, Tanana F, Hashizume T, Kikuchi K, Yamamoto Y, Yamamoto T, Kodaira S. Hepatocyte growth factor and c-Met/hepatocyte growth factor receptor in pulmonary adenocarcinomas: an evaluation of their expression as prognostic markers. *Oncology*. 1996;53(5):392-7. Epub 1996/09/01. PubMed PMID: 8784474.

88. Jagadeeswaran R, Ma PC, Seiwert TY, Jagadeeswaran S, Zumba O, Nallasura V, Ahmed S, Filiberti R, Paganuzzi M, Puntoni R, Kratzke RA, Gordon GJ, Sugarbaker DJ, Bueno R, Janamanchi V, Bindokas VP, Kindler HL, Salgia R. Functional analysis of c-Met/hepatocyte growth factor pathway in malignant pleural mesothelioma. *Cancer research*. 2006;66(1):352-61. Epub 2006/01/07. doi: 10.1158/0008-5472.CAN-04-4567. PubMed PMID: 16397249.

89. Wong AS, Pelech SL, Woo MM, Yim G, Rosen B, Ehlen T, Leung PC, Auersperg N. Coexpression of hepatocyte growth factor-Met: an early step in ovarian carcinogenesis?

Oncogene. 2001;20(11):1318-28. Epub 2001/04/21. doi: 10.1038/sj.onc.1204253. PubMed PMID: 11313876.

90. Zeng ZS, Weiser MR, Kuntz E, Chen CT, Khan SA, Forslund A, Nash GM, Gimbel M, Yamaguchi Y, Culliford ATt, D'Alessio M, Barany F, Paty PB. c-Met gene amplification is associated with advanced stage colorectal cancer and liver metastases. *Cancer letters*. 2008;265(2):258-69. Epub 2008/04/09. doi: 10.1016/j.canlet.2008.02.049. PubMed PMID: 18395971.

91. Tolgay Ocal I, Dolled-Filhart M, D'Aquila TG, Camp RL, Rimm DL. Tissue microarray-based studies of patients with lymph node negative breast carcinoma show that met expression is associated with worse outcome but is not correlated with epidermal growth factor family receptors. *Cancer*. 2003;97(8):1841-8. Epub 2003/04/04. doi: 10.1002/cncr.11335. PubMed PMID: 12673709.

92. Carracedo A, Egervari K, Salido M, Rojo F, Corominas JM, Arumi M, Corzo C, Tusquets I, Espinet B, Rovira A, Albanell J, Szollosi Z, Serrano S, Sole F. FISH and immunohistochemical status of the hepatocyte growth factor receptor (c-Met) in 184 invasive breast tumors. *Breast cancer research : BCR*. 2009;11(2):402. Epub 2009/05/15. doi: 10.1186/bcr2239. PubMed PMID: 19439036; PubMed Central PMCID: PMC2688943.

93. Cappuzzo F, Ciuleanu T, Stelmakh L, Cicens S, Szesna A, Juzasz E, Esteban Gonzalez E, Molinier O, Klingelschmitt G, Giaccone GobotSI. SATURN: A double-blind, randomized, phase III study of maintenance erlotinib versus placebo following nonprogression with first-line platinum-based chemotherapy in patients with advanced NSCLC. *J Clin Oncol*. 2009;15s:(suppl; abstr 8001).

94. Schmidt L, Duh FM, Chen F, Kishida T, Glenn G, Choyke P, Scherer SW, Zhuang Z, Lubensky I, Dean M, Allikmets R, Chidambaram A, Bergerheim UR, Feltis JT, Casadevall C, Zamarron A, Bernues M, Richard S, Lips CJ, Walther MM, Tsui LC, Geil L, Orcutt ML, Stackhouse T, Lipan J, Slife L, Brauch H, Decker J, Niehans G, Hughson MD, Moch H, Storkel

S, Lerman MI, Linehan WM, Zbar B. Germline and somatic mutations in the tyrosine kinase domain of the MET proto-oncogene in papillary renal carcinomas. *Nature genetics*. 1997;16(1):68-73. Epub 1997/05/01. doi: 10.1038/ng0597-68. PubMed PMID: 9140397.

95. Ma PC, Kijima T, Maulik G, Fox EA, Sattler M, Griffin JD, Johnson BE, Salgia R. c-MET mutational analysis in small cell lung cancer: novel juxtamembrane domain mutations regulating cytoskeletal functions. *Cancer research*. 2003;63(19):6272-81. Epub 2003/10/16. PubMed PMID: 14559814.

96. Graveel C, Su Y, Koeman J, Wang LM, Tessarollo L, Fiscella M, Birchmeier C, Swiatek P, Bronson R, Vande Woude G. Activating Met mutations produce unique tumor profiles in mice with selective duplication of the mutant allele. *Proceedings of the National Academy of Sciences of the United States of America*. 2004;101(49):17198-203. Epub 2004/11/24. doi: 10.1073/pnas.0407651101. PubMed PMID: 15557554; PubMed Central PMCID: PMC535398.

97. Hammond ME, Hayes DF, Dowsett M, Allred DC, Hagerty KL, Badve S, Fitzgibbons PL, Francis G, Goldstein NS, Hayes M, Hicks DG, Lester S, Love R, Mangu PB, McShane L, Miller K, Osborne CK, Paik S, Perlmutter J, Rhodes A, Sasano H, Schwartz JN, Sweep FC, Taube S, Torlakovic EE, Valenstein P, Viale G, Visscher D, Wheeler T, Williams RB, Wittliff JL, Wolff AC. American Society of Clinical Oncology/College Of American Pathologists guideline recommendations for immunohistochemical testing of estrogen and progesterone receptors in breast cancer. *J Clin Oncol*.28(16):2784-95. Epub 2010/04/21. doi: JCO.2009.25.6529 [pii]

10.1200/JCO.2009.25.6529. PubMed PMID: 20404251.

98. Wolff AC, Hammond ME, Schwartz JN, Hagerty KL, Allred DC, Cote RJ, Dowsett M, Fitzgibbons PL, Hanna WM, Langer A, McShane LM, Paik S, Pegram MD, Perez EA, Press MF, Rhodes A, Sturgeon C, Taube SE, Tubbs R, Vance GH, van de Vijver M, Wheeler TM, Hayes DF. American Society of Clinical Oncology/College of American Pathologists guideline

recommendations for human epidermal growth factor receptor 2 testing in breast cancer. *J Clin Oncol.* 2007;25(1):118-45. Epub 2006/12/13. doi: JCO.2006.09.2775 [pii]

10.1200/JCO.2006.09.2775. PubMed PMID: 17159189.

99. Hennessy BT, Lu Y, Gonzalez-Angulo AM, Carey MS, Myhre S, Ju Z, Davies MA, Liu W, Coombes K, Meric-Bernstam F, Bedrosian I, McGahren M, Agarwal R, Zhang F, Overgaard J, Alsner J, Neve RM, Kuo WL, Gray JW, Borresen-Dale AL, Mills GB. A Technical Assessment of the Utility of Reverse Phase Protein Arrays for the Study of the Functional Proteome in Non-microdissected Human Breast Cancers. *Clin Proteomics.*6(4):129-51. Epub 2011/06/22. doi: 10.1007/s12014-010-9055-y. PubMed PMID: 21691416.

100. Leo B. *Classification & Regression Trees* Wadsworth Co; 1984.

101. Cooper CS, Park M, Blair DG, Tainsky MA, Huebner K, Croce CM, Vande Woude GF. Molecular cloning of a new transforming gene from a chemically transformed human cell line. *Nature.* 1984;311(5981):29-33. Epub 1984/09/06. PubMed PMID: 6590967.

102. Birchmeier C, Birchmeier W, Gherardi E, Vande Woude GF. Met, metastasis, motility and more. *Nat Rev Mol Cell Biol.* 2003;4(12):915-25. Epub 2003/12/20. doi: 10.1038/nrm1261 nrm1261 [pii]. PubMed PMID: 14685170.

103. Ponzetto C, Bardelli A, Zhen Z, Maina F, dalla Zonca P, Giordano S, Graziani A, Panayotou G, Comoglio PM. A multifunctional docking site mediates signaling and transformation by the hepatocyte growth factor/scatter factor receptor family. *Cell.* 1994;77(2):261-71. Epub 1994/04/22. doi: 0092-8674(94)90318-2 [pii]. PubMed PMID: 7513258.

104. Camp RL, Rimm EB, Rimm DL. Met expression is associated with poor outcome in patients with axillary lymph node negative breast carcinoma. *Cancer.* 1999;86(11):2259-65. Epub 1999/12/11. doi: 10.1002/(SICI)1097-0142(19991201)86:11<2259::AID-CNCR13>3.0.CO;2-2 [pii]. PubMed PMID: 10590366.

105. Lengyel E, Prechtel D, Resau JH, Gauger K, Welk A, Lindemann K, Salanti G, Richter T, Knudsen B, Vande Woude GF, Harbeck N. C-Met overexpression in node-positive breast cancer identifies patients with poor clinical outcome independent of Her2/neu. *Int J Cancer*. 2005;113(4):678-82. Epub 2004/09/30. doi: 10.1002/ijc.20598. PubMed PMID: 15455388.
106. Berg D, Hipp S, Malinowsky K, Bollner C, Becker KF. Molecular profiling of signalling pathways in formalin-fixed and paraffin-embedded cancer tissues. *Eur J Cancer*.46(1):47-55. Epub 2009/11/17. doi: S0959-8049(09)00774-6 [pii]
10.1016/j.ejca.2009.10.016. PubMed PMID: 19914823.
107. Grote T, Siwak DR, Fritsche HA, Joy C, Mills GB, Simeone D, Whitcomb DC, Logsdon CD. Validation of reverse phase protein array for practical screening of potential biomarkers in serum and plasma: accurate detection of CA19-9 levels in pancreatic cancer. *Proteomics*. 2008;8(15):3051-60. Epub 2008/07/11. doi: 10.1002/pmic.200700951. PubMed PMID: 18615426.
108. Tibes R, Qiu Y, Lu Y, Hennessy B, Andreeff M, Mills GB, Kornblau SM. Reverse phase protein array: validation of a novel proteomic technology and utility for analysis of primary leukemia specimens and hematopoietic stem cells. *Mol Cancer Ther*. 2006;5(10):2512-21. Epub 2006/10/17. doi: 5/10/2512 [pii]
10.1158/1535-7163.MCT-06-0334. PubMed PMID: 17041095.
109. Kermorgant S, Aparicio T, Dessirier V, Lewin MJ, Lehy T. Hepatocyte growth factor induces colonic cancer cell invasiveness via enhanced motility and protease overproduction. Evidence for PI3 kinase and PKC involvement. *Carcinogenesis*. 2001;22(7):1035-42. Epub 2001/06/16. PubMed PMID: 11408346.
110. Bussolino F, Di Renzo MF, Ziche M, Bocchietto E, Olivero M, Naldini L, Gaudino G, Tamagnone L, Coffer A, Comoglio PM. Hepatocyte growth factor is a potent angiogenic factor which stimulates endothelial cell motility and growth. *J Cell Biol*. 1992;119(3):629-41. Epub 1992/11/01. PubMed PMID: 1383237.

111. Previdi S, Maroni P, Matteucci E, Broggin M, Bendinelli P, Desiderio MA. Interaction between human-breast cancer metastasis and bone microenvironment through activated hepatocyte growth factor/Met and beta-catenin/Wnt pathways. *Eur J Cancer*.46(9):1679-91. Epub 2010/03/31. doi: S0959-8049(10)00163-2 [pii]
- 10.1016/j.ejca.2010.02.036. PubMed PMID: 20350802.
112. Khoury H, Naujokas MA, Zuo D, Sangwan V, Frigault MM, Petkiewicz S, Dankort DL, Muller WJ, Park M. HGF converts ErbB2/Neu epithelial morphogenesis to cell invasion. *Mol Biol Cell*. 2005;16(2):550-61. Epub 2004/11/19. doi: E04-07-0567 [pii]
- 10.1091/mbc.E04-07-0567. PubMed PMID: 15548598.
113. Fan S, Wang JA, Yuan RQ, Rockwell S, Andres J, Zlatapolskiy A, Goldberg ID, Rosen EM. Scatter factor protects epithelial and carcinoma cells against apoptosis induced by DNA-damaging agents. *Oncogene*. 1998;17(2):131-41. Epub 1998/07/23. doi: 10.1038/sj.onc.1201943. PubMed PMID: 9674697.
114. Fan S, Ma YX, Wang JA, Yuan RQ, Meng Q, Cao Y, Laterra JJ, Goldberg ID, Rosen EM. The cytokine hepatocyte growth factor/scatter factor inhibits apoptosis and enhances DNA repair by a common mechanism involving signaling through phosphatidyl inositol 3' kinase. *Oncogene*. 2000;19(18):2212-23. Epub 2000/05/24. doi: 10.1038/sj.onc.1203566. PubMed PMID: 10822371.
115. De Bacco F, Luraghi P, Medico E, Reato G, Girolami F, Perera T, Gabriele P, Comoglio PM, Boccaccio C. Induction of MET by ionizing radiation and its role in radioresistance and invasive growth of cancer. *J Natl Cancer Inst*.103(8):645-61. Epub 2011/04/06. doi: djr093 [pii]
- 10.1093/jnci/djr093. PubMed PMID: 21464397.
116. Davies G, Watkins G, Mason MD, Jiang WG. Targeting the HGF/SF receptor c-met using a hammerhead ribozyme transgene reduces in vitro invasion and migration in prostate

cancer cells. *Prostate*. 2004;60(4):317-24. Epub 2004/07/21. doi: 10.1002/pros.20068. PubMed PMID: 15264243.

117. Zou HY, Li Q, Lee JH, Arango ME, McDonnell SR, Yamazaki S, Koudriakova TB, Alton G, Cui JJ, Kung PP, Nambu MD, Los G, Bender SL, Mroczkowski B, Christensen JG. An orally available small-molecule inhibitor of c-Met, PF-2341066, exhibits cytoreductive antitumor efficacy through antiproliferative and antiangiogenic mechanisms. *Cancer Res*. 2007;67(9):4408-17. Epub 2007/05/08. doi: 67/9/4408 [pii]

10.1158/0008-5472.CAN-06-4443. PubMed PMID: 17483355.

118. Gewinner C, Wang ZC, Richardson A, Teruya-Feldstein J, Etemadmoghadam D, Bowtell D, Barretina J, Lin WM, Rameh L, Salmena L, Pandolfi PP, Cantley LC. Evidence that inositol polyphosphate 4-phosphatase type II is a tumor suppressor that inhibits PI3K signaling. *Cancer Cell*. 2009;16(2):115-25. Epub 2009/08/04. doi: 10.1016/j.ccr.2009.06.006. PubMed PMID: 19647222; PubMed Central PMCID: PMC2957372.

119. Ghossein RA, Dillon DA, D'Aquila T, Rimm EB, Fearon ER, Rimm DL. Expression of c-met is a strong independent prognostic factor in breast carcinoma. *Cancer*. 1998;82(8):1513-20. Epub 1998/04/29. PubMed PMID: 9554529.

120. Eder JP, Vande Woude GF, Boerner SA, LoRusso PM. Novel therapeutic inhibitors of the c-Met signaling pathway in cancer. *Clin Cancer Res*. 2009;15(7):2207-14. Epub 2009/03/26. doi: 10.1158/1078-0432.ccr-08-1306. PubMed PMID: 19318488.

121. Wu G, Xing M, Mambo E, Huang X, Liu J, Guo Z, Chatterjee A, Goldenberg D, Gollin SM, Sukumar S, Trink B, Sidransky D. Somatic mutation and gain of copy number of PIK3CA in human breast cancer. *Breast Cancer Res*. 2005;7(5):R609-16. Epub 2005/09/20. doi: 10.1186/bcr1262. PubMed PMID: 16168105; PubMed Central PMCID: PMC1242128.

122. Kadota M, Sato M, Duncan B, Ooshima A, Yang HH, Diaz-Meyer N, Gere S, Kageyama S, Fukuoka J, Nagata T, Tsukada K, Dunn BK, Wakefield LM, Lee MP. Identification of novel gene amplifications in breast cancer and coexistence of gene

amplification with an activating mutation of PIK3CA. *Cancer Res.* 2009;69(18):7357-65. Epub 2009/08/27. doi: 10.1158/0008-5472.can-09-0064. PubMed PMID: 19706770; PubMed Central PMCID: PMC2745517.

123. Lopez-Knowles E, O'Toole SA, McNeil CM, Millar EK, Qiu MR, Crea P, Daly RJ, Musgrove EA, Sutherland RL. PI3K pathway activation in breast cancer is associated with the basal-like phenotype and cancer-specific mortality. *Int J Cancer.* 2010;126(5):1121-31. Epub 2009/08/18. doi: 10.1002/ijc.24831. PubMed PMID: 19685490.

124. Engelman JA, Luo J, Cantley LC. The evolution of phosphatidylinositol 3-kinases as regulators of growth and metabolism. *Nat Rev Genet.* 2006;7(8):606-19. Epub 2006/07/19. doi: 10.1038/nrg1879. PubMed PMID: 16847462.

125. Liu P, Cheng H, Roberts TM, Zhao JJ. Targeting the phosphoinositide 3-kinase pathway in cancer. *Nat Rev Drug Discov.* 2009;8(8):627-44. Epub 2009/08/01. doi: 10.1038/nrd2926. PubMed PMID: 19644473; PubMed Central PMCID: PMC3142564.

126. Samuels Y, Wang Z, Bardelli A, Silliman N, Ptak J, Szabo S, Yan H, Gazdar A, Powell SM, Riggins GJ, Willson JK, Markowitz S, Kinzler KW, Vogelstein B, Velculescu VE. High frequency of mutations of the PIK3CA gene in human cancers. *Science.* 2004;304(5670):554. Epub 2004/03/16. doi: 10.1126/science.1096502. PubMed PMID: 15016963.

127. Vogt PK, Kang S, Elsliger MA, Gymnopoulos M. Cancer-specific mutations in phosphatidylinositol 3-kinase. *Trends Biochem Sci.* 2007;32(7):342-9. Epub 2007/06/15. doi: 10.1016/j.tibs.2007.05.005. PubMed PMID: 17561399.

128. Yuan TL, Cantley LC. PI3K pathway alterations in cancer: variations on a theme. *Oncogene.* 2008;27(41):5497-510. Epub 2008/09/17. doi: 10.1038/onc.2008.245. PubMed PMID: 18794884; PubMed Central PMCID: PMC3398461.

129. Zhao JJ, Liu Z, Wang L, Shin E, Loda MF, Roberts TM. The oncogenic properties of mutant p110alpha and p110beta phosphatidylinositol 3-kinases in human mammary epithelial cells. *Proc Natl Acad Sci U S A.* 2005;102(51):18443-8. Epub 2005/12/13. doi:

10.1073/pnas.0508988102. PubMed PMID: 16339315; PubMed Central PMCID: PMC1317954.

130. Engelman JA, Chen L, Tan X, Crosby K, Guimaraes AR, Upadhyay R, Maira M, McNamara K, Perera SA, Song Y, Chirieac LR, Kaur R, Lightbown A, Simendinger J, Li T, Padera RF, Garcia-Echeverria C, Weissleder R, Mahmood U, Cantley LC, Wong KK. Effective use of PI3K and MEK inhibitors to treat mutant Kras G12D and PIK3CA H1047R murine lung cancers. *Nat Med.* 2008;14(12):1351-6. Epub 2008/11/26. doi: 10.1038/nm.1890. PubMed PMID: 19029981; PubMed Central PMCID: PMC2683415.

131. Isakoff SJ, Engelman JA, Irie HY, Luo J, Brachmann SM, Pearlman RV, Cantley LC, Brugge JS. Breast cancer-associated PIK3CA mutations are oncogenic in mammary epithelial cells. *Cancer Res.* 2005;65(23):10992-1000. Epub 2005/12/03. doi: 10.1158/0008-5472.can-05-2612. PubMed PMID: 16322248.

132. Kang S, Bader AG, Vogt PK. Phosphatidylinositol 3-kinase mutations identified in human cancer are oncogenic. *Proc Natl Acad Sci U S A.* 2005;102(3):802-7. Epub 2005/01/14. doi: 10.1073/pnas.0408864102. PubMed PMID: 15647370; PubMed Central PMCID: PMC545580.

133. Samuels Y, Diaz LA, Jr., Schmidt-Kittler O, Cummins JM, DeLong L, Cheong I, Rago C, Huso DL, Lengauer C, Kinzler KW, Vogelstein B, Velculescu VE. Mutant PIK3CA promotes cell growth and invasion of human cancer cells. *Cancer Cell.* 2005;7(6):561-73. Epub 2005/06/14. doi: 10.1016/j.ccr.2005.05.014. PubMed PMID: 15950905.

134. Muellner MK, Uras IZ, Gapp BV, Kerzendorfer C, Smida M, Lechtermann H, Craig-Mueller N, Colinge J, Duernberger G, Nijman SM. A chemical-genetic screen reveals a mechanism of resistance to PI3K inhibitors in cancer. *Nat Chem Biol.* 2011;7(11):787-93. Epub 2011/09/29. doi: 10.1038/nchembio.695. PubMed PMID: 21946274; PubMed Central PMCID: PMC3306898.

135. Haber DA, Gray NS, Baselga J. The evolving war on cancer. *Cell*. 2011;145(1):19-24. Epub 2011/04/05. doi: 10.1016/j.cell.2011.03.026. PubMed PMID: 21458664.
136. Sellers WR. A blueprint for advancing genetics-based cancer therapy. *Cell*. 2011;147(1):26-31. Epub 2011/10/04. doi: 10.1016/j.cell.2011.09.016. PubMed PMID: 21962504.
137. Zhang H, Liu G, Dziubinski M, Yang Z, Ethier SP, Wu G. Comprehensive analysis of oncogenic effects of PIK3CA mutations in human mammary epithelial cells. *Breast Cancer Res Treat*. 2008;112(2):217-27. Epub 2007/12/13. doi: 10.1007/s10549-007-9847-6. PubMed PMID: 18074223.
138. Muthuswamy SK, Li D, Lelievre S, Bissell MJ, Brugge JS. ErbB2, but not ErbB1, reinitiates proliferation and induces luminal repopulation in epithelial acini. *Nat Cell Biol*. 2001;3(9):785-92. Epub 2001/09/05. doi: 10.1038/ncb0901-785. PubMed PMID: 11533657; PubMed Central PMCID: PMC2952547.
139. Zhang YW, Su Y, Lanning N, Gustafson M, Shinomiya N, Zhao P, Cao B, Tsarfaty G, Wang LM, Hay R, Vande Woude GF. Enhanced growth of human met-expressing xenografts in a new strain of immunocompromised mice transgenic for human hepatocyte growth factor/scatter factor. *Oncogene*. 2005;24(1):101-6. Epub 2004/11/09. doi: 10.1038/sj.onc.1208181. PubMed PMID: 15531925.
140. Hanahan D, Weinberg RA. The hallmarks of cancer. *Cell*. 2000;100(1):57-70. Epub 2000/01/27. PubMed PMID: 10647931.
141. Zhao L, Vogt PK. Helical domain and kinase domain mutations in p110alpha of phosphatidylinositol 3-kinase induce gain of function by different mechanisms. *Proc Natl Acad Sci U S A*. 2008;105(7):2652-7. Epub 2008/02/13. doi: 10.1073/pnas.0712169105. PubMed PMID: 18268322; PubMed Central PMCID: PMC2268191.
142. Huang CH, Mandelker D, Schmidt-Kittler O, Samuels Y, Velculescu VE, Kinzler KW, Vogelstein B, Gabelli SB, Amzel LM. The structure of a human p110alpha/p85alpha complex

- elucidates the effects of oncogenic PI3K α mutations. *Science*. 2007;318(5857):1744-8. Epub 2007/12/15. doi: 10.1126/science.1150799. PubMed PMID: 18079394.
143. Meyer DS, Brinkhaus H, Muller U, Muller M, Cardiff RD, Bentires-Alj M. Luminal expression of PIK3CA mutant H1047R in the mammary gland induces heterogeneous tumors. *Cancer Res*. 2011;71(13):4344-51. Epub 2011/04/13. doi: 10.1158/0008-5472.can-10-3827. PubMed PMID: 21482677.
144. Miller TW. Initiating breast cancer by PIK3CA mutation. *Breast Cancer Res*. 2012;14(1):301. Epub 2012/02/10. doi: 10.1186/bcr3103. PubMed PMID: 22315990; PubMed Central PMCID: PMC3496136.
145. Saal LH, Holm K, Maurer M, Memeo L, Su T, Wang X, Yu JS, Malmstrom PO, Mansukhani M, Enoksson J, Hibshoosh H, Borg A, Parsons R. PIK3CA mutations correlate with hormone receptors, node metastasis, and ERBB2, and are mutually exclusive with PTEN loss in human breast carcinoma. *Cancer Res*. 2005;65(7):2554-9. Epub 2005/04/05. doi: 10.1158/0008-5472.can-04-3913. PubMed PMID: 15805248.
146. Charafe-Jauffret E, Ginestier C, Monville F, Finetti P, Adelaide J, Cervera N, Fekairi S, Xerri L, Jacquemier J, Birnbaum D, Bertucci F. Gene expression profiling of breast cell lines identifies potential new basal markers. *Oncogene*. 2006;25(15):2273-84. Epub 2005/11/17. doi: 10.1038/sj.onc.1209254. PubMed PMID: 16288205.
147. Smolen GA, Muir B, Mohapatra G, Barmettler A, Kim WJ, Rivera MN, Haserlat SM, Okimoto RA, Kwak E, Dahiya S, Garber JE, Bell DW, Sgroi DC, Chin L, Deng CX, Haber DA. Frequent met oncogene amplification in a Brca1/Trp53 mouse model of mammary tumorigenesis. *Cancer Res*. 2006;66(7):3452-5. Epub 2006/04/06. doi: 10.1158/0008-5472.can-05-4181. PubMed PMID: 16585167.
148. Jin L, Fuchs A, Schnitt SJ, Yao Y, Joseph A, Lamszus K, Park M, Goldberg ID, Rosen EM. Expression of scatter factor and c-met receptor in benign and malignant breast tissue. *Cancer*. 1997;79(4):749-60. Epub 1997/02/15. PubMed PMID: 9024713.

149. Gastaldi S, Comoglio PM, Trusolino L. The Met oncogene and basal-like breast cancer: another culprit to watch out for? *Breast Cancer Res.* 2010;12(4):208. Epub 2010/09/02. doi: 10.1186/bcr2617. PubMed PMID: 20804567; PubMed Central PMCID: PMC2949647.
150. Graveel CR, DeGroot JD, Su Y, Koeman J, Dykema K, Leung S, Snider J, Davies SR, Swiatek PJ, Cottingham S, Watson MA, Ellis MJ, Sigler RE, Furge KA, Vande Woude GF. Met induces diverse mammary carcinomas in mice and is associated with human basal breast cancer. *Proc Natl Acad Sci U S A.* 2009;106(31):12909-14. Epub 2009/07/02. doi: 10.1073/pnas.0810403106. PubMed PMID: 19567831; PubMed Central PMCID: PMC2722304.
151. Ma PC, Kijima T, Maulik G, Fox EA, Sattler M, Griffin JD, Johnson BE, Salgia R. c-MET mutational analysis in small cell lung cancer: novel juxtamembrane domain mutations regulating cytoskeletal functions. *Cancer Res.* 2003;63(19):6272-81. Epub 2003/10/16. PubMed PMID: 14559814.
152. Lefebvre J, Ancot F, Leroy C, Muharram G, Lemiere A, Tulasne D. Met degradation: more than one stone to shoot a receptor down. *FASEB J.* 2012;26(4):1387-99. Epub 2012/01/10. doi: 10.1096/fj.11-197723. PubMed PMID: 22223753.
153. Burke WM, Jin X, Lin HJ, Huang M, Liu R, Reynolds RK, Lin J. Inhibition of constitutively active Stat3 suppresses growth of human ovarian and breast cancer cells. *Oncogene.* 2001;20(55):7925-34. Epub 2001/12/26. doi: 10.1038/sj.onc.1204990. PubMed PMID: 11753675.
154. Kunigal S, Lakka SS, Sodadasu PK, Estes N, Rao JS. Stat3-siRNA induces Fas-mediated apoptosis in vitro and in vivo in breast cancer. *Int J Oncol.* 2009;34(5):1209-20. Epub 2009/04/11. PubMed PMID: 19360334; PubMed Central PMCID: PMC2668130.
155. Dave B, Landis MD, Dobrolecki LE, Wu MF, Zhang X, Westbrook TF, Hilsenbeck SG, Liu D, Lewis MT, Tweardy DJ, Chang JC. Selective small molecule Stat3 inhibitor reduces

breast cancer tumor-initiating cells and improves recurrence free survival in a human-xenograft model. *PLoS One*. 2012;7(8):e30207. Epub 2012/08/11. doi: 10.1371/journal.pone.0030207. PubMed PMID: 22879872; PubMed Central PMCID: PMC3412855.

156. Zhang Q, Thomas SM, Lui VW, Xi S, Siegfried JM, Fan H, Smithgall TE, Mills GB, Grandis JR. Phosphorylation of TNF-alpha converting enzyme by gastrin-releasing peptide induces amphiregulin release and EGF receptor activation. *Proc Natl Acad Sci U S A*. 2006;103(18):6901-6. Epub 2006/04/28. doi: 10.1073/pnas.0509719103. PubMed PMID: 16641105; PubMed Central PMCID: PMC1458991.

157. Yuen HF, Chan KK, Grills C, Murray JT, Platt-Higgins A, Eldin OS, O'Byrne K, Janne P, Fennell DA, Johnston PG, Rudland PS, El-Tanani M. Ran is a potential therapeutic target for cancer cells with molecular changes associated with activation of the PI3K/Akt/mTORC1 and Ras/MEK/ERK pathways. *Clin Cancer Res*. 2012;18(2):380-91. Epub 2011/11/18. doi: 10.1158/1078-0432.ccr-11-2035. PubMed PMID: 22090358; PubMed Central PMCID: PMC3272446.

158. Yuen HF, Abramczyk O, Montgomery G, Chan KK, Huang YH, Sasazuki T, Shirasawa S, Gopesh S, Chan KW, Fennell D, Janne P, El-Tanani M, Murray JT. Impact of oncogenic driver mutations on feedback between the PI3K and MEK pathways in cancer cells. *Biosci Rep*. 2012;32(4):413-22. Epub 2012/06/07. doi: 10.1042/bsr20120050. PubMed PMID: 22668349; PubMed Central PMCID: PMC3392104.

159. Maulik G, Madhiwala P, Brooks S, Ma PC, Kijima T, Tibaldi EV, Schaefer E, Parmar K, Salgia R. Activated c-Met signals through PI3K with dramatic effects on cytoskeletal functions in small cell lung cancer. *J Cell Mol Med*. 2002;6(4):539-53. Epub 2003/03/04. PubMed PMID: 12611639.

160. G SK. Targeting Notch Signaling And Hepatocyte Growth Factor In Breast Cancer 2008. Available from: <http://ww5.komen.org/Abstracts.aspx?qn=KG080310&cycle=2007-2008>.

161. Gama Sosa MA, De Gasperi R, Elder GA. Animal transgenesis: an overview. *Brain Struct Funct.* 2010;214(2-3):91-109. Epub 2009/11/26. doi: 10.1007/s00429-009-0230-8. PubMed PMID: 19937345.

VITA

Ana Maria Gonzalez-Angulo M.D. was born and raised in Columbia. She joined the medical program at the Universidad del Cauca School of Health Sciences in Colombia, and graduated as the top ranker of her class. She then joined the Mount Sinai Medical Center in Miami, FL to complete her Internal Medicine internship and residency, after which she earned a Medical Oncology Fellowship at the Ochsner Clinic Foundation in New Orleans, LA. Owing to her interest in an academic career and her focus on breast cancer, she extended her training for an additional year and completed the Susan G. Komen Fellowship at The University of Texas MD Anderson Cancer Center (MDACC) in 2004. She then joined the faculty in Breast Medical Oncology (BMO) as a non-tenure track Assistant Professor attracted by the institution's reputation, and her desire to become a leading physician-scientist in the area of breast cancer. After receiving peer-reviewed funding, she switched to the tenure track with a joint appointment in Systems Biology. She has earned a Masters of Research Sciences (Translational Research Track) from The University of Texas Health Science Center at Houston. In 2009 she received early promotion as an Associate Professor, with Tenure. In 2013, she was named as Section Chief of Clinical Research and Drug Development in BMO. Her translational and clinical research have been significantly impactful. Specifically, her research has led to a change in the management of patients with small tumors, reinforced the need for biopsies at the time of metastatic diagnosis, and supported the development of clinical trials using metformin in breast cancer. She designed and chaired a clinical trial that validated the use of genomic signatures to select the patients that have node-positive and hormone receptor-positive breast cancer, and who may not benefit from chemotherapy. The results of this study will be practice changing and will allow physicians to better personalize breast cancer treatment. Outside MDACC, she participates on multiple committees, task forces and study sessions. As a member of SWOG, she serves on the Breast Cancer Steering Committee, and chairs the endocrine therapy resistance research group. She also serves on various committees for ASCO and AACR, and co-chairs the ASCO Breast Cancer Tumor Marker Guidelines. She has been invited as a speaker at several national and international meetings, and has presented Institutional Grand Rounds at Dana Farber Cancer Institute, Massachusetts General Hospital, Columbia University, Vall d'Hebron University Hospital, and the European Institute of Cancer, among others. After graduate school, Ana will continue in her position as a physician scientist at MD Anderson with the goal of continuing to build a robust breast cancer translational research and drug development program.